Hydraulics of Flow near Wells in Unconsolidated Sediments
Volume 2; Field Studies

Errata Sheet

Page	Location	Correct From	To
E2	Lines 11 and 12 from top	...pumped at a maximum estimated discharge for a period of 48 hours.	...pumped over a further series of 3 tests.
	Fig. 1.1	Site 'A' Site 'B'	Site 'B' Site 'A'
	Fig. 2.3(a) top right hand side	35 ft. 10 ft.	m' m
E20	Line 1 para. 3	Figs. 2.34 & 2.33	Figs. 2.24 & 2.28
E21	Line 4 from top	(r = 1, 8 ft.)	(r = 1, 7 ft.)
E22	Line 3 from bottom	Fig. 2.38	Fig. 2.33
E26	Line 9 from bottom	$t = \frac{m's'}{10k'}$	$t = \frac{m'^2 S_s'}{10K'}$
E28	Line 10 from top	...Tables 3.8 and 3.9	...Tables 3.6 and 3.7
	Table 3.8	Table 3.8	Table 3.6
	Table 3.9	Table 3.9	Table 3.7
	Table 3.8 (now 3.6)	Hantush Method T S	Hantush Method T S β
	Table 3.8 (now 3.6) Col. 2 Line 1	14	4
E29	Line 10 & 11 from top	...Tables 3.8 and 3.9	Tables 3.6 and 3.7

Errata Sheet (Page 2)

Page	Location	From	To (Correct)
E31	Eq. (3.8a)	$\frac{\partial}{\partial r}(K_e \partial s)+\ldots$	$\frac{\partial}{\partial r}(K_e \frac{\partial s}{\partial r})+\ldots$
E32	Last line paragraph 2	$(t \leq \frac{m'^2 S_s'}{10k'}$	$(t \leq \frac{m'^2 S_s'}{10K'}$
E34	Eq. (3.14)	$\ldots = \overset{e}{\Sigma} \ldots$	$\ldots = \underset{e}{\Sigma} \ldots\ldots$
	Eq. (3.15b)	$\alpha' S'_y \int_t^{t+\Delta t/2} \frac{\partial s'}{\partial \tau} e^{-\alpha(..)}$	$\alpha' S_y' \int_t^{t+\Delta t/2} \frac{\partial s'}{\partial \tau} J e^{-\alpha(...)}$
	Eq. (3.16a)	$+S_e' \left.\frac{\partial s'}{\partial \tau}\right\|_{\tau=t+\frac{\Delta t}{2}}$	$+S_e' \left.\frac{\partial s'}{\partial \tau} J\right\|_{\tau=t+\frac{\Delta t}{2}}$
E35	Fig. 3.16 right hand side	S_{y_r}'	S_{y_α}'
	Fig. 3.23 bottom right hand side	$bQT/(2\pi m^2 r)$	$bQT/(8\pi m^2 r)$
		$b=6.5\ min^2/ft^2$	$b=26 min^2/ft^2$
E40	Line 3 from bottom of paragraph 1	Knowing the nonlinear...	Knowing λ the nonlinear...
	Fig. 3.24 top left hand corner	$b=6.5\ min^2/ft^2$	$b=26 min^2/ft^2$

The University of New South Wales
WATER RESEARCH LABORATORY

Australian Water Resources Council Research Project 68/8
Extraction of Water from Unconsolidated Sediments

HYDRAULICS OF FLOW NEAR WELLS IN UNCONSOLIDATED SEDIMENTS

Volume 1: Theoretical and Experimental Studies

Volume 2: Field Studies

by

C.R.Dudgeon, P.S.Huyakorn and W.H.C. Swan

Report No. 126

Key Words

Aquifers
Aquitards
Groundwater
Pumping
Testing
Gumly Gumly Island, N.S.W.
Rosevale, Q'ld.
Porous Media
Drawdown
Water Wells
Computer Programmes
Mathematical Models

0.85824-081-5

Preface

This report covers the field studies performed as part of the Australian Water Resources Council's Research Project 68/8 "Extraction of Water from Unconsolidated Sediments'. The purpose of the studies was to provide verification under field conditions of the theory and numerical techniques reported in Volume 1. They were carried out with the co-operation of the Water Conservation and Irrigation Commission, New South Wales and the Irrigation and Water Supply Commission, Queensland. Their co-operation and assistance is gratefully acknowledged.

D.N. Foster,
Senior Lecturer in Civil Engineering,
Officer-in-Charge.

31st March 1973.

SECTION E

FIELD STUDIES

OF

THE GUMLY GUMLY ISLAND AND ROSEVALE WELL-AQUIFER SYSTEMS

by

W. H. C. Swan and P. S. Huyakorn

Table of Contents

Table of Contents
(cont'd.)

Nomenclature

		Dimension
a	linear coefficient of hydraulic resistance	TL^{-1}
b	non-linear coefficient of hydraulic resistance	T^2L^{-2}
m, m'	thickness of aquifer and aquitard, respectively	L
r, r_p	radial distance from pumped well to observation well	L
r_i	radial distance from image well to observation well	L
r_w	well radius	L
s, s'	drawdown in main aquifer and aquitard respectively	L
s_w	well drawdown	L
t	elapsed time from the commencement of pumping	T
t_e	required elapsed time for the straight line method	T
t_i	time after pumping started, after the boundary becomes effective, when the divergence of the time-drawdown curve caused by the influence of the image well to the particular value of drawdown at time t_p	T
t_p	time after pumping started, before the boundary becomes effective, for a particular drawdown to be observed	T
u	$\frac{r^2S}{4Tt}$	
z	vertical co-ordinate above the bottom of the main aquifer	L
z'	z-m	L
A	linear coefficient of well loss	TL^{-2}
B	non-linear coefficient of well loss	T^2L^{-5}
K, K'	hydraulic conductivity of aquifer and aquitard respectively	LT^{-1}
K_e	$\frac{1}{a+b\lvert V\rvert}$	LT^{-1}

Nomenclature (cont'd.)

		Dimension
Q	well discharge	L^3T^{-1}
$\frac{r}{D}$	$r \Big/ \left[\frac{Km}{\alpha' S_y'} + \frac{Kmm'}{K'}\right]^{\frac{1}{2}}$	
$\frac{r}{B}$	$r \Big/ \left[\frac{K'}{Kmm'}\right]^{\frac{1}{2}}$	
$\frac{r}{D_t}$	$r \Big/ \left[\frac{Km}{\alpha' S_y'}\right]^{\frac{1}{2}}$	
S	storage coefficient of main aquifer	
S_s, S_s'	specific storage of aquifer and aquitard respectively	L^{-1}
S_y, S_y'	specific yield of aquifer and aquitard respectively	
T	transmissivity of main aquifer	L^2T^{-1}
$\|V\|$	absolute flow velocity	LT^{-1}
$W(u)$	$\frac{4\pi\ sT}{Q}$	
α'	reciprocal of the delayed yield index for water table aquitard	T
β	$\frac{r}{4m}\left[\frac{K'S_s'}{K\ S_s}\right]^{\frac{1}{2}}$	
λ	$(bQT/2\pi\ m^2r)$	

1. Introduction

The primary objectives of the field studies described herein were to apply the theory and numerical studies presented in Section B to actual field problems, to develop new methods for analysing pumping test data and to evaluate aquifer and aquitard properties with the aid of the finite element digital computer programmes.

To achieve these objectives, an extensive programme of field tests was carried out at two widely separated sites, (Fig. 1.1), where differing problems in extracting water have been encountered, namely:-

(i) Site A - Gumly Gumly Island, Wagga Wagga, New South Wales, where high yields are possible from a deep aquifer overlain by a confining aquitard. A 16 inch diameter gravel packed production well was constructed in a 24 inch diameter hole and screened through the entire thickness of the main aquifer. Piezometer tubes were installed in the gravel pack of the production well and in a nearby observation well to allow the measurement of head losses during the early period of pumping.

(ii) Site B - Rosevale, South East Queensland, where a highly variable aquifer is overlain by a water table aquitard. Difficulties have been experienced in extracting water at this site due to small available drawdown and variability in thickness and physical characteristics of the aquifer. Due to these difficulties, significant aquifer losses near the production well have been recorded.

Two 4 inch diameter production wells, fully screened through the entire aquifer thickness were constructed. The two production wells were required for trial in-situ two well tests designed to determine independently the hydraulic characteristics of the aquifer material local to the pumped wells. Samples from the two production wells were collected for permeability tests and sieve analysis in the laboratory. Six nearby observation wells were also constructed to record the response at various radial distances from the pumped well.

One of the 4 inch diameter production wells was later reamed to 8 inch diameter to evaluate the effects of diameter on well yield. Selection of the size and screen of this reamed hole was based on the knowledge of the physical characteristics of the collected samples.

The following test programmes were executed:

(i) Site A - A 72 hour constant discharge pump test was performed.

Water levels were recorded in the pumped well, in the nearby observation wells and in three existing distant observation wells, throughout the duration of the test.

(ii) Site B - A series of pump tests and recovery tests at various constant discharges was performed on each of the 4 inch diameter production wells. Water levels were recorded in the pumped wells and the nearby observation wells.

The in-situ two well tests were then conducted using the two 4 inch diameter production wells.

Finally, to investigate the effects of diameter on well yield, the reamed 8 inch diameter production well was then pumped at a maximum estimated discharge for a period 48 hours.

Data collected from the tests at both sites were analysed by the following approach:-

(i) Conventional methods of pumping test analysis were first applied to obtain approximate values of the gross transmissivity T and storage coefficient S for the main aquifer. Existing boundary effects were also analysed by image well theory. The results of the foregoing analyses were then verified with the aid of a finite difference digital computer programme developed by Prickett and Lonnquist (1971).

(ii) New methods with the aid of the finite element digital computer programmes were used to examine more closely the flow behaviour local to the pumped well, and to obtain more accurate values of the hydraulic coefficients for the aquifer and aquitard. Predictions of the non-Darcy effects and effects of well diameter on yield were also made.

(iii) The results obtained from the conventional and new methods were compared. New field methods for pumping test evaluation of the aquifer and aquitard properties are proposed.

The following section is intended to be a brief presentation of the results of these studies. A general discussion of the conventional and proposed methods of pumping test analysis is presented. Development of the finite element models for both well-aquifer systems and predicted behaviour of transient flow is also discussed.

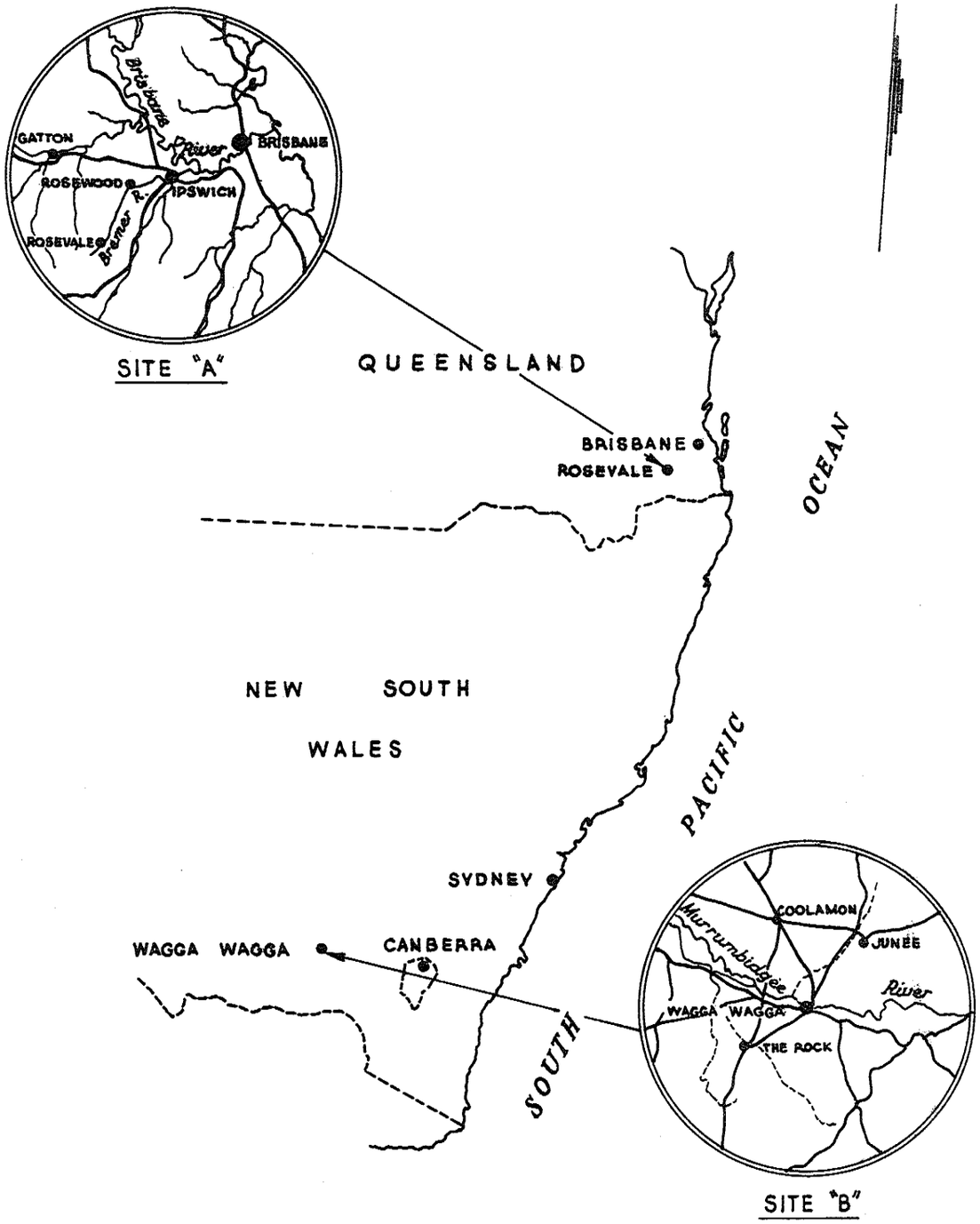

Fig. 1.1: Sites selected for Field Studies.

2. Site A- Gumly Gumly Island, Wagga Wagga, New South Wales

2.1 General

The aquifer test at this site was performed in co-operation with the Water Conservation and Irrigation Commission of New South Wales, from September 26 to 29, 1972. The group of wells (Fig. 2.1) is located on an alluvial area of the Murrumbidgee River, known as Gumly Gumly Island, approximately five miles east of Wagga Wagga. The construction features, available drillers logs and geophysical logs in and near the test site are presented in Figs. 2.2, 2.3 and 2.4.

The gravel packed production well 30638 and the observation well 30577 were each fitted with four slotted P.V.C. piezometers, (Fig. 2.4), placed at depths indicated in Table 2.1 and Fig. 2.2.. The production well piezometers were placed equidistantly around and against the outside edge of the well casing. Piezometers in observation well 30577 were spaced several inches apart and the well hydraulically sealed between 52 ft. and 110 ft. below ground level.

The remaining observation wells 30568, 30031, 30032 and 30602 were screened at intervals shown in Table 2.1 and Fig. 2.2.

The effects of pumping production well 30638 were measured in that well and the gravel pack piezometers, piezometers in observation well 30577 and observation wells 30568, 30602, 30031 and 30032. Water levels in the production well 30638 and observation wells 30568, 30031 and 30032 were measured by float and tape. Observation well 30602 was monitored by a continuous recorder. The gravel pack piezometers and the piezometers in well 30577 were measured by means of a multiple contact electric probe developed for the measurement of rapidly falling water levels (see Appendix III).

Pumping was started at 3.00 pm on September 26 and was continued until 3.00 pm on September 29, a period of 4320 minutes. A continuous record of water levels in the production well, observation wells and piezometers was maintained for only 3960 minutes. The pumping rate, nominally 48,000 igph, varied between 50, 100 and 47,000 igph.

The time-drawdown field data collected for all wells and piezometers which responded to the pumping is presented in Appendix I. The two piezometers which penetrated the shallow aquifer at observation wells 30031 and 30032 were monitored but showed no response to

Table 2.1: Radial Distances from well 30638 and screened intervals of observation wells and piezometers at Site A.

Well	Piezometer No.	Radial Distance from 30638 (ft.)	Screened Interval R.L. above sea level (ft.)	Remarks
30638		-	412 - 452	Inside production well
	1	-	555 - 557)	
	2*	-	480 - 482)	Gravel pack
	3*	-	440 - 442)	piezometers
	4	-	420 - 422)	
30577**	5	8	555 - 557	No response to pumping 30638
	6	8	485 - 487	
	7	8	465 - 467	
	8	8	420 - 422	
30568		22	416 - 436	
30602		1385	398 - 437	
30032	1	2600	355 - 375	No response to pumping 30638
	3	2600	457 - 465	
	2	2600	540 - 560	
30031	1	3050	533 - 553	
	2	3050	353 - 413	No response to pumping 30638

* Blocked during construction

** Well 30577 hydraulically sealed from 52 ft. to 110 ft. below ground surface.

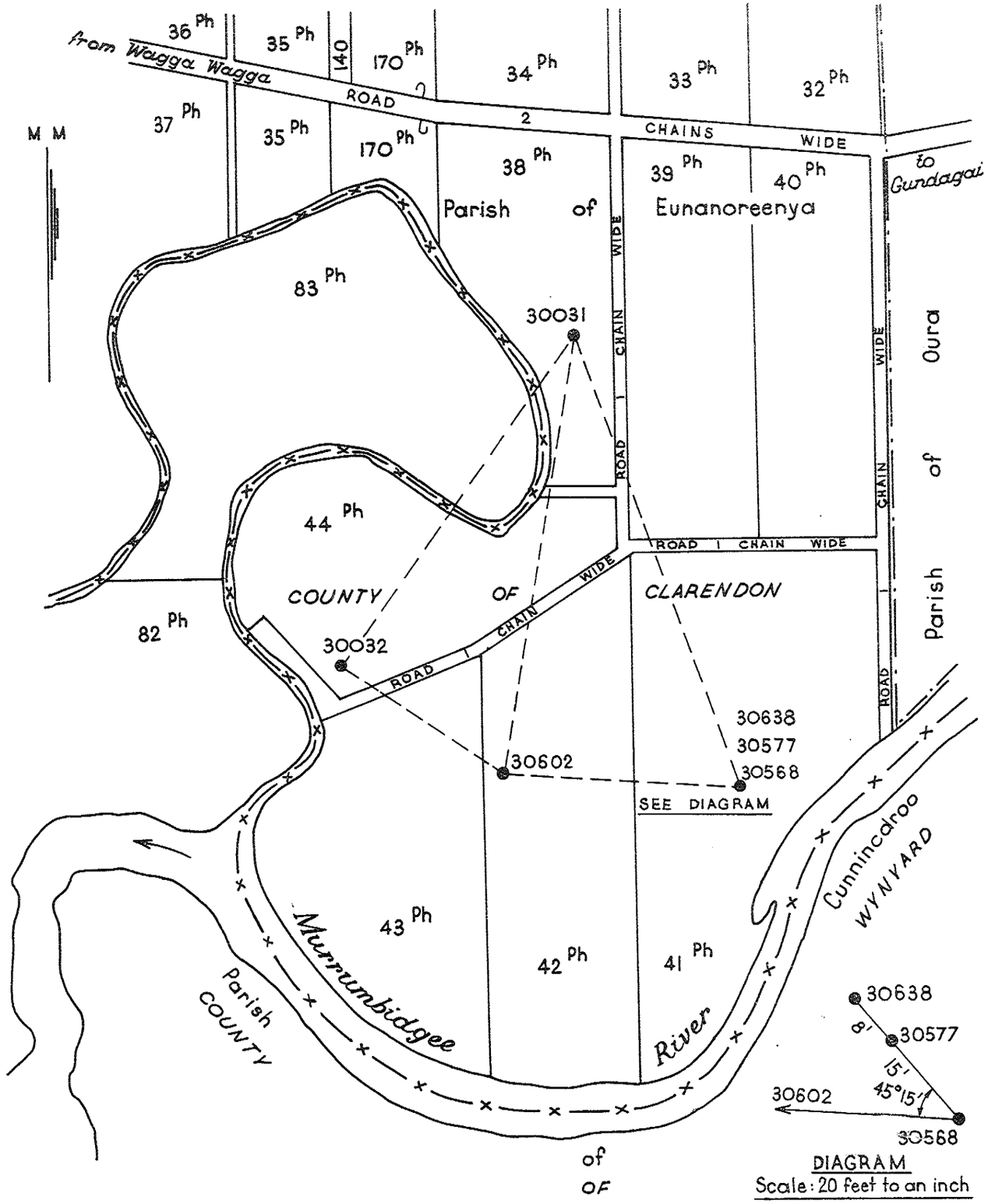

Fig. 2.1: General Plan of Site A.

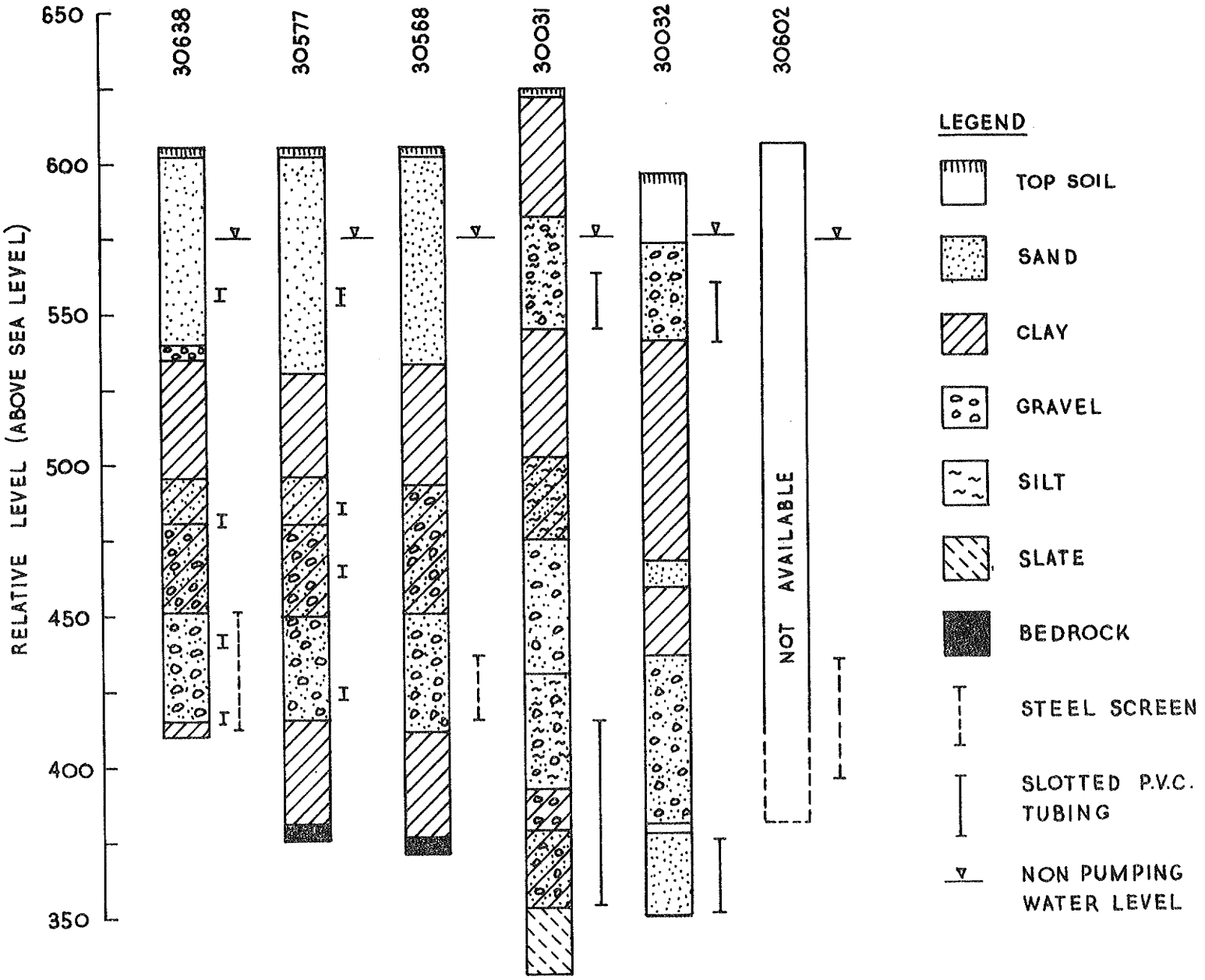

Fig. 2.2 Construction features and available drillers logs of wells at Site A.

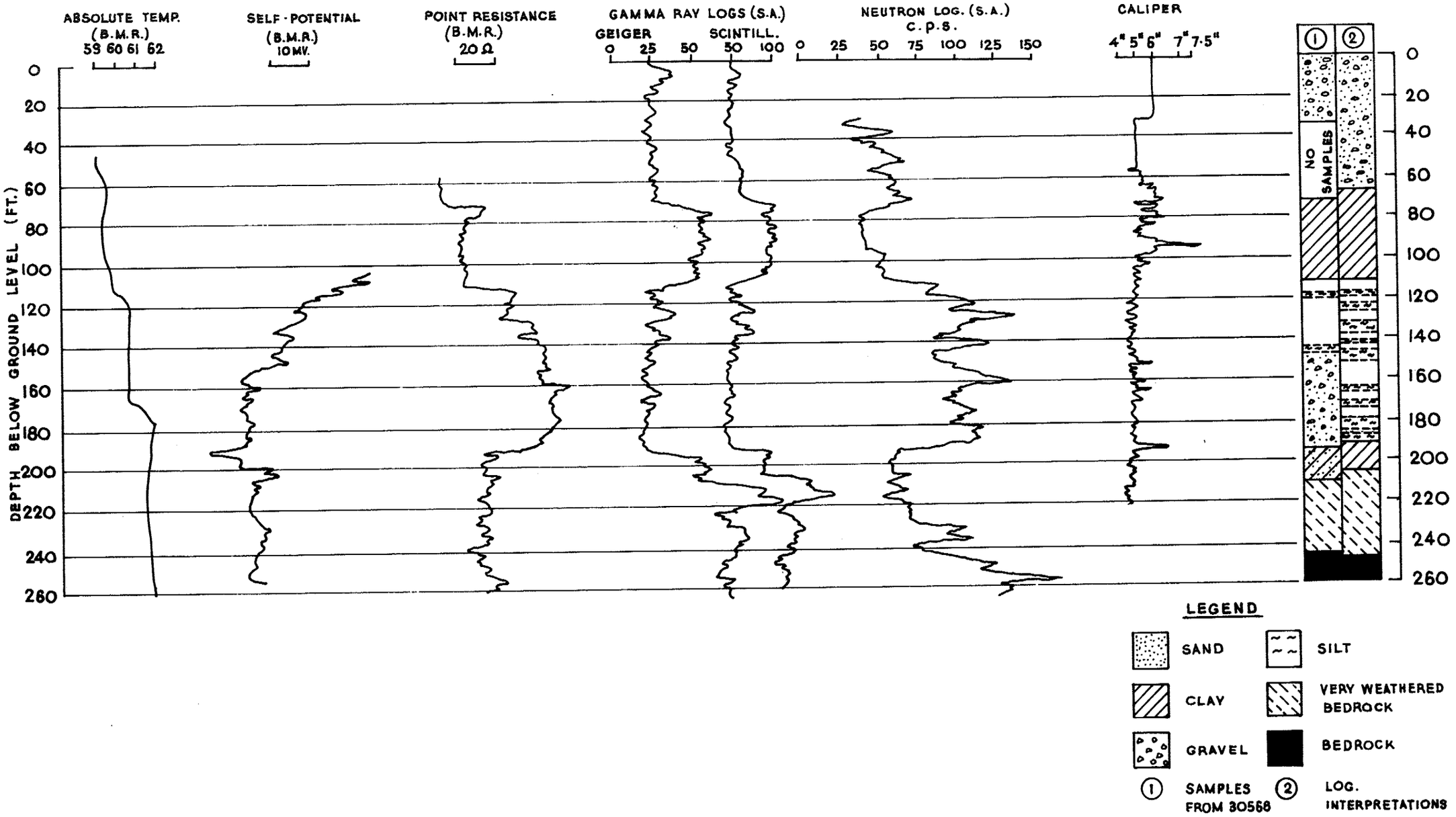

Fig. 2.3: Geophysical log of observation well 30568.

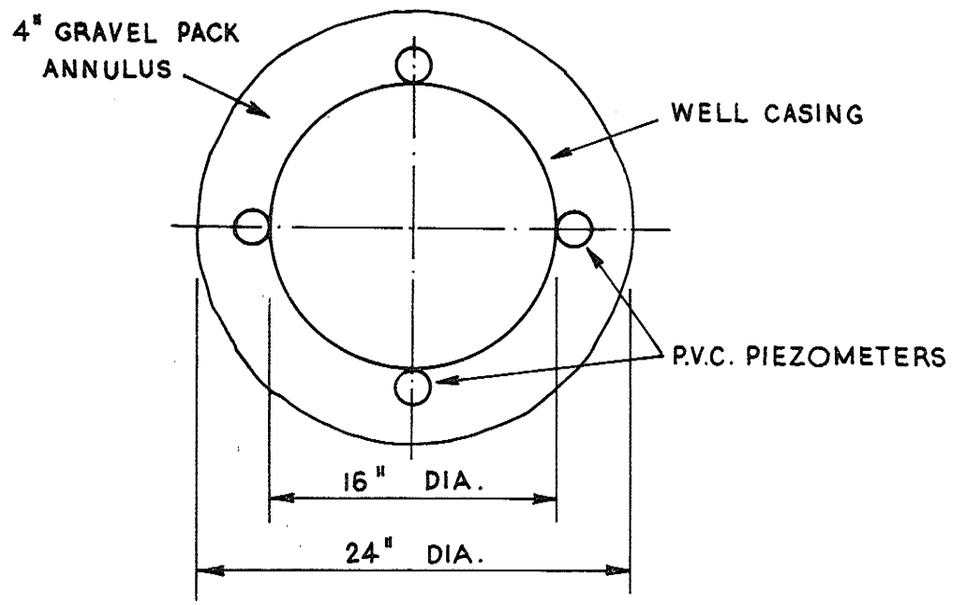

(a)

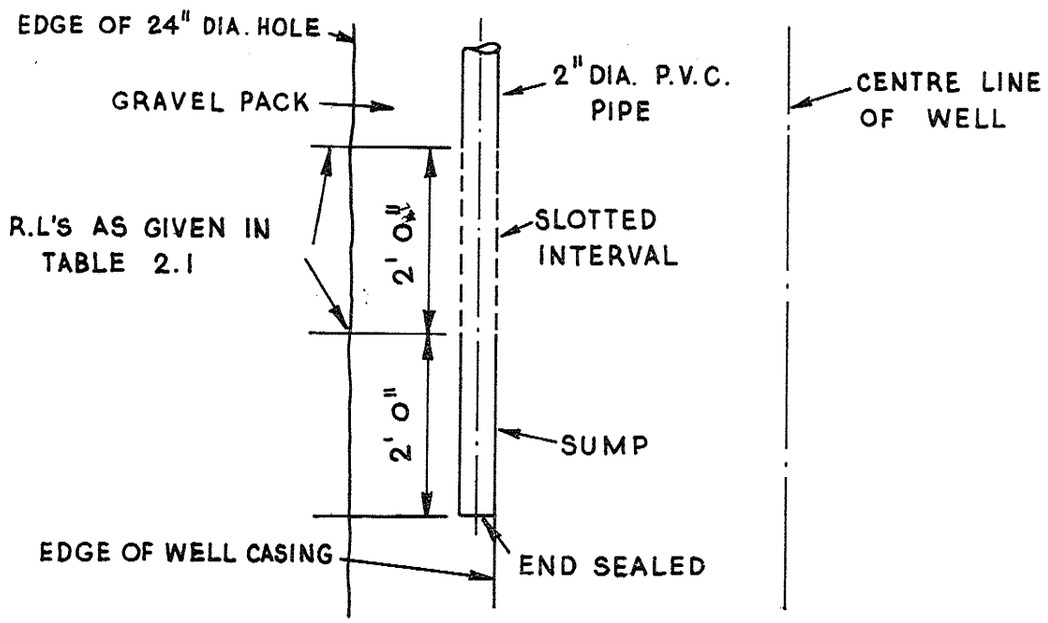

(b)

Fig. 2.4: Positioning and details of slotted P.V.C. piezometers in production well 30638.

the pumping of well 30638 and consequently have not been included.

2.2 Conventional Methods of Pumping Test Analysis

2.2.1 Selection of Applicable Methods

The methods available for analysing unsteady state constant discharge pumping test data are based on the method of analysis for a fully penetrating well in a non-leaky confined aquifer and constant discharge introduced by Theis (1935).

The validity of the results obtained by using any of the methods currently available depends to a large extent on the degree to which the hydrogeologic characteristics of the system under investigation agree with the basic assumptions of that method. In the absence of supporting data, observed variation of drawdown with time and distance may be interpreted in several ways. However, if careful consideration of all possible interpretations is pursued, valuable information in addition to the hydraulic properties of the aquifer can frequently be obtained. Such information includes the nature and location of the hydraulic boundaries and the average thickness of the aquifer.

The applicability of a method of analysis depends on the governing factors in a particular situation. The main governing factors which influence the applicability of any particular method include the flow system geometry, the time range within which the observed data falls and the distribution with time and distance of the collected data.

The methods available for the analysis of unsteady state pumping test data may be divided into two main categories, namely -

(i) Type curve methods
(ii) Straight line methods

(i) Type Curve Methods

The available hydrogeologic information suggests possible application of the following type curve methods for the Gumly Gumly Island pumping tests.

(a) Theis curve for a non-leaky confined aquifer and fully penetrating well, constant discharge conditions and allowance for existing barrier boundaries (Theis 1935, Ferris et al, 1962).

(b) Hantush type curves for a leaky confined aquifer and fully pen-

etrating well, constant discharge conditions and water released from storage in the overlying aquitard (Hantush, 1964).

After an initial attempt to match the time-drawdown field data on the above curves, it was found that the Theis curve was more suitable as the collected field data fell well outside the short time range of validity of the Hantush curves. The Theis curve was used in the subsequent analysis to obtain the coefficient of transmissivity T and coefficient of storage S for the main aquifer and to locate the barrier boundaries.

(ii) Straight Line Methods

In view of the findings of the previous section the straight line method of analysis introduced by Cooper and Jacob (1946) was also considered valid and selected for use.

The assumption (Hantush, 1964)

$$t_e > \frac{5\,Sr^2}{T}$$

or $$u \leq 0.05$$

where t_e = required elapsed time

$$u = \frac{r^2 S}{4Tt_e}$$

for the straight line method to apply was checked using the "early time" type curve values of S and T before proceeding with the analysis.

The "required elapsed time" values, t_e, that must be attained before the straight line method can be applied to the time-drawdown field test data for observation wells 30602, 30031 and 30032 are presented in Table 2.2.

Table 2.2: Required elapsed time for applicability of the straight line method

Well	Required elapsed time t_e (min.)
30602	496
30031	1916
30032	2038

A check of subsequent values of t_e obtained using the values of S

and T from the straight line method was made with the values given in Table 2.2.

Values of t_e for the production well 30638, gravel pack piezometers, piezometers in 30577 and observation well 30568 were not calculated as only values of transmissivity T were obtained for those locations.

2.2.2 Application of Conventional Methods to the Field System

(i) Type curve Method

The observation well 30568 and piezometers in well 30577 and in the gravel pack of well 30638 are very close to the pumped well, and their logarithmic time-drawdown graphs are too flat to be matched on the Theis curve. Consequently, emphasis was placed on the time-drawdown graphs of wells 30602, 30031 and 30032 in determining T and S of the main aquifer. The Theis curve trace was superimposed on the time-drawdown graphs of these wells as shown in Figs. 2.5, 2.6 and 2.7. After a relatively early time, the time-drawdown graphs departed upward from the Theis curve, indicating the presence of barrier boundaries.

The type curve trace was fitted to the early time-drawdown field data for these observation wells. Match point co-ordinates (W(u), $\frac{1}{u}$), and (s,t) were substituted in the following equations to determine T and S for the aquifer.

$$T = \frac{Q}{4\pi s} W(u) \qquad (2.1)$$

and

$$S = \frac{4Ttu}{r^2} \qquad (2.2)$$

The departures of the time-drawdown field data graphs from the type curve trace were recorded and plotted as subsequent time-drawdown curves and the type curve trace refitted to these new graphs in an attempt to detect the presence of multiple barrier boundaries.

It was found that the replotted departures of the time-drawdown field data graph for observation well 30032 departed from the type curve trace, indicating the presence of multiple barrier boundaries. The replotted departures of observation wells 30602 and 30031 did not depart significantly from the type curve trace for the period of available record.

Reference to available geologic data of the area surrounding the pumped well revealed the presence of two probable barrier boundaries,

which took the general shape and direction of the valley bedrock formation contours as shown in Fig. 2.8. Consideration of the likely location and direction of the two boundaries and the positions of observation wells 30602, 30031 and 30032 resulted in the following conclusions.

(a) Observation well 30602 would appear to be closer to the southern barrier boundary than to the northern barrier boundary. Consequently its time-drawdown graph would reflect the existence of the southern boundary more readily than the existence of the northern boundary.

(b) Observation well 30031 would appear to be closer to the northern barrier boundary and its time-drawdown graph would reflect the existence of the northern boundary more readily than the southern boundary.

(c) Observation well 30032, being situated at approximately the same distance from either boundary as the production well 30638 would tend to reflect the existence of both boundaries. The southern boundary, being closer to observation well 30032 than the northern boundary, would be detected first in the time-drawdown graph of this well.

These deductions were supported by the time-drawdown curves.

In view of this, the analysis was performed using observation wells 30032 and 30602 to locate the position of the southern barrier boundary and observation wells 30032 and 30031 to locate the northern barrier boundary. The location and direction of the barrier boundaries, the bedrock formation contours and the approximate locations of the production well 30638 and observation wells 30031, 30032 and 30602 are presented in Fig. 2.8.

The Theis curve was also fitted to the late time-drawdown field data of observation wells 30602, 30031 and 30032 and values of T and S obtained for the aquifer.

The values of T and S obtained by fitting the Theis curve to early and late time-drawdown data of observation wells 30031, 30032 and 30602 are presented in Table 2.3.

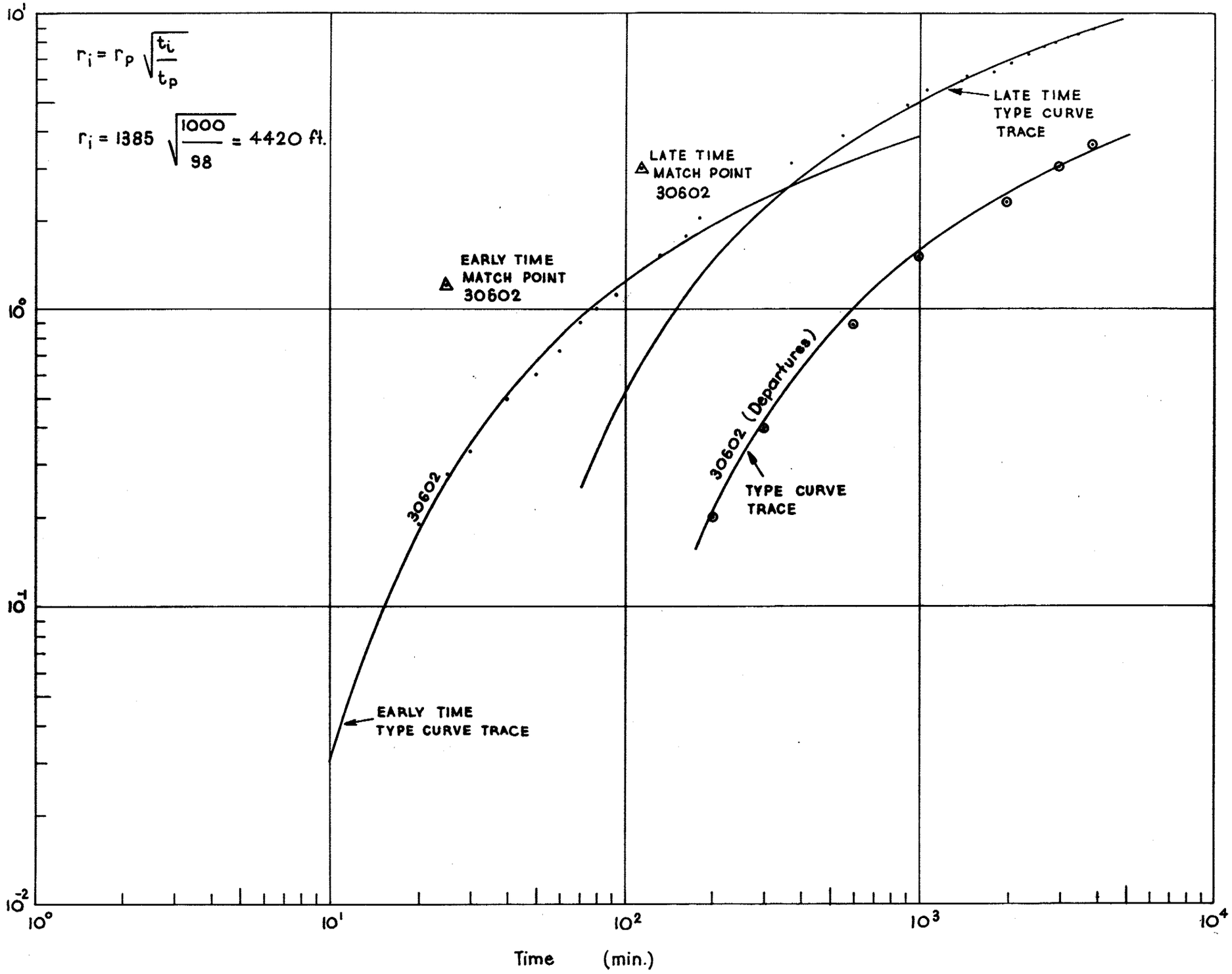

Fig. 2.5: Time-Drawdown Graph of Observation Well 30602.

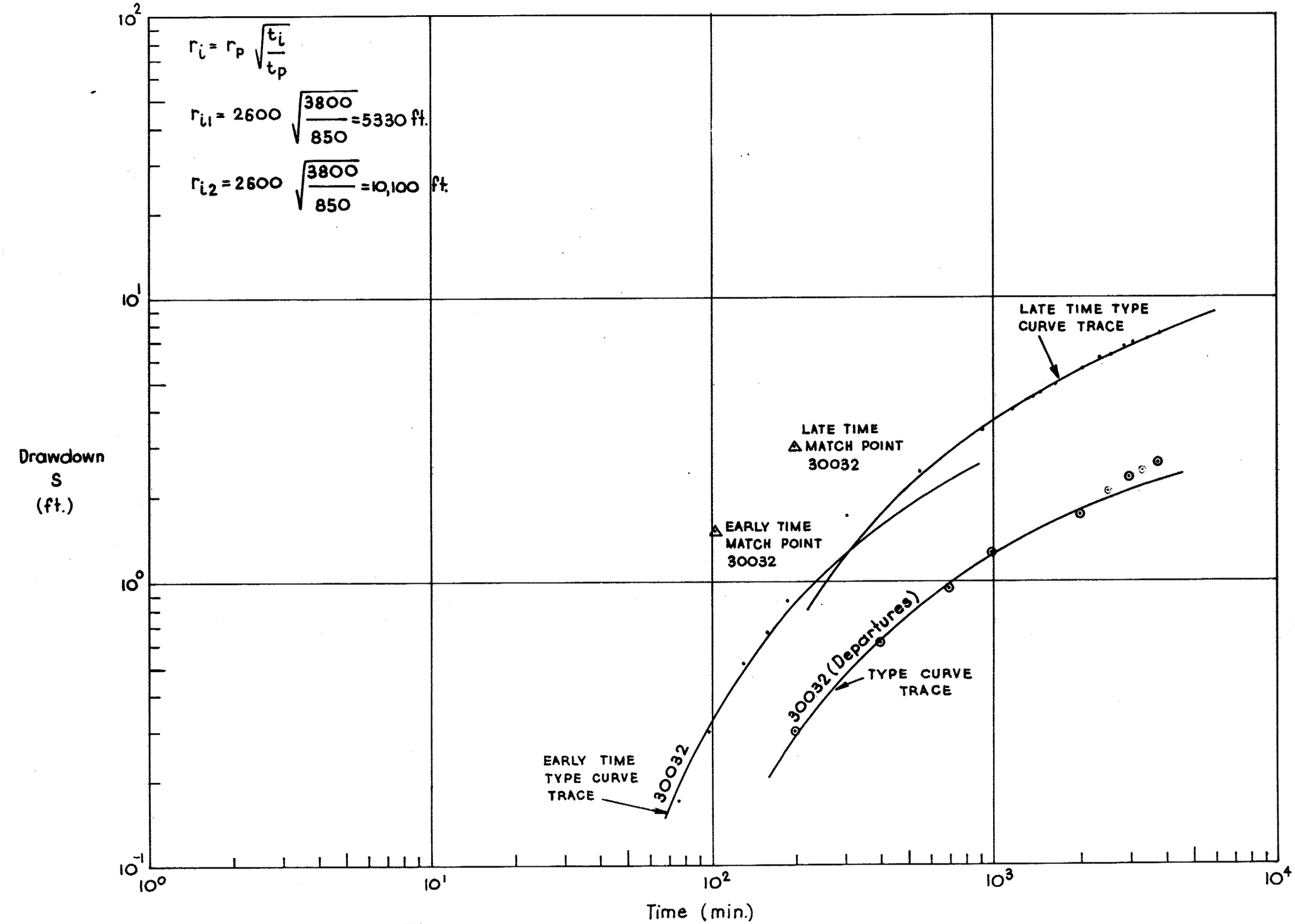

Fig. 2.6: Time-Drawdown Graph of Observation Well 30032.

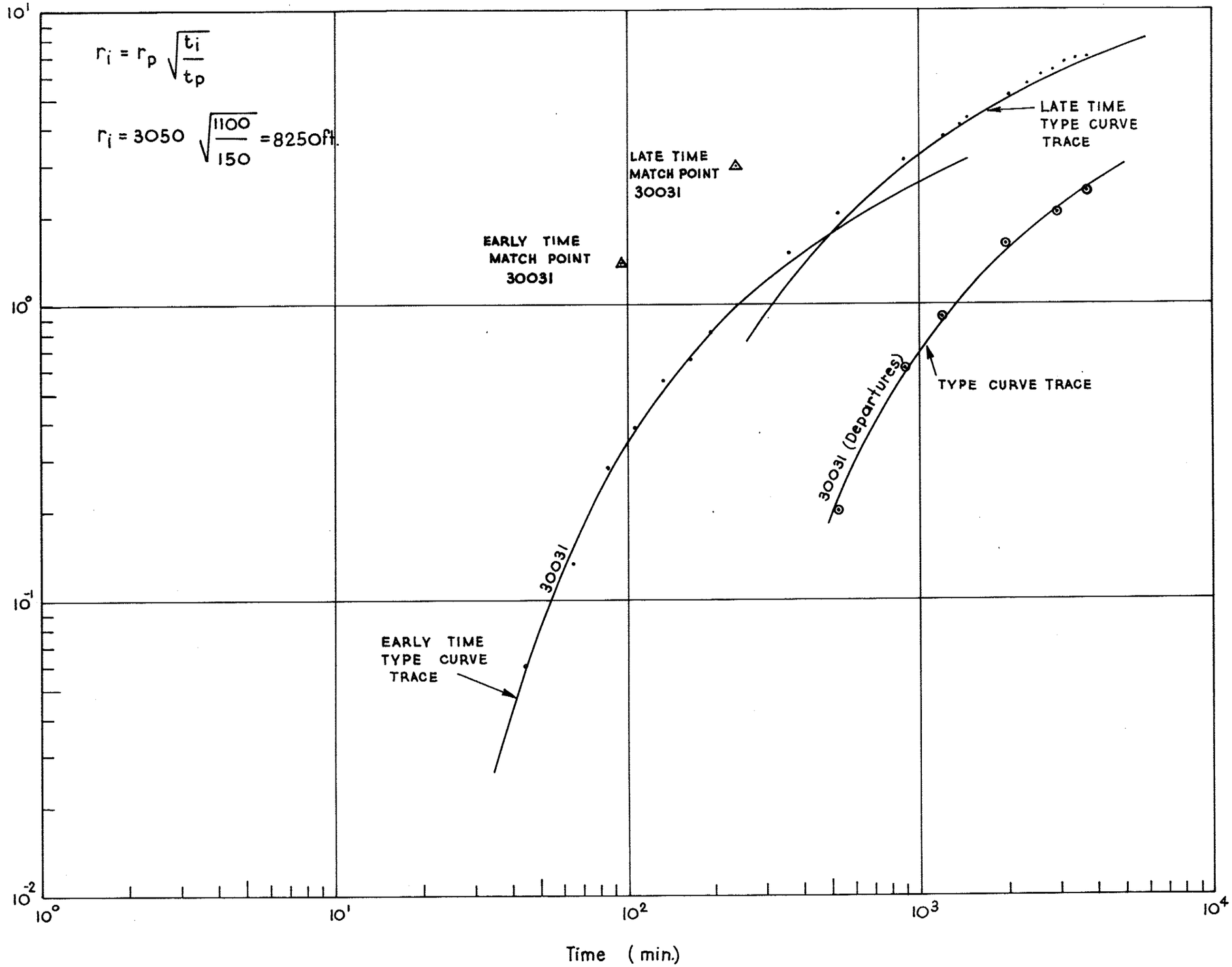

Fig. 2.7: Time Drawdown Graph of Observation Well 30031.

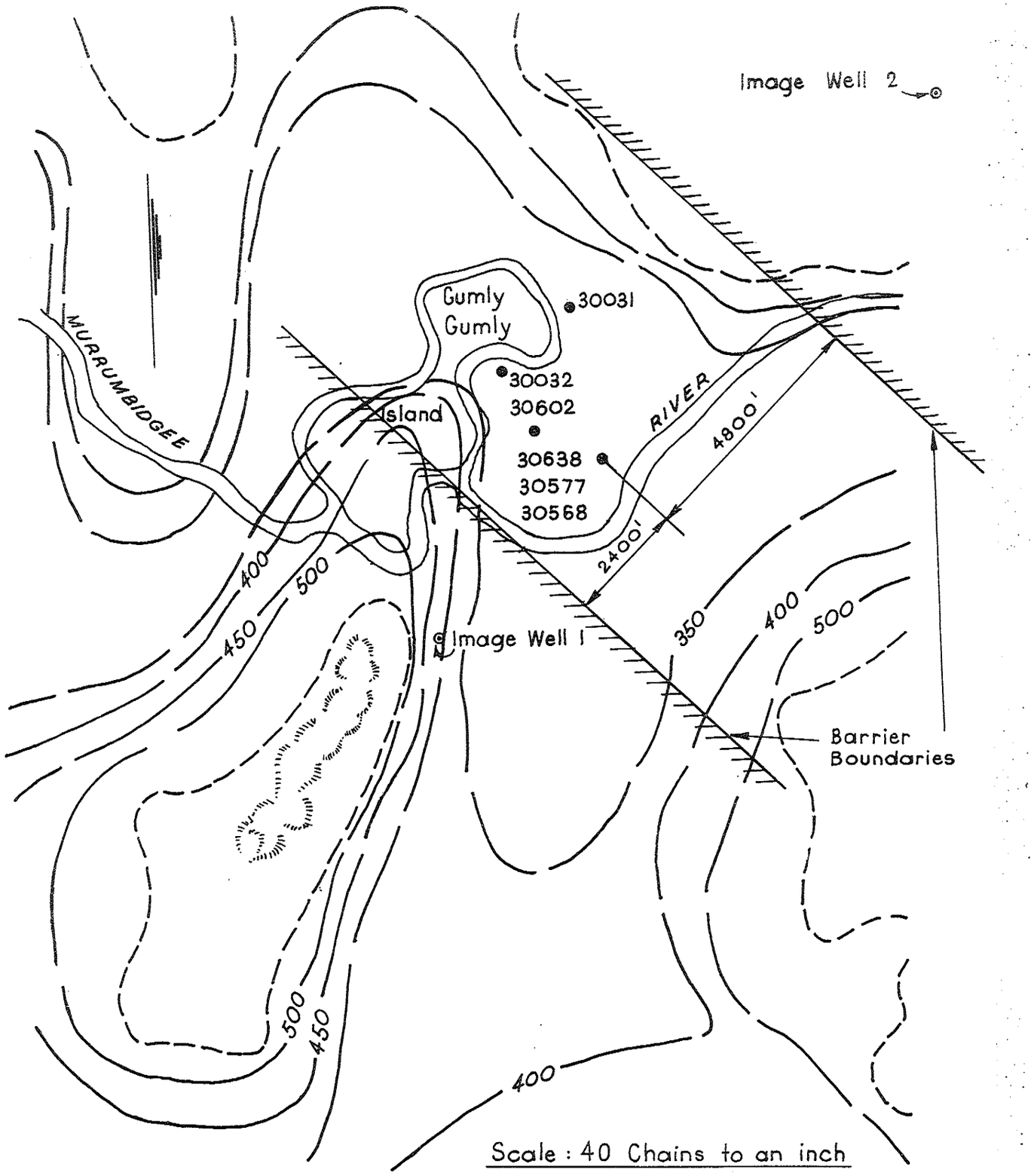

Fig. 2.8: Location and direction of Barrier Boundaries.

Table 2.3: Summary of T and S values obtained by fitting the Theis curve to early time and late time-drawdown data.

Well	Radial Distance (ft.)	$T(ft^2/min)$	S
Theis curve fit - early time			
30602	1385	8.5	4.4×10^{-4}
30031	3050	7.28	3.0×10^{-4}
30032	2600	6.8	4.1×10^{-4}
	Mean values	7.52	3.83×10^{-4}
Theis curve fit - late time			
30602	1385	3.42	8.2×10^{-4}
30031	3050	3.42	3.53×10^{-4}
30032	2600	3.42	4.05×10^{-4}
	Mean values	3.42	5.26×10^{-4}

(ii) Straight Line Method

The time-drawdown field data for the pumped well 30638, observation piezometers 30638 (1), 30638 (4), 30577 (6), 30577 (7), 30577 (8) and observation wells 30568, 30031, 30032 and 30602 were plotted on semilogarithmic paper.

A straight line was fitted to the time-drawdown field data graph of all wells as shown in Figs. 2.9, 2.10 and 2.11. The slope of the straight line was substituted in Equation (2.3).

$$T = \frac{2.3Q}{4\pi \frac{\Delta s}{\Delta \log_{10} t}} \qquad (2.3)$$

to obtain the coefficient of transmissivity T. The coefficient of storage S was determined for observation wells 30602, 30031 and 30032. No attempt was made to obtain values of the coefficient of storage for the production well 30638, observation piezometers 30638 (1), 30638 (4), 30577(6), 30577 (7), 30577 (8) and observation well 30568. The intercept t_o of the straight line at zero drawdown and the coefficient of transmissivity T were used to determine the value of the storage coefficient S by substitution in Equation (2.4).

$$S = 2.25 \frac{T\ t_o}{r^2} \qquad (2.4)$$

A summary of T and S values obtained are presented in Table 2.4.

Table 2.4: Summary of T and S values obtained from the straight line method.

Well	Piezometer No.	Radial Distance (ft.)	T (ft^2/min)	S
30638		-	4.26	-
	(1)	-	3.34	-
	(4)	-	4.25	-
30577	(6)	8	4.04	-
	(7)	8	4.18	-
	(8)	8	4.18	-
30568		22	4.26	-
30602		1385	3.21	8.85×10^{-4}
30031		3050	3.21	3.03×10^{-4}
30032		2600	3.21	3.85×10^{-4}
		Mean	3.81	5.24×10^{-4}

Revised values of the required elapsed time t_e were computed using the values of T and S obtained from the straight line method for observation wells 30602, 30031 and 30032. A summary of the values of t_e obtained using the "early time" type curve method and the straight line method is presented in Table 2.5.

Table 2 5: Comparison of t_e values obtained from type curve and straight line methods.

Well	Early time type curve method t_e (min)	Straight line method t_e (min)
30602	496	2644
30031	1916	4390
30032	2036	4054

(iii) Radial Distance-Drawdown Graphs

A semi-logarithmic graph of radial distance against drawdown (natural scale) was made using the drawdowns in wells 30638, 30638 (4), 30577(8), 30568, 30602, 30031 and 30032 for a time t of approximately 3800 minutes, and is presented in Fig. 2.12.

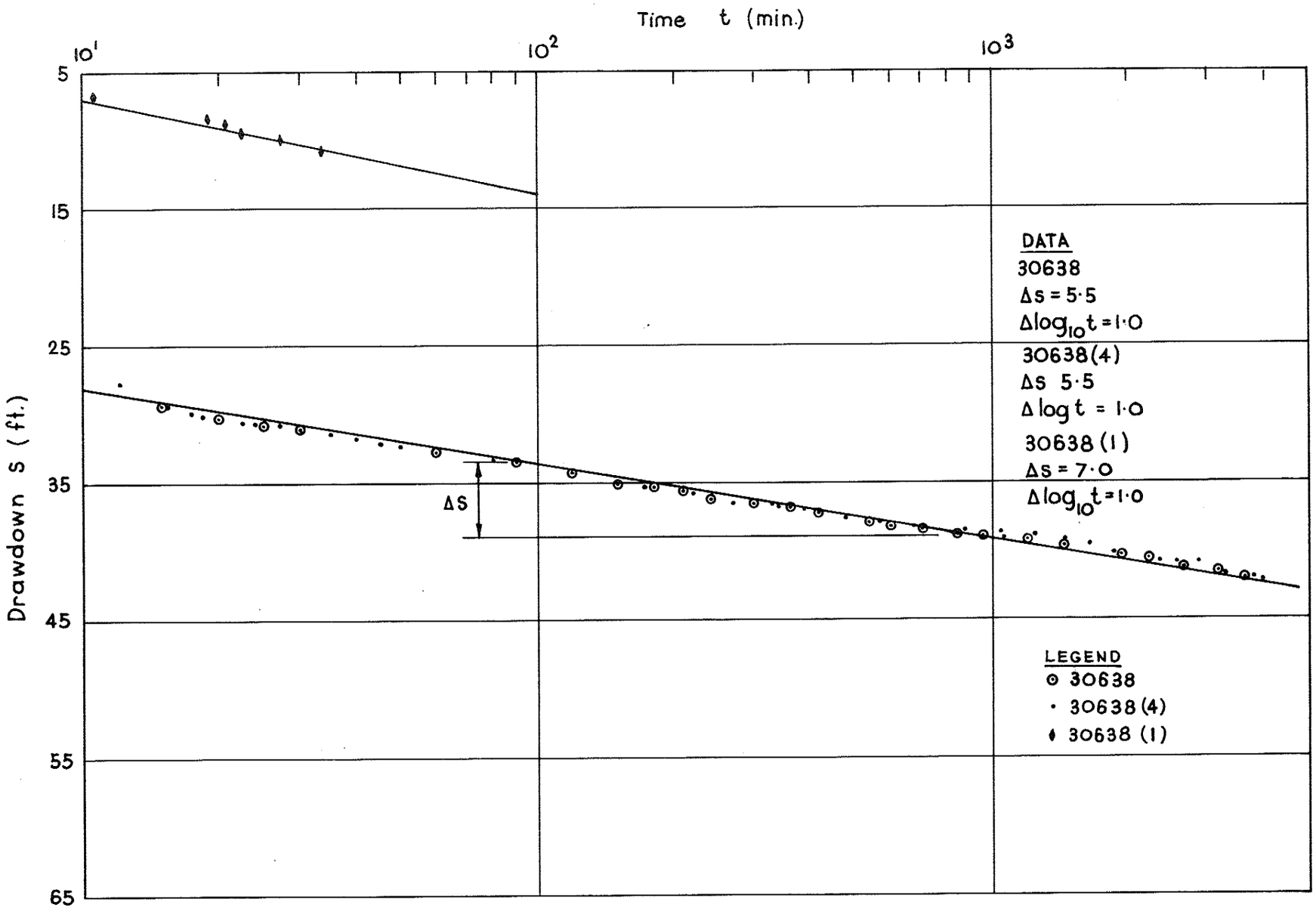

Fig. 2.9: Straight Line Graph of Time-Drawdown Data - Site A.

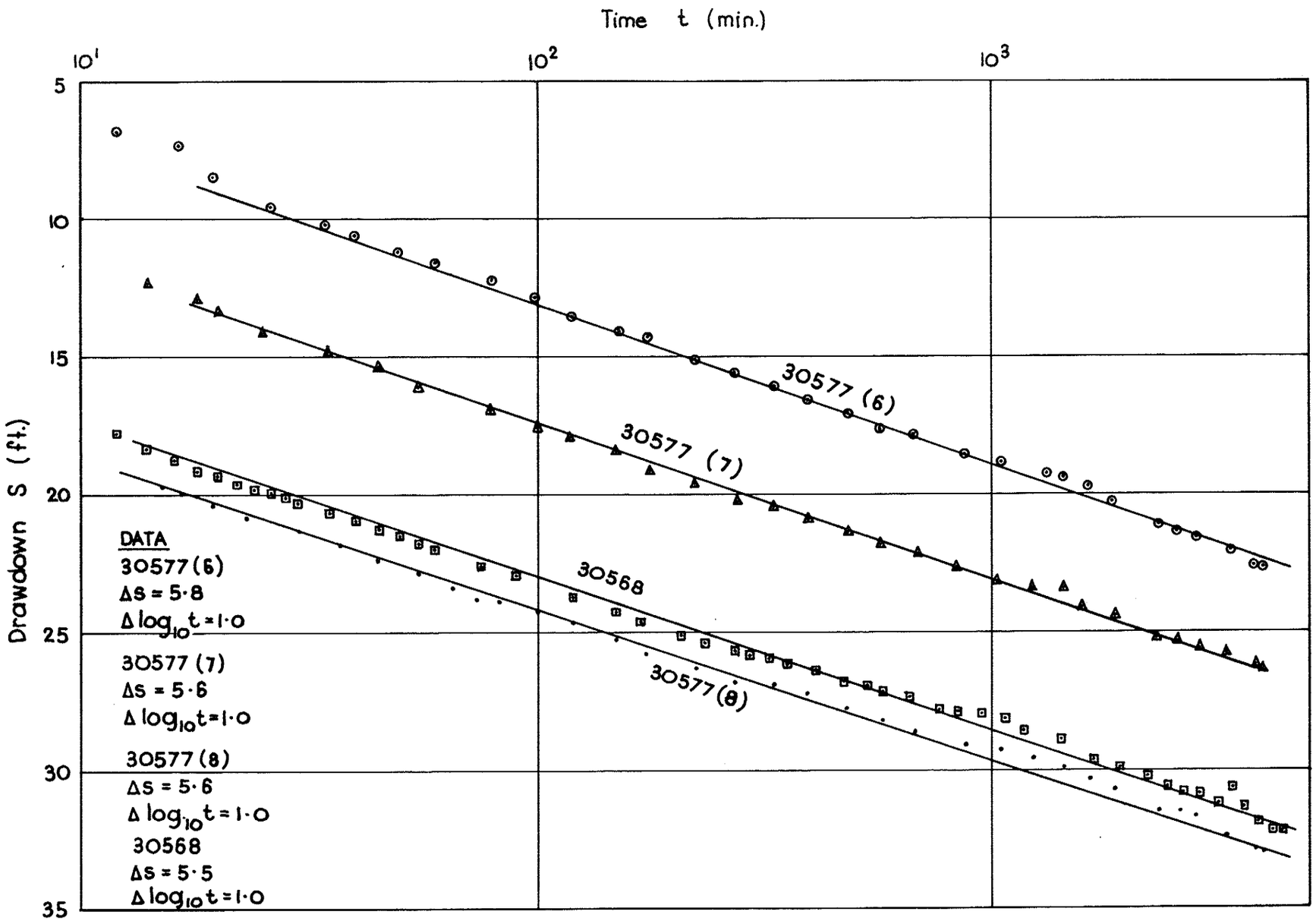

Fig. 2.10: Straight Line Graph of Time Drawdown Data - Site A.

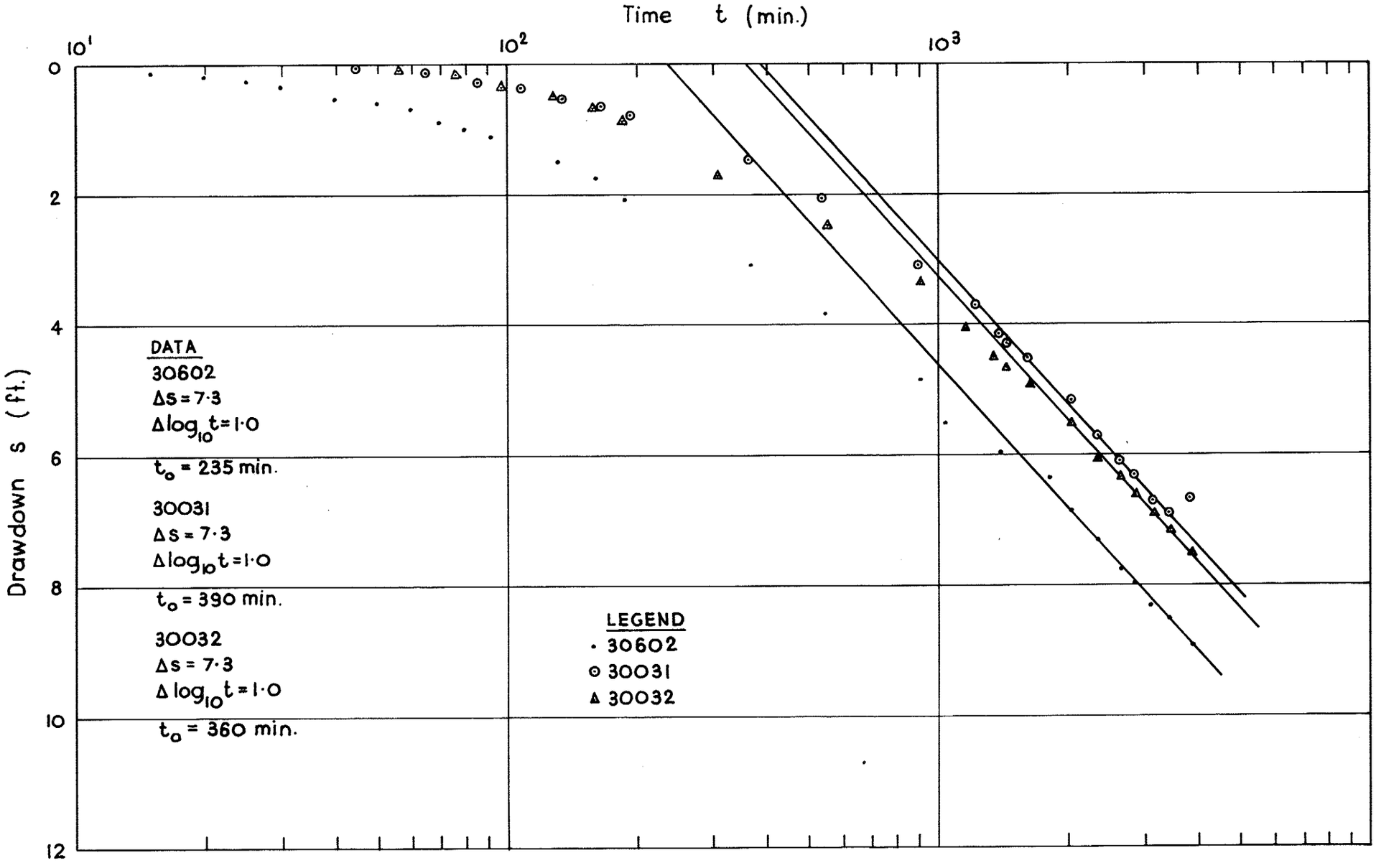

Fig. 2.11: Straight Line Graph of Time-Drawdown Data - Site A.

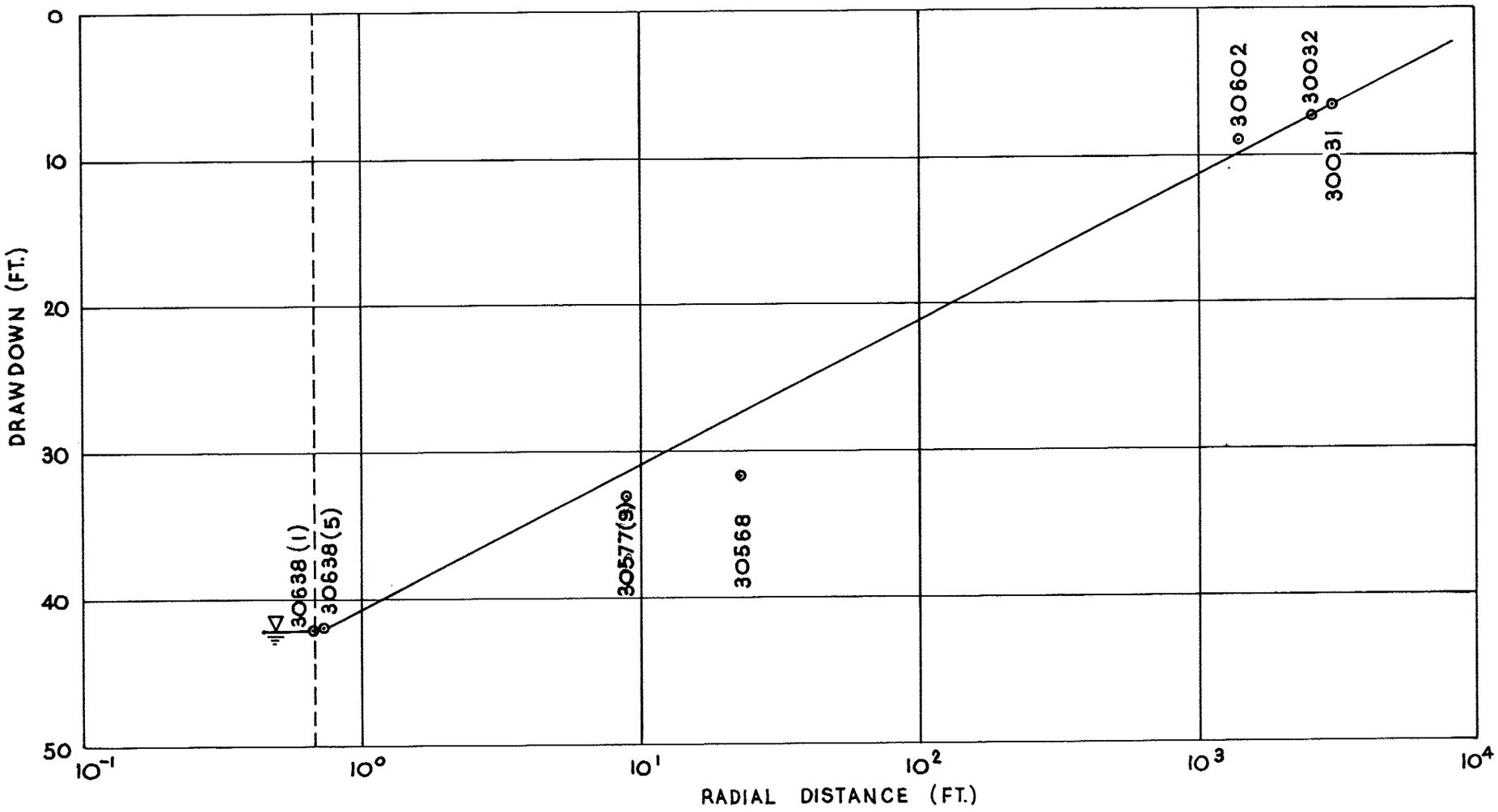

Fig. 2.12: Radial Distance - Drawdown Graph - Site A.

This graph would suggest the flow of water through the system falls in the linear regime of aquifer losses as no significant screen loss or non-linear aquifer loss can be detected.

2.2.3 Regional Flow Model Verification

The results of the analysis of Sec. 2.2.2 using the conventional methods of pumping test analysis can be verified with the aid of two methods currently available, namely:-

(i) finite differences digital computer programme
(ii) image well simulation digital computer programme.

(i) Finite Differences Digital Computer Programme

Prickett and Lonnquist (1971) presented generalised digital computer programmes that can simulate two and three dimensional nonsteady regional flow of groundwater in heterogeneous aquifers under water table and non-leaky and leaky confined conditions.

They used the finite difference approach to approximate the governing differential equation of groundwater flow and adopted a modified alternating implicit direction method to solve the resulting set of finite difference equations. For given T and S values and boundary geometry, drawdowns can be predicted for given pumping conditions.

Their two dimensional non-leaky confined aquifer digital computer programme has been adapted and used to check the results obtained for the Gumly Gumly Island aquifer. Written in FORTRAN IV, it has been modified for use on an IBM 360 system model 50 computer with a G level compiler. A flow chart diagram of the programme is presented in Fig. 2.13 and a listing of the programme presented in Appendix IV.

The early time mean values of T and S of Table 2.3 and the boundary geometry of Fig. 2.8 were inserted as data in the programme.

A uniform finite difference grid (Fig. 2.14) of 13x61 nodes, at 600 ft. spacings, with non-uniform time increments was used to simulate the field situation.

The results of the computer simulation and the time-drawdown field data for observation wells 30602, 30031 and 30032 are presented in Figs. 2.15, 2.16 and 2.17.

For observation wells 30031 and 30032, the time-drawdown field data have been compared with the computed time-drawdown curves of the two nearest nodal points. The time-drawdown field data of well 30602 have been compared with the time-drawdown computer simulation data at the nearest nodal point (Table 2.6).

Table 2.6: Nodal Points chosen for comparison with Field Data

Well	Computer Simulation Nodal Points
30602	(4,29)
30031	(5,26) (5,27)
30032	(9,27) (9,28)

The computer simulation results show a tendency to deviate from the field data points at time values greater than 1000 minutes from the commencement of the test. This is due, in part, to the fact that the end node rows (j=1 and j = 61), of the finite difference grid behave as if a barrier boundary exists one half nodal distance beyond these end rows.

To eliminate the end node effects would have required an enormous increase in the number of nodes with a resultant increase in the computational time. Alternatively, a non-uniform grid spacing could have been used but the saving in computational time on the computer is not offset by the increase in time of data preparation for insertion in the programme as presented by Prickett and Lonnquist. Use of a non uniform grid spacing would require preparation of node cards for each node in the grid.

However, with the finite difference grid used, the digital computer simulation of the regional flow, as suggested by the conventional methods of pumping test analyses, agrees reasonably well with the time-drawdown field data for times less than 1000 minutes for each of the observation wells 30602, 30031 and 30032.

(ii) Image Well System Simulation

An alternative method of verifying the results of conventional methods of pumping test analyses is to feed back the data obtained into the analysed image well system. The image well system used is presented in Fig. 2.18.

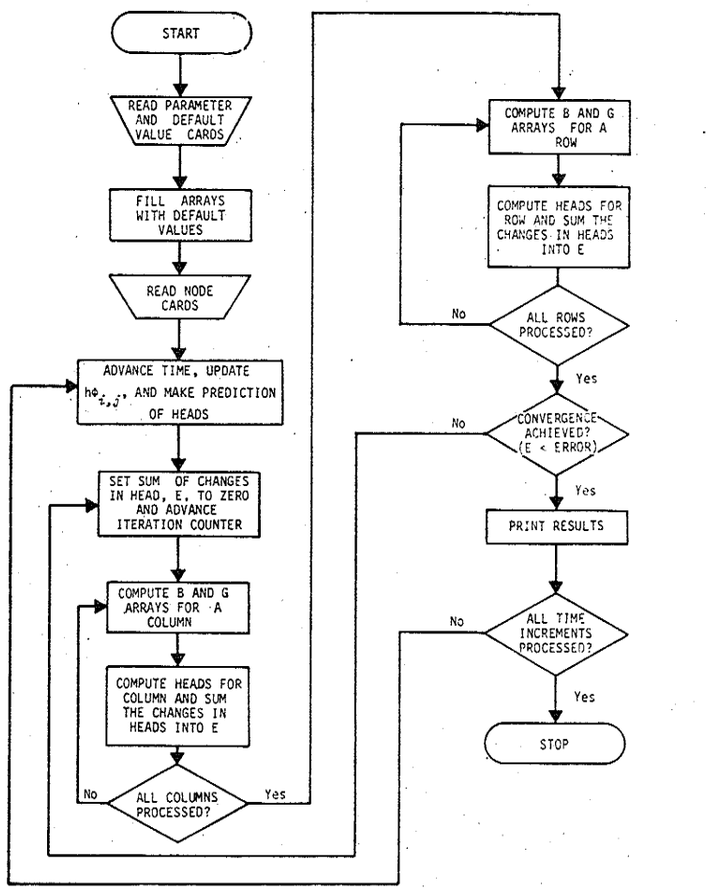

Fig. 2.13: Flow chart diagram of aquifer simulation programme (after Prickett and Lonnquist, 1971).

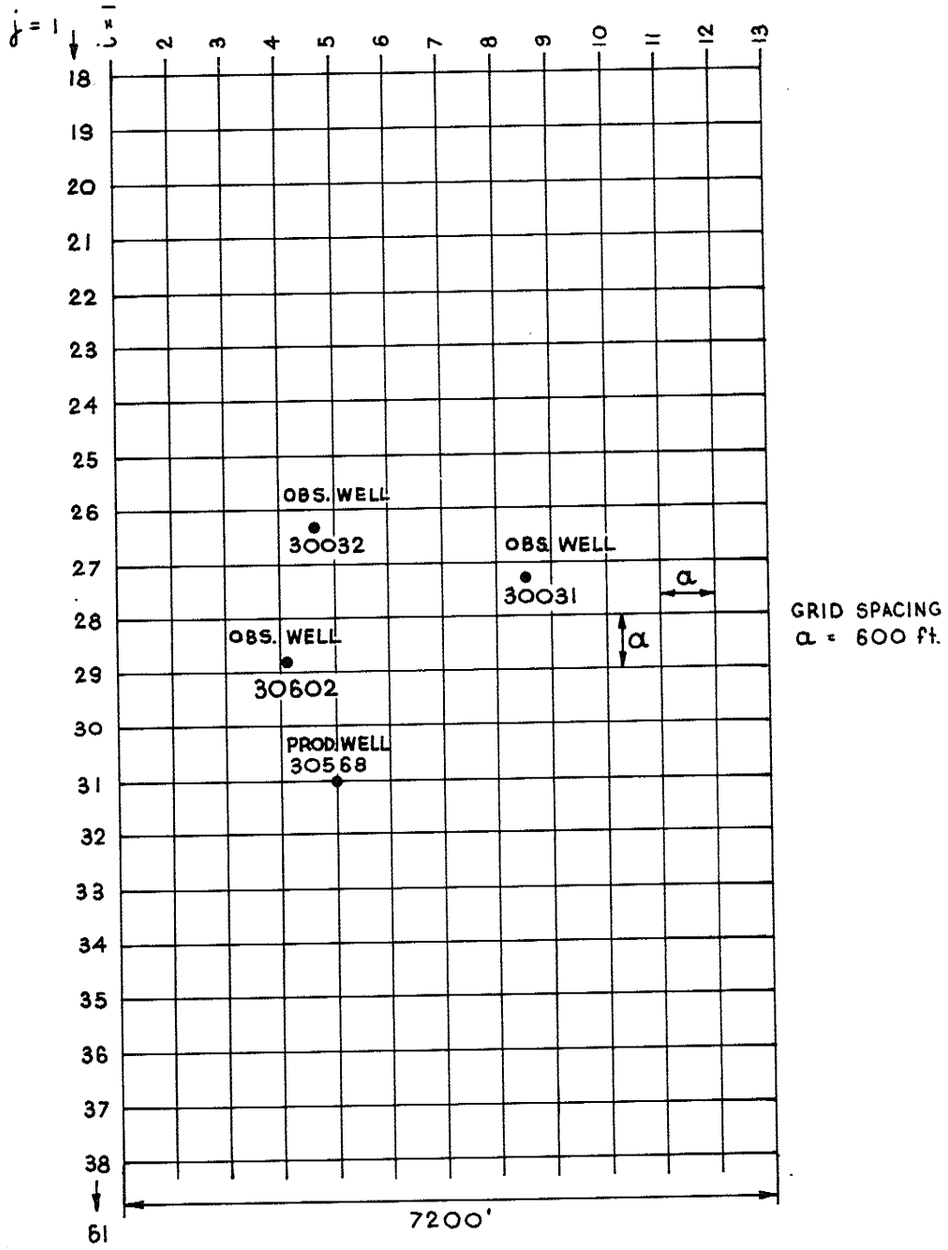

Fig. 2.14: Finite Difference Grid adopted for Site A.

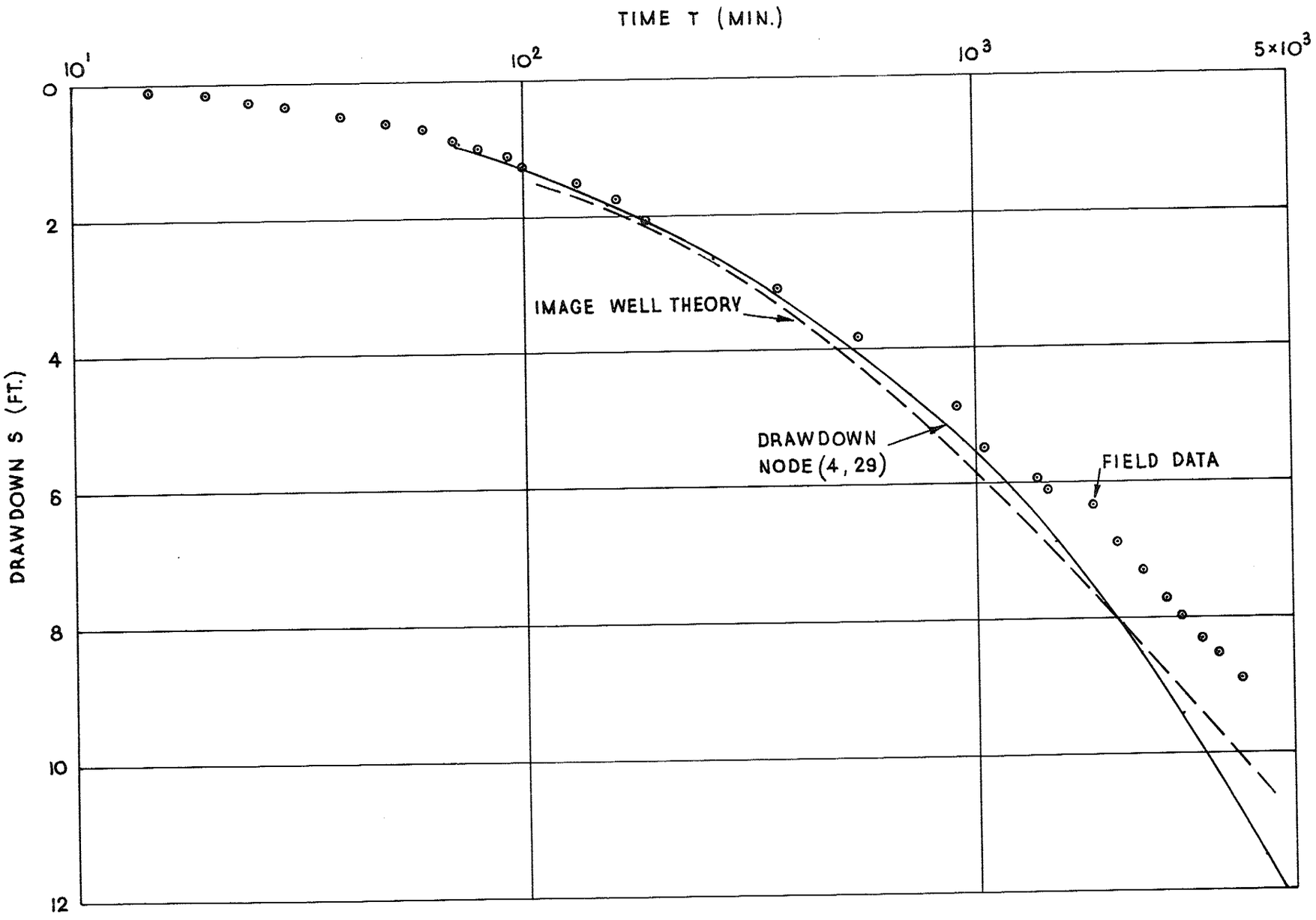

Fig. 2. 15: Theoretical and Field Data Correlation for Observation Well 30602.

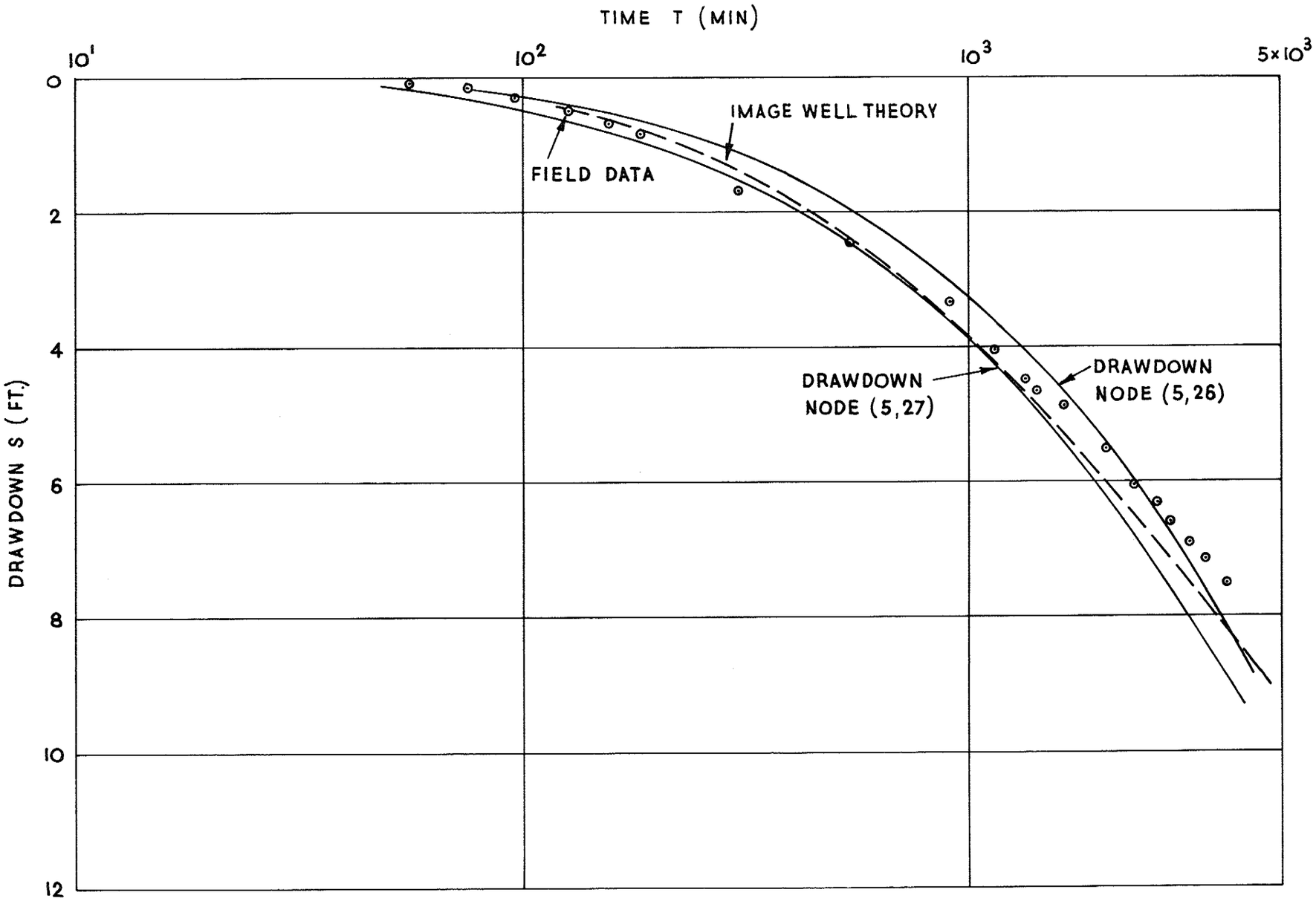

Fig. 2.16: Theoretical and Field Data Correlation for Observation Well 30032.

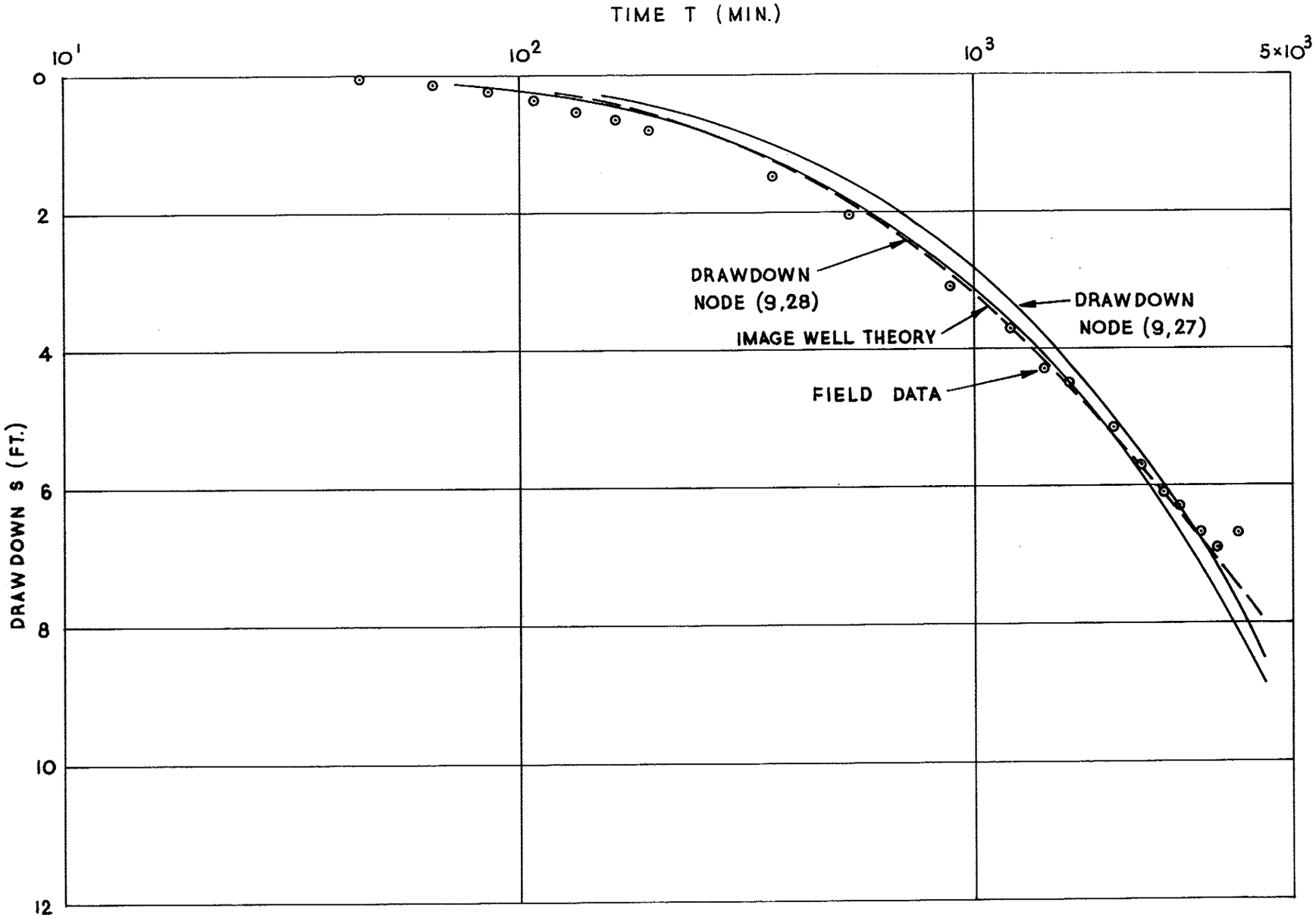

Fig. 2.17: Theoretical and Field Data Correlation for Observation Well 30031.

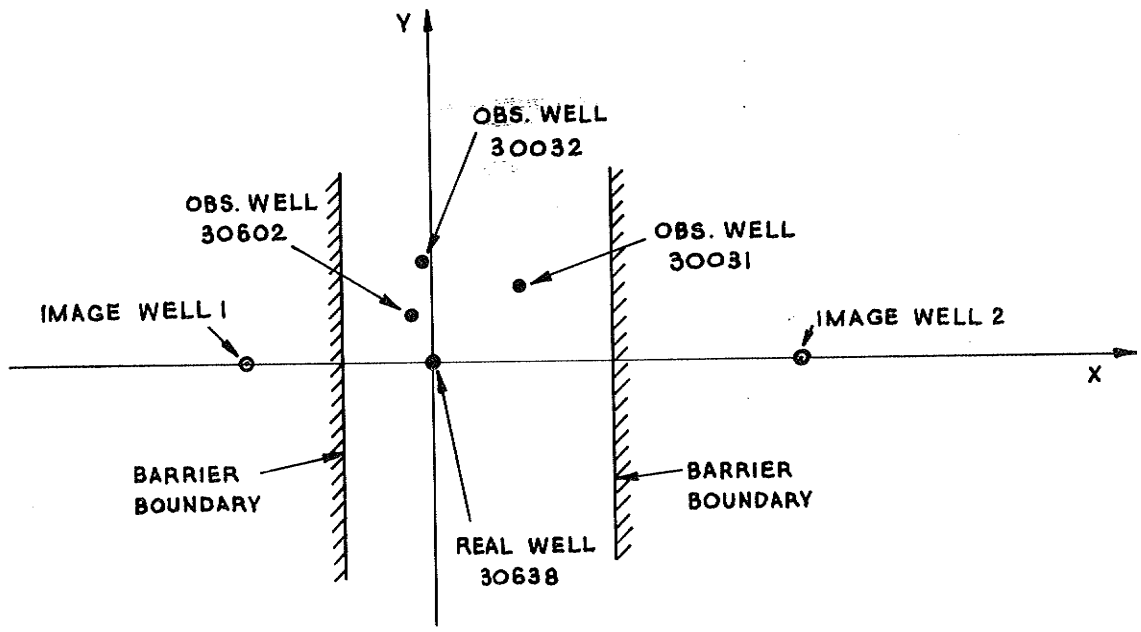

Scale - 1 inch = 5000 ft.

CO-ORDINATES

WELL	X	Y
30638	0	0
30031	2300	2000
30032	-200	2600
30602	-500	1300

IMAGE WELL	X	Y
1	-4800	0
2	9600	0

Fig. 2.18: Image System for Site A.

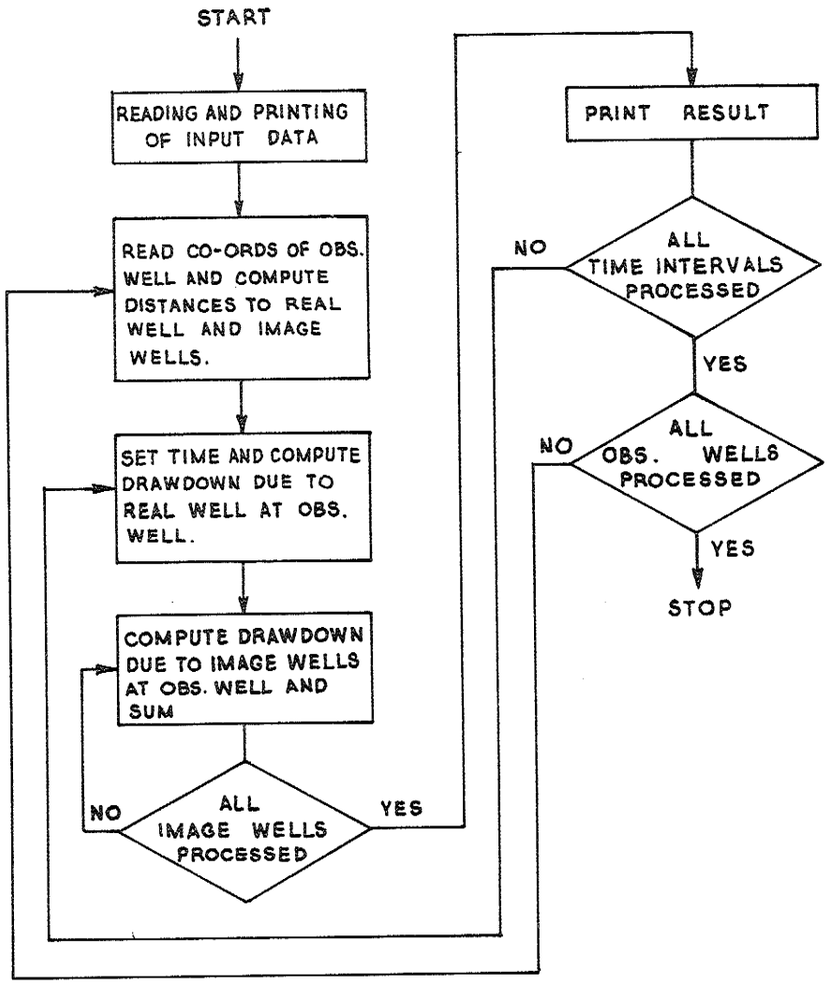

Fig. 2.19: Flow Chart Diagram of Image Well System Simulation Digital Computer Programme.

The method is based on the image well theory of Ferris et al (1962). A simple FORTRAN IV digital computer programme based on this theory was prepared and used on an IBM 360 system model 50 digital computer. A flow chart of the programme is presented in Fig. 2.19 and a listing of the programme in Appendix V.

Again the early time mean values of transmissivity T and storage coefficient S for observation wells 30602, 30031 and 30032 and the boundaries analysed were used as data.

Graphical comparison between the field data points and the image well simulation curves are presented in Figs. 2.15, 2.16 and 2.17.

2.3 Computer Method of Pumping Test Analysis

2.3.1 Introduction

The basic approach in investigating well flow by finite element technique, previously outlined in Section C, was adopted. A mathematical model for the existing well-aquifer system was first developed, and a finite element model was constructed to simulate the actual flow behaviour of the system. Type curves representing the general flow behaviour were produced and matched against the actual field data to obtain approximate values of the hydraulic coefficients for the aquifer and the overlying aquitard. The computed coefficients were then fed into the model to predict the actual response to pumping of the field system, and the predicted behaviour compared to the measured response. Adjustments were made to the values of the hydraulic coefficients until satisfactory agreement between the predicted and measured responses was obtained.

2.3.2 Mathematical Formulation of Flow Problem

A sketch of the mathematical model for the Wagga Wagga aquifer system is as shown in Fig. 2.20. The following assumptions were made:-

(i) The aquifer and the aquitard are of infinite radial extent and of constant thicknesses.

(ii) Both the aquifer and the aquitard are homogeneous and isotropic. The flow is considered radial in the aquifer and vertically downward in the aquitard.

(iii) The pumped well is fully screened through the entire thickness of the main aquifer, and pumping occurs at a constant rate.

(iv) Non-Darcy flow and resulting non-Darcy and screen losses are negligible. (The losses actually measured were very small as the pumping rate of 48,000 igph was not sufficiently great to induce non-Darcy flow around the 16 inch screen well with 4 inch thick gravel pack).

(v) The top of the overlying aquitard is impermeable and hence no flow across it is permitted.

Following these assumptions, the equations describing flow in the system and the corresponding initial and boundary conditions are as follows:-

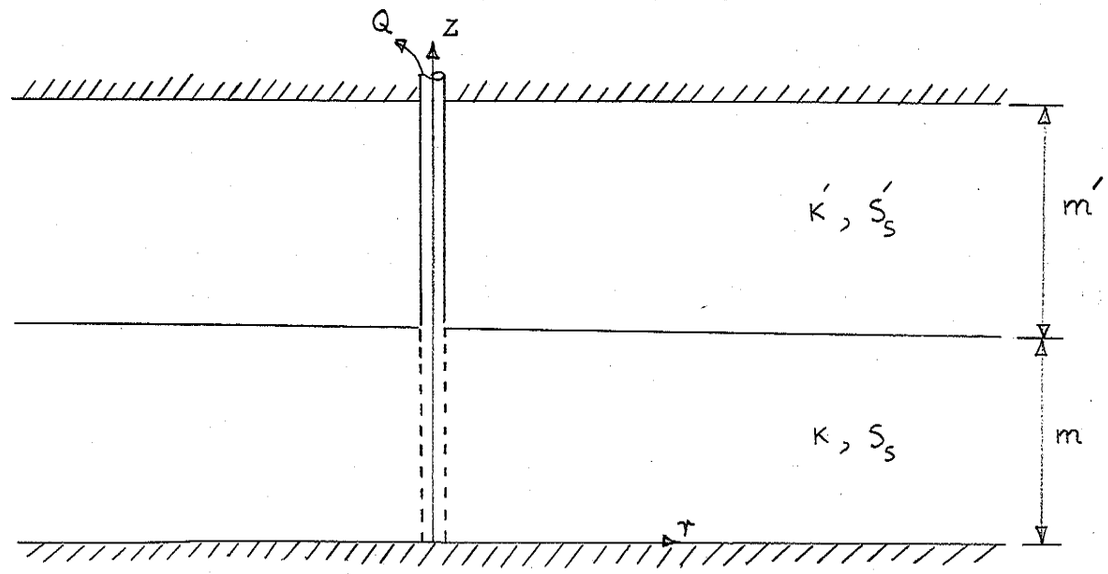

Fig. 2.20 and Mathematical Model of the Wagga Wagga Well-Aquifer System.

Let s and s' denote drawdowns in the aquifer and the aquitard respectively. The equation for drawdown in the main aquifer is:

$$K\left(\frac{\partial^2 s}{\partial r^2} + \frac{1}{r}\frac{\partial s}{\partial r}\right) + \frac{K'}{m}\frac{\partial s'}{\partial z}\,(r,m,t) = S_s\frac{\partial s}{\partial t} \qquad (2.5a)$$

The corresponding initial and boundary conditions are given by -

$$s(r, 0) = 0 \qquad (2.5b)$$

$$s(\infty, t) = 0 \qquad (2.5c)$$

$$\frac{\partial s}{\partial r}(r_w, t) = \frac{-Q}{2\pi K m r_w} \qquad (2.5d)$$

The equation for drawdown in the aquitard takes the form

$$K' \frac{\partial^2 s'}{\partial z^2} = S_s' \frac{\partial s'}{\partial t} \qquad (2.6a)$$

With the following initial and boundary conditions

$$s'(r, z, 0) = 0 \qquad (2.6b)$$

$$s'(r, m, t) = s(r, m, t) \qquad (2.6c)$$

$$\frac{\partial s'}{\partial z}(r, m + m', t) = 0 \qquad (2.6d)$$

where

K, S_s, m and K', S_s', m' are the coefficients of hydraulic conductivity, specific storage and thickness of the aquifer and the aquitard respectively.

Asymptotic solutions of short and long time drawdowns in the aquifer were first obtained by Hantush (1964). They may be written in the following forms:-

(i) Short time solution $t \leqslant \frac{S_s' m'^2}{10K'}$

$$W(u, \beta) = \int_u^\infty \frac{e^{-y}}{y} \operatorname{erfc}\left[\frac{\beta\sqrt{u}}{\sqrt{y(y-u)}}\right] dy \qquad (2.7a)$$

where

$$\beta = \frac{r}{4m}\sqrt{\frac{K'S_s'}{K S_s}} \; ; \quad u = \frac{r^2 S_s}{4Kt} \qquad (2.7b)$$

(ii) Long time solution, $t \geqslant$ both $\frac{2m'^2 S_s'}{K'}$ and $30\, \delta_2\, r_w^2\, \frac{S_s}{K}$

$$s = \frac{Q}{4\pi Km} \int_{\delta_2 u}^\infty \frac{e^{-u}}{u} du \qquad (2.8a)$$

where $\delta_2 = 1 + \frac{S_s' m'}{S_s m}$ (2.8b)

A short time solution of drawdown in the aquitard was first obtained by Neuman and Witherspoon (1969), and may be written as

$$s' = \frac{Q}{4\pi K m} W(u, \beta, \bar{t}_{D1}, z'/m') \quad (2.9a)$$

where

$$W = \int_u^\infty \frac{e^{-y}}{y} \left\{ \operatorname{erfc}\left[\frac{\beta\sqrt{u} + y(z'/m')/\sqrt{4\bar{t}_{D1}}}{\sqrt{y(y-u)}} \right] - \operatorname{erfc}\left[\frac{\beta\sqrt{u} + y(2 - z'/m')/\sqrt{4\bar{t}_{D1}}}{\sqrt{y(y-u)}} \right] \right\} dy \quad (2.9b)$$

$$z'/m' = (z-m)/m' \quad (2.9c)$$

$$\bar{t}_{D1} = \frac{K't}{S_s' m'^2} \quad (2.9d)$$

The above asymptotic solutions are readily evaluated numerically. Computer subroutines for their evaluation were written so that they may be used to check the finite element results. The short time solutions were also used as starting values for the finite element programme to compute approximate solutions at later times.

2.3.3 Design and Construction of Finite Element Model

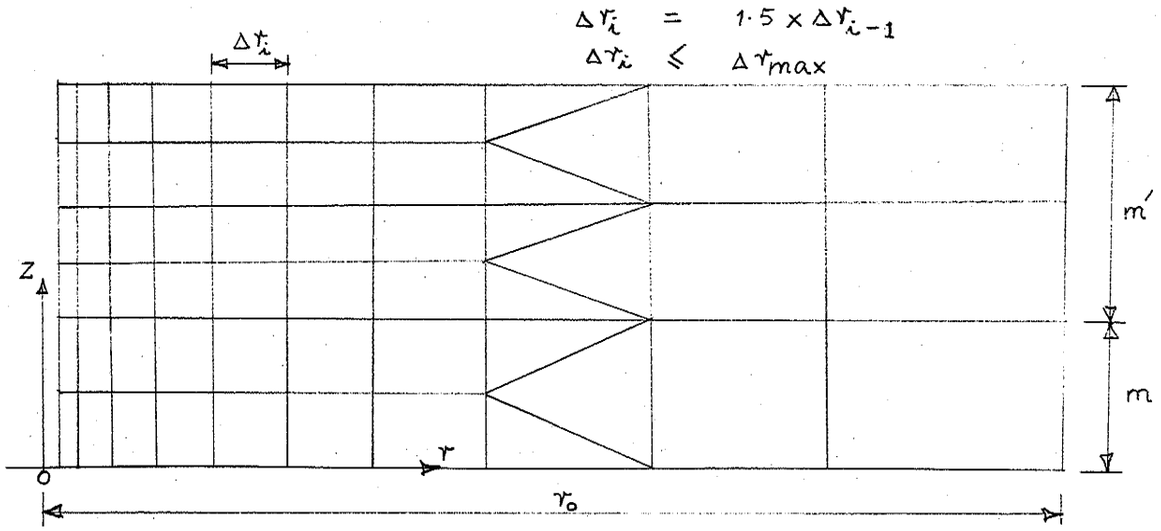

Fig. 2.21: Typical two-dimensional finite element network.

Designing a finite element model involves selection of the type of network and elements in the network. A more elaborate network usually means a greater degree of accuracy but an increase in computational time. Thus, in making a proper choice, one needs to balance the required accuracy with computational cost.

A two-dimensional finite element model for a general multi-layered well-aquifer system was constructed. A typical network representing a radial cross-section through the three-dimensional axisymmetric region of a two-layered system is shown in Fig. 2.21. The network is automatically generated by the computer programme. Rectangular ring elements are employed in each subregion of each layer whilst triangular ring elements are used in the transition zone connecting the two adjacent subregions. The sizes of elements are graded uniformly with radial distance from the pump well. To cover a reasonably large value of the external radius r_o,(approximately 5000 to 10,000 ft.), the horizontal width of the elements in a vertical block is made 1.5 times the width of those in the previous block ($\Delta r_i = 1.5 \Delta r_{i-1}$) until a maximum width Δr_{max} is exceeded. As flow in the aquitard region is associated with steep vertical hydraulic gradients, the region is split up into a larger number of elements, particularly in the zone in close proximity to the pumped well.

2.3.4 Calibration of Finite Element Model

Finite element model calibration involves comparison of the model results with known analytical solutions or other kinds of solution obtained for the same flow cases. From the comparisons, assessment of the accuracy of the model solution may be made, and a minimum number of nodes in the network determined to achieve a certain required accuracy.

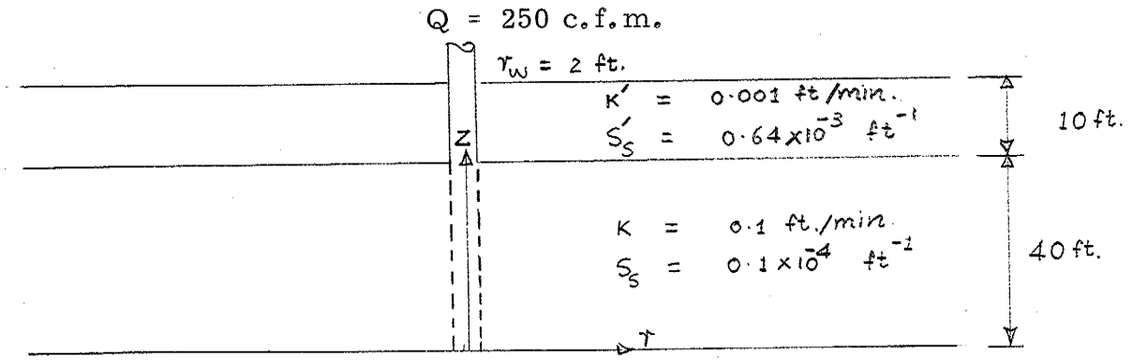

Fig. 2.22: Flow System for Test Problem

A typical flow problem was formulated for the purpose of model calibration. The problem data are given in Fig. 2.22. Two combinations of mesh pattern and time discretisation were used, as shown in Fig. 2.23, to allow the study of convergence and stability of the finite element solutions. For the first combination, a coarser mesh and time steps were used. The mesh and time steps were later refined to obtain better accuracy.

Fig. 2.24 shows dimensionless logarithmic plot of drawdown vs time for various nodes located in the aquifer whilst the plot in Fig. 2.25 represents general drawdown-time relationship for different nodes in the aquitard, all located at the same radius from the pumped well. It is seen that the finite element results check quite closely with the analytical solutions. Some deviation from the analytical curves are present along the steep portions of the curves. The deviation becomes much smaller when the second combination of refined mesh and time steps is used.

For the coarser mesh, a study aimed at finding out whether the use of rectangular ring elements is beneficial was also performed. The results show that for the same number of nodes a combination of rectangular and triangular elements gives more accurate results than triangular elements alone. This is to be expected since constant hydraulic gradient is assumed within each triangle.

2.3.5 Behaviour of Well-Aquifer System

The general behaviour of transient flow towards a pumped well in multi-layered aquifers is best described in terms of dimensionless relationships between drawdown in the system and time. For a two layered confined aquifer-aquitard system, the general drawdown-time relations may be written in the following forms:-

For the main aquifer

$$\frac{4\pi TS}{Q} = W(u, \beta, r/B) \qquad (2.12a)$$

and for the aquitard

$$\frac{4\pi TS'}{Q} = W(u, \beta, r/B, z'/m') \qquad (2.12b)$$

where

W = generalised well function

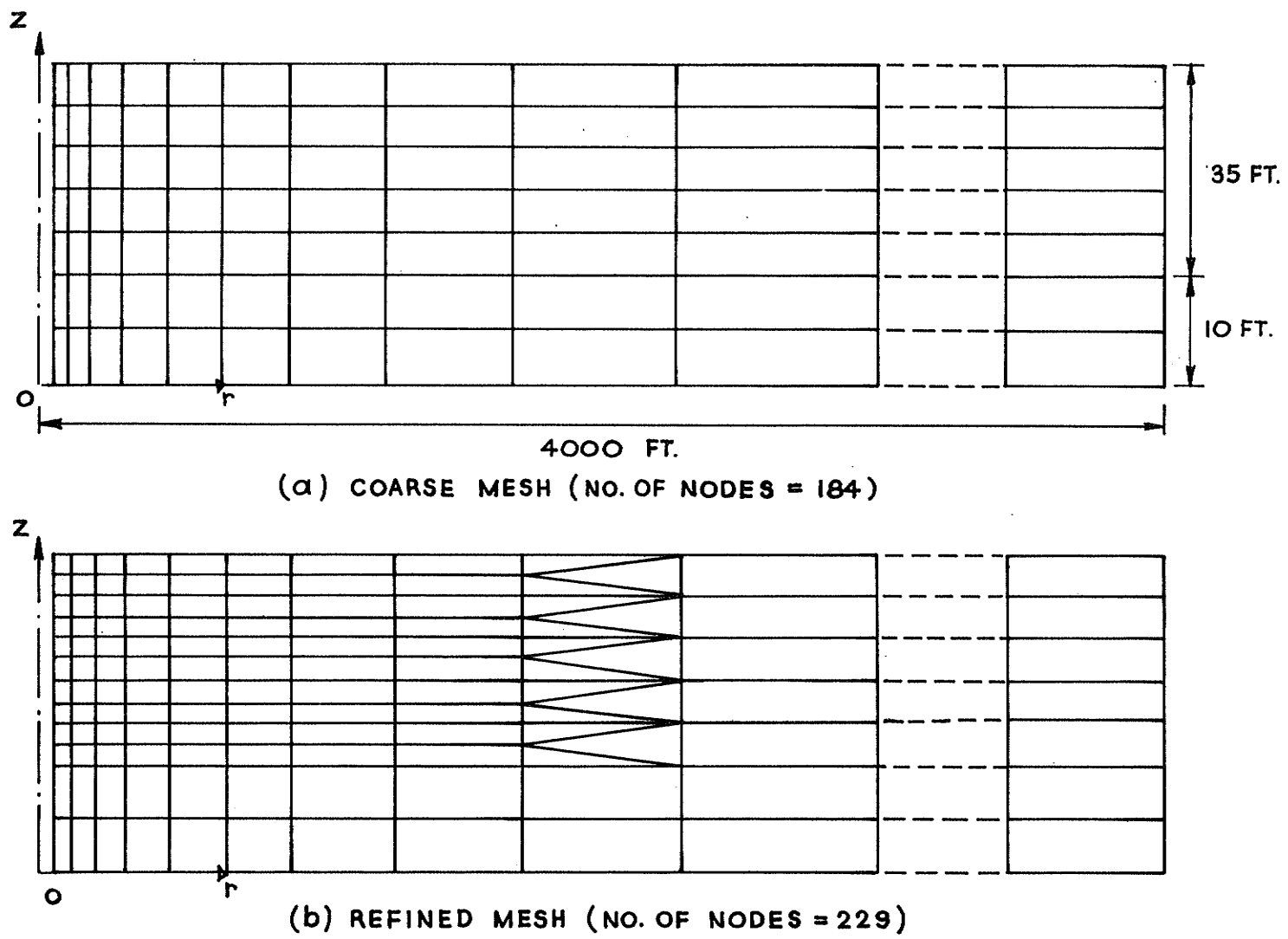

Fig. 2.23· Coarse and Refined Meshes adopted for Test Problem.

$$u = \frac{r^2 S_s}{4Kt}$$

$$\beta = \frac{r}{4m}\sqrt{\frac{K' S_s'}{K S_s}}$$

$$\frac{r}{B} = r\sqrt{\frac{K'}{Kmm'}}$$

T = transmissivity of the aquifer = Km

$z'/m' = (z-m)/m'$

Q = well discharge

s , s' = drawdowns in the aquifer and aquitard respectively

$\beta/(r/B) = \frac{1}{4}\sqrt{S_s' m'/S_s m}$

β and $\frac{r}{B}$ may be referred to as dimensionless storage and leakage factors for the flow system respectively.

Equations (2.12a) and (2.12b) may be represented by type curves of 1/u versus W (u) for various values of β , $\frac{r}{B}$ and z'/m'

To obtain families of such curves for a practical period of pumping time, several flow problems were formulated and solved by employing the previously calibrated finite element model. To save computer time, a value of initial time $t_o = \frac{S_s' m'^2}{10K'}$, was used for all problems. The initial nodal drawdowns in the system were computed from equations (2.7) and (2.9) respectively. Knowing the initial drawdowns, the drawdowns at the end of the first and subsequent time steps could be computed by the programme. Due to good stability characteristics of the solution scheme previously described in Section B, large time steps could be used. The time steps were graded uniformly such that the next time step was approximately 1.4 to 2.0 times the current time step ($\Delta t_{i+1} = f \times \Delta t_i$, f = 1.4 to 2). Approximately 25 time steps were required to cover 6 to 7 log cycles of the type curve plot. For each flow problem solved, the ratio $\beta/(\frac{r}{B})$ is constant for all the type curves so obtained. Typical results are shown in Figs. (2.24) to (2.29). It is seen that each type curve consists of a steep portion for early times when the response to pumping is rapid, and a flatter portion for later times when the response becomes much slower.

The curves in Figs. 2.25 to 2.27 correspond to the points in the system situated at the same radius from the pumped well but at different heights above the top of the main aquifer. As indicated, the type curves are vertically and horizontally spread in each figure. The vertical spread represents the vertical hydraulic gradient at different points in the aquitard at a certain radius from the pumped well whilst the horizontal spread provides a direct measure of time lag in the drawdown between these points. It is noted that the spread between the type curves decreases as the magnitudes of β and $\frac{r}{B}$ increase, for constant $\beta/(\frac{r}{B})$, and that when the ratio $\beta/(\frac{r}{B})$ increases the spread also increases. This fact was used to great advantage in matching the field data against the computed type curves.

It can also be seen that the curves in Fig. 2.26 and 2.27 all merge into one curve at a certain time when there is negligible vertical leakage from the aquitard into the top of the aquifer; for a radial distance $r \gg m + m'$ where the partial penetration effect is negligible.

Figs. 2.34 and 2.33 show the family of type curves of drawdown versus time for various points in the aquifer located at different radii from the pumped well. In each figure, the early and late time Theis curves are also shown. The late time Theis curve was constructed by using Equation 2.8 whilst the early time curve was constructed in the usual manner. It can be seen that the horizontal spacing between the two Theis curves is directly proportional to the ratio $\beta/(\frac{r}{B}) = \frac{1}{4}\sqrt{S_s' m'/S_s m}$ and that all type curves for the main aquifer approach and coincide with it for $t \geqslant \frac{2m'^2 S_s'}{K'}$. This fact suggests that the conventional method of matching the long time field data obtained from a distance observation well against the classical Theis curve should give an accurate estimate of the transmissivity coefficient for the aquifer but a gross over-estimate of its coefficient of storage.

2.3.6 Evaluation of Hydraulic Properties of Aquifer and Aquitard

A preliminary estimate of the gross hydraulic properties of the main aquifer was made by applying conventional methods of pumping test analysis, which neglect vertical leakage from the overlying aquitard to the top of the aquifer.

To determine more accurately the values of the hydraulic coefficients of the aquifer material local to the pumped well and the hydraulic properties of the aquitard, the following procedures were adopted.

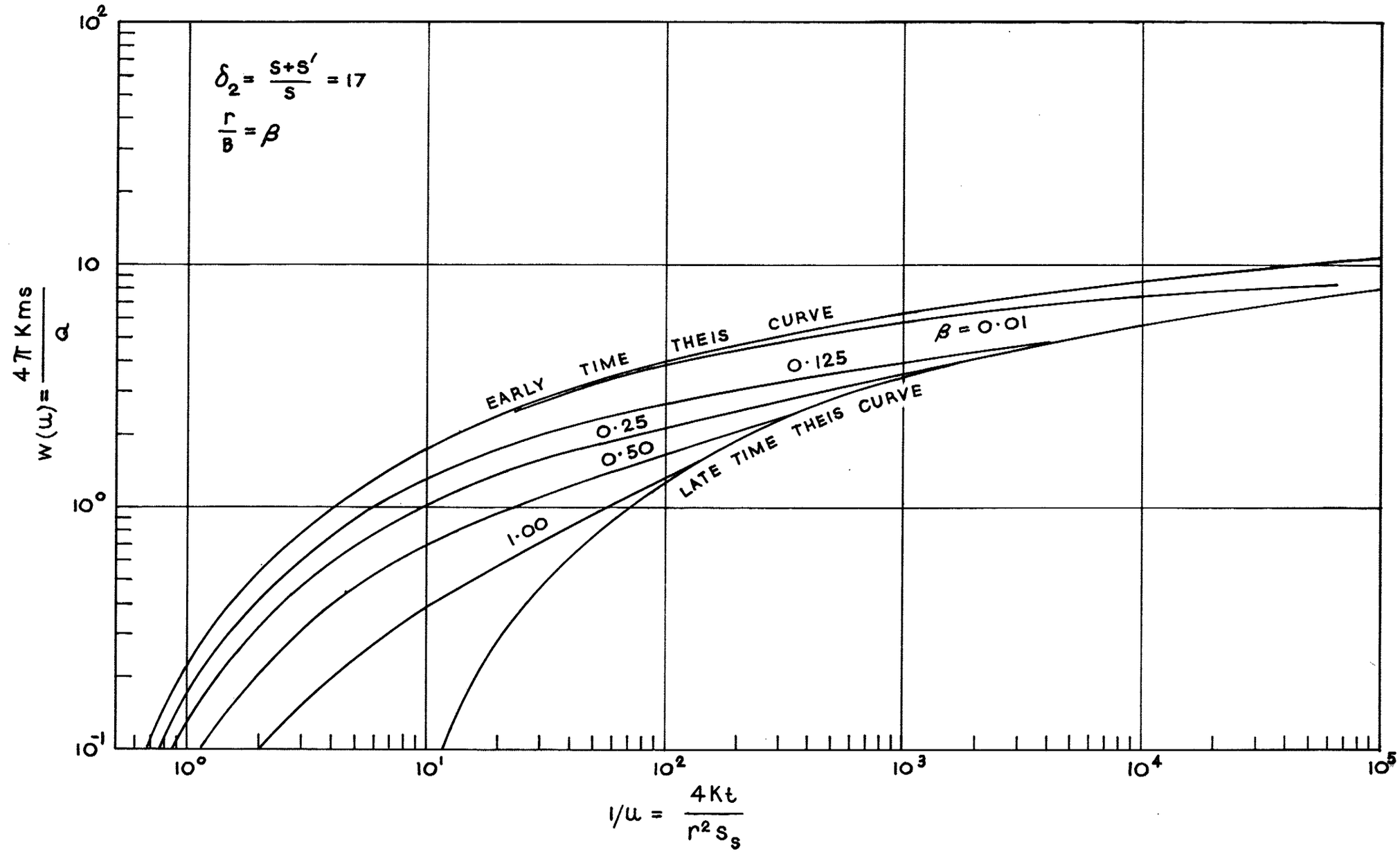

Fig. 2.24: Type curves for the main aquifer of a confined aquifer-aquitard system.

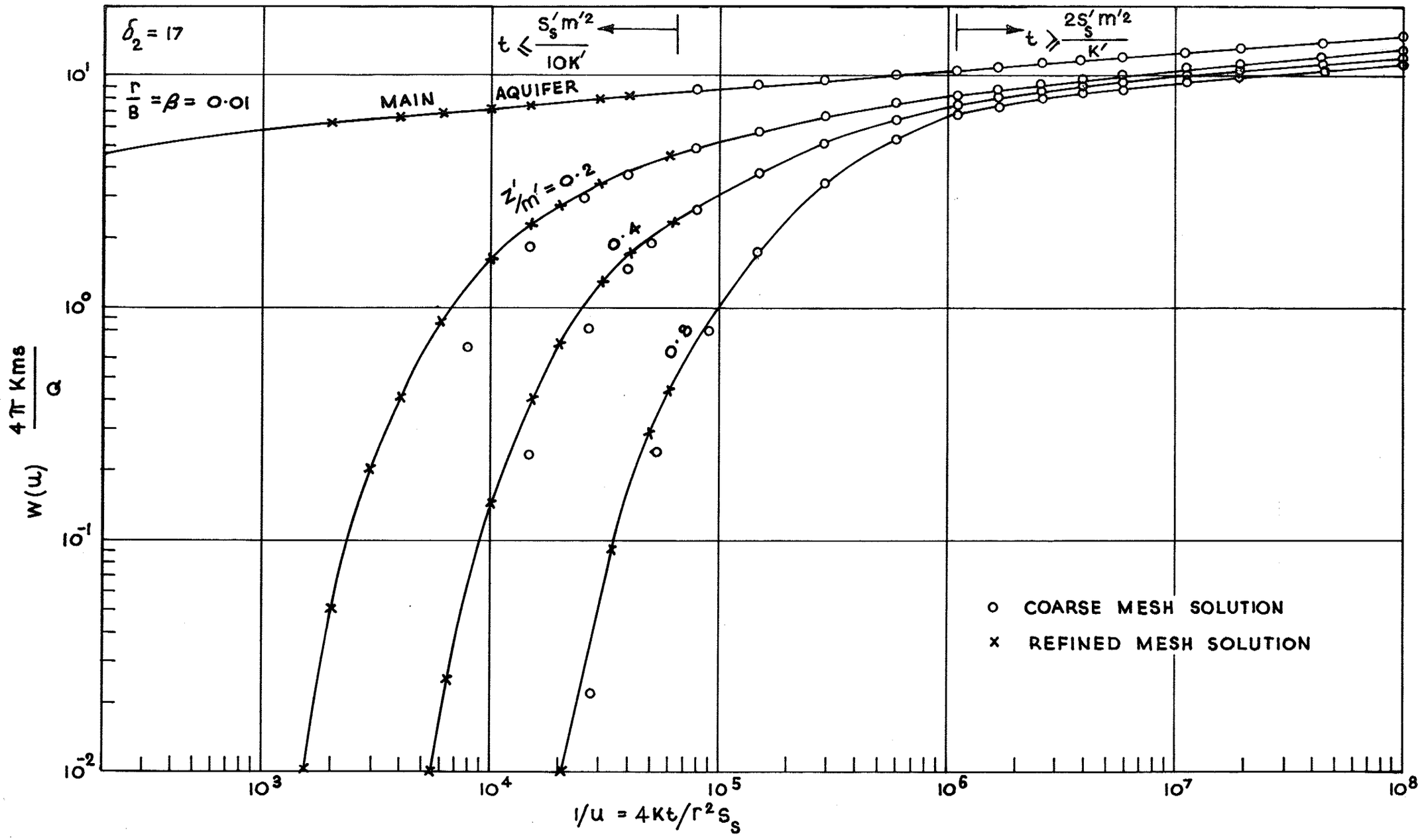

Fig. 2.25: Type curves for the overlying aquitard of a confined aquifer-aquitard system, showing convergence of the finite element solutions.

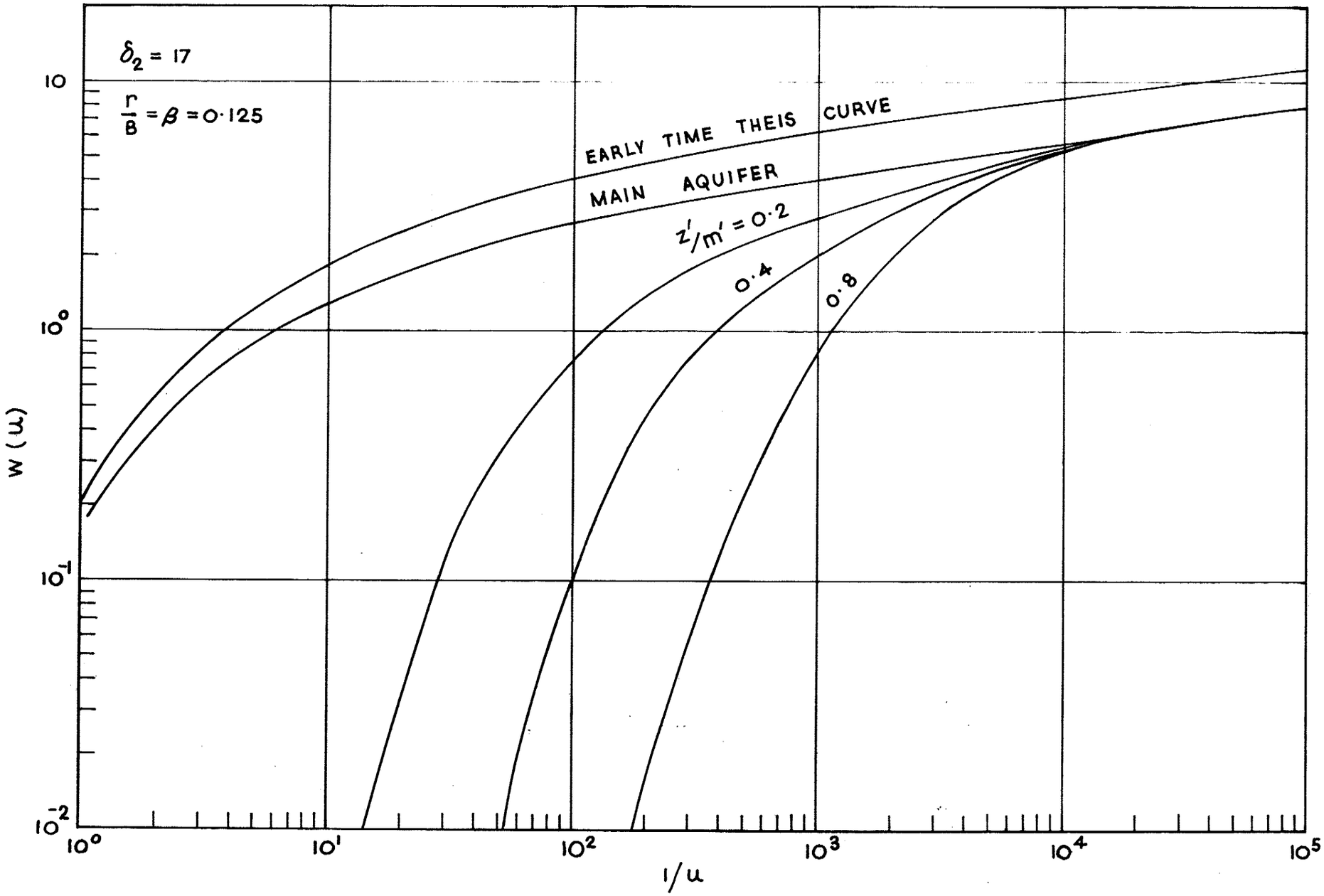

Fig. 2.26: Type curves for the overlying aquitard of a confined aquifer-aquitard system.

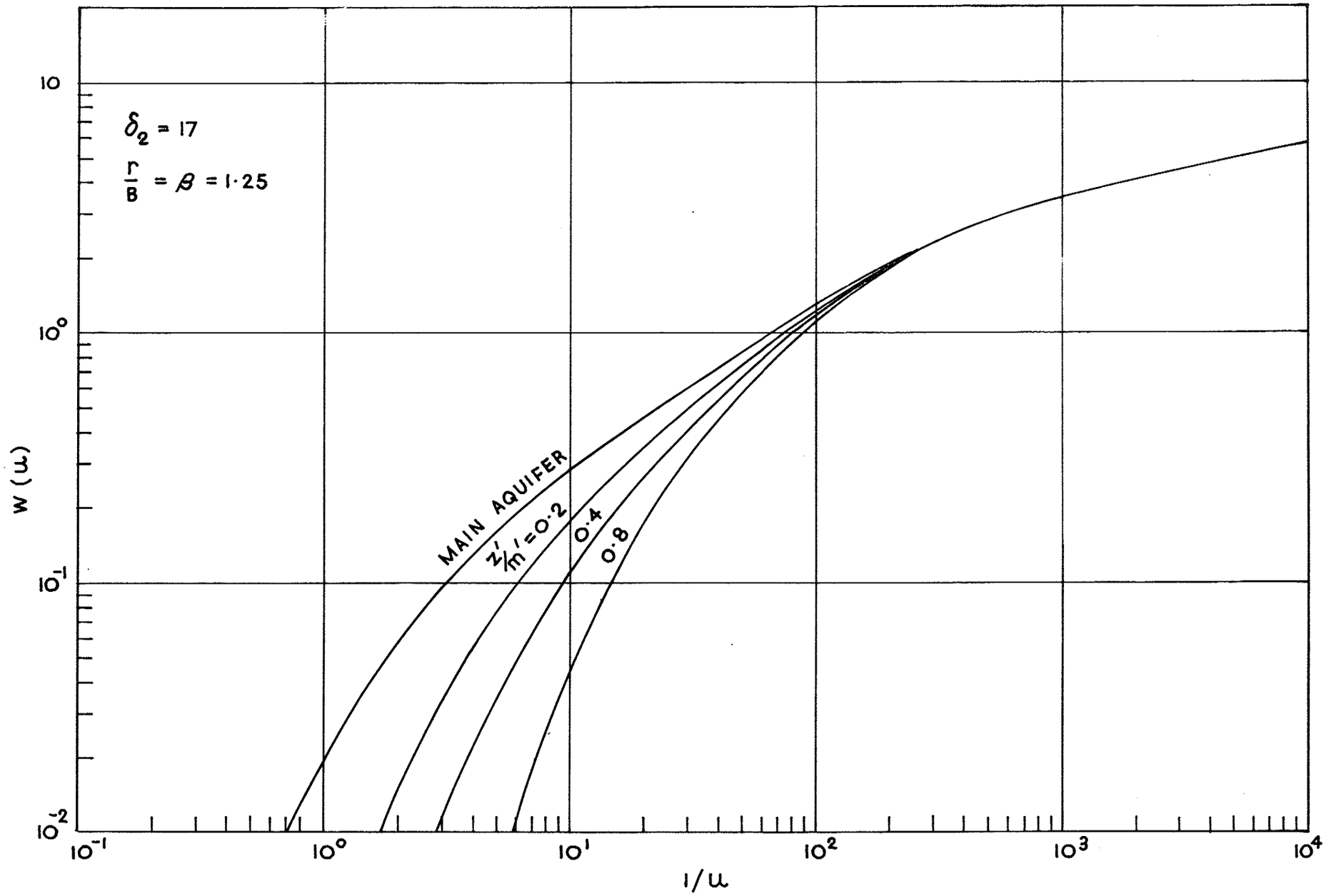

Fig. 2.27: Type curves for the overlying aquitard of a confined aquifer-aquitard system.

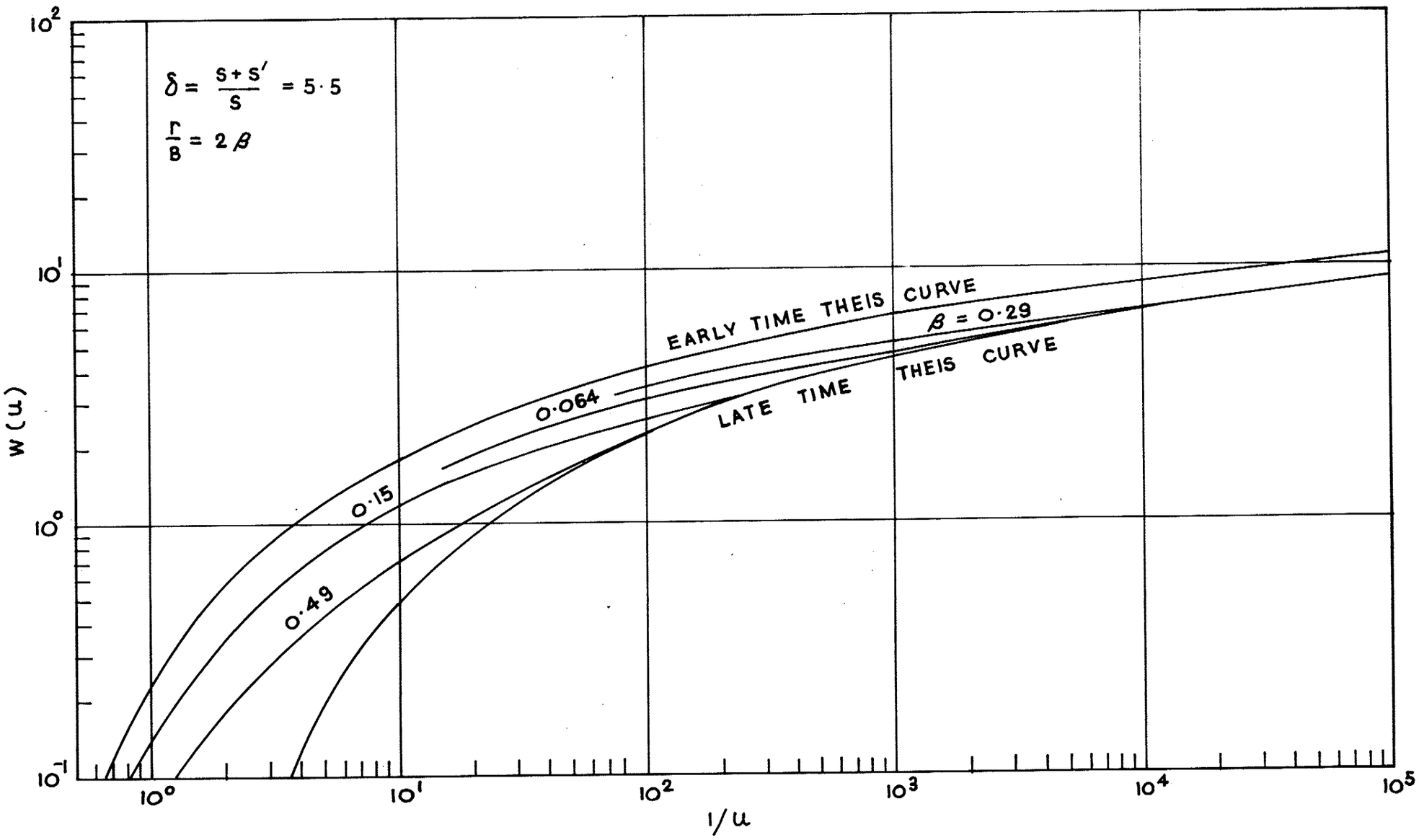

Fig. 2.28: Type curves for the main aquifer of a confined aquifer-aquitard system.

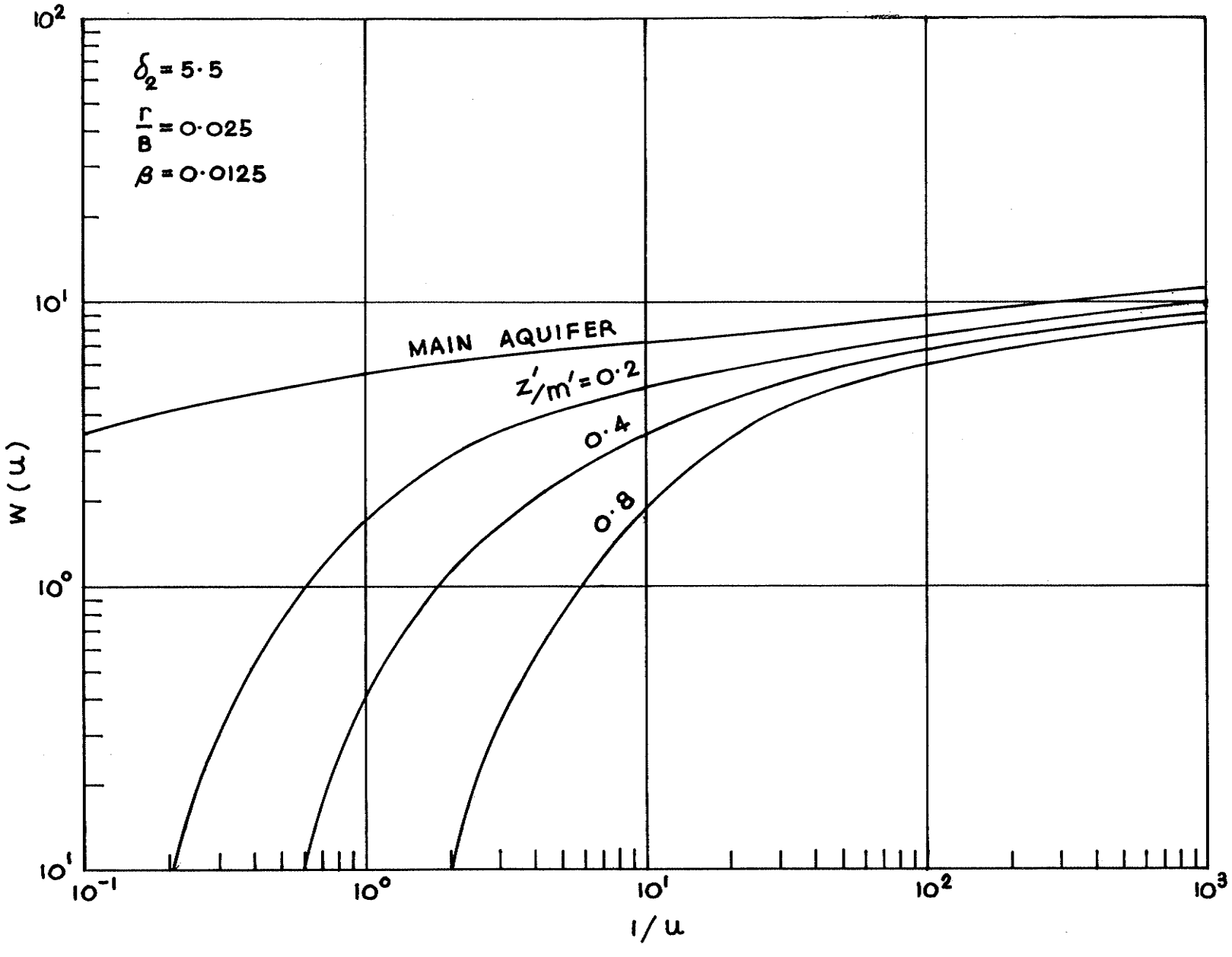

Fig. 2.29: Type curves for the overlying aquitard of a confined aquifer-aquitard system.

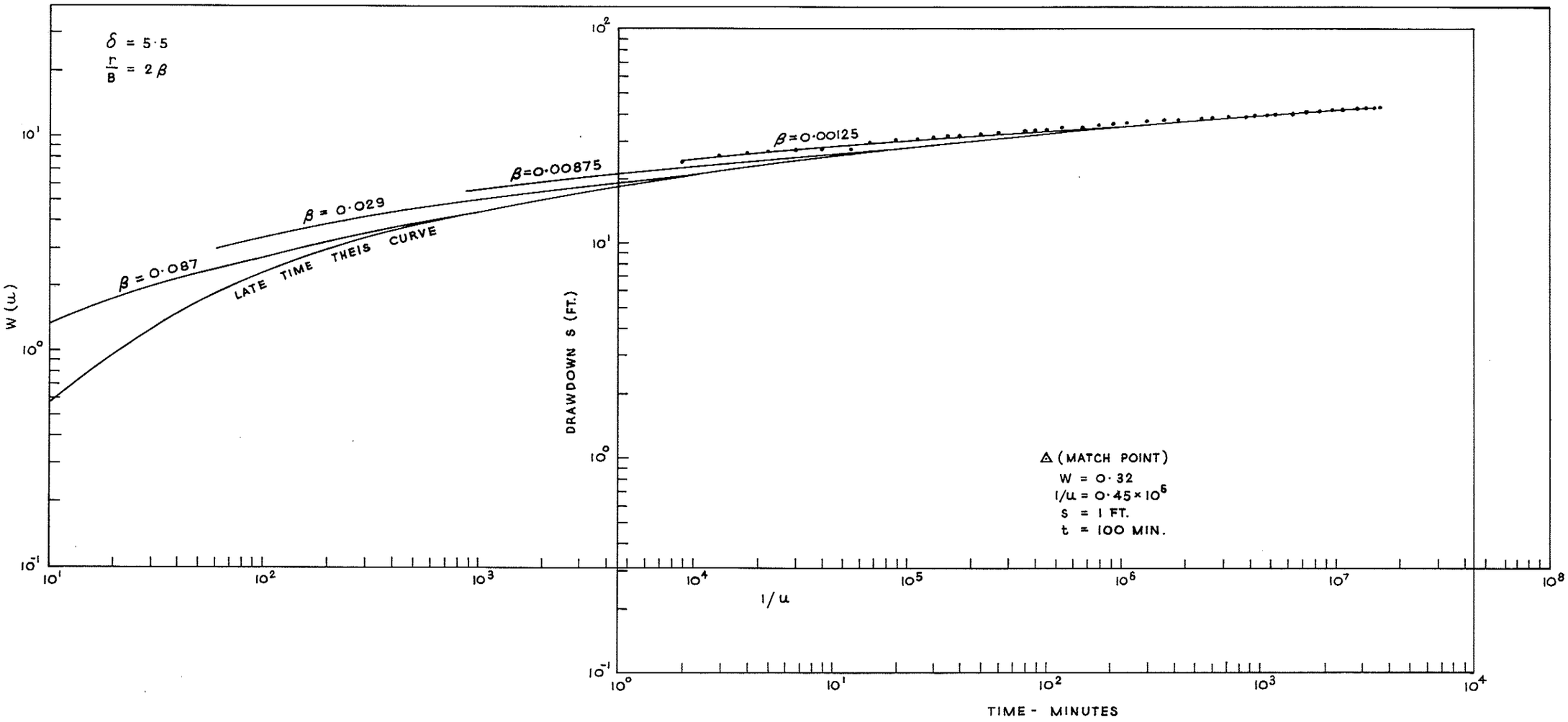

Fig. 2.30: Matching of Field Data on Type Curves for Main Aquifer.

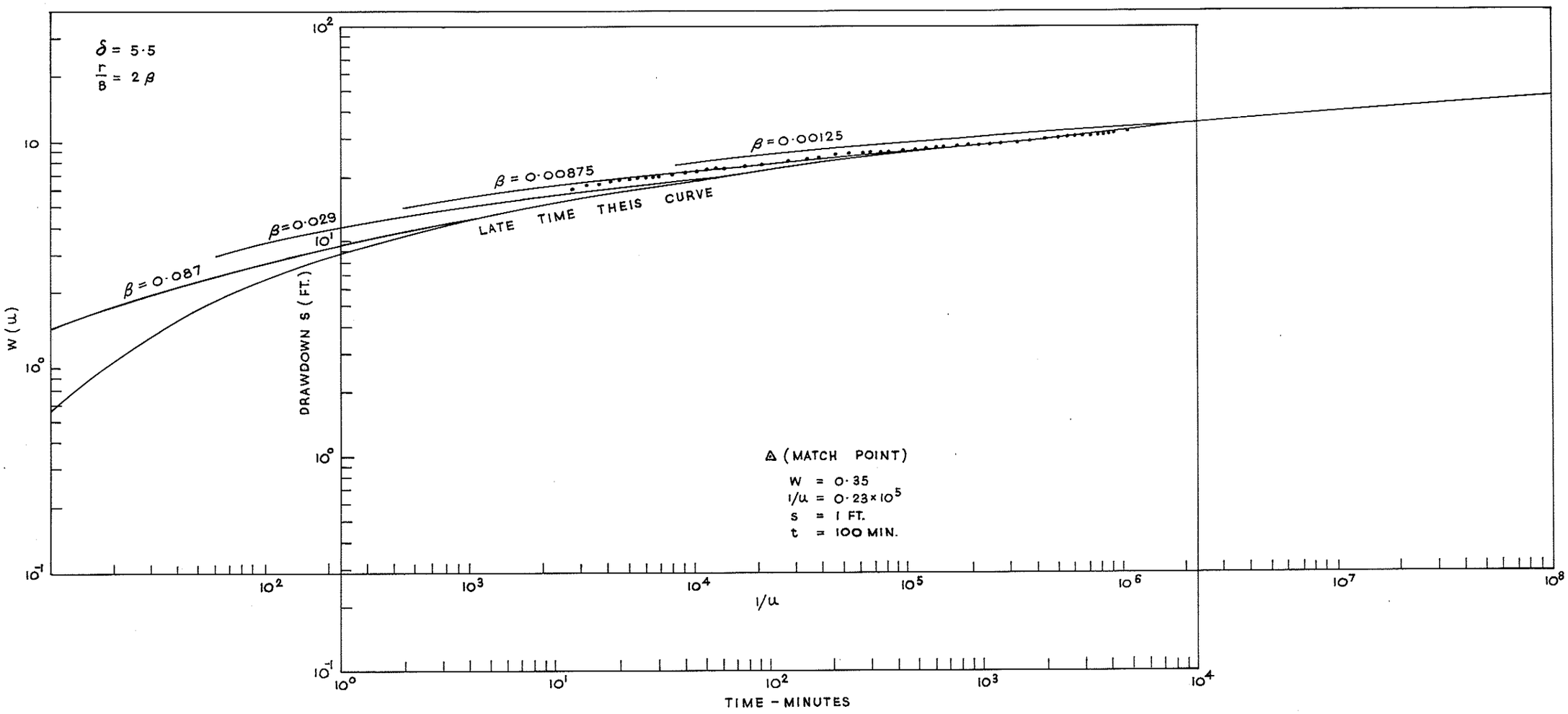

Fig. 2.31: Matching of Field Data on Type Curves for Main Aquifer.

(i) The drawdown-time data collected from pumped well 30638, and observation wells 30577 and 30538 were converted to a log-log plot of s versus t on a piece of transparent paper for observation points in the main aquifer inside and close to the pumped well (r = 1,8 ft.). The plot was then matched on a selected family of dimensionless drawdown-time curves for the main aquifer as shown in Figs. 2.30 and 2.31. Matching was performed by shifting the field data over the type curve plot while maintaining their axes parallel and ensuring the late time portion of the field data fell on the late time Theis curve. Satisfactory matching was found when the remaining portion of the field data coincide with the corresponding type curve branching from the late time Theis curve. The final match is shown in Fig. 2.33. The values of the dimensionless parameters for the matched family of curves β and $\frac{r}{B}$ were determined.

(ii) Time-drawdown data for all derivation points in well 30577 (at $z'/m' = 0,\ 0.25$ and 0.75) were plotted on another piece of transparent paper. Using the values of β and $\frac{r}{B}$ obtained from (i), the type curves for $z'/m' = 0,\ 0.25$ and 0.75 were constructed and matched on the field data plot. Minor adjustments of the values of β and $\frac{r}{B}$ were found necessary to obtain a satisfactory match. The final match and values of β and $\frac{r}{B}$ are shown in Fig. 2.32. A match point was selected to determine the hydraulic coefficients K, S_s and K', S'_s for the aquifer and aquitard respectively. The calculation is presented as follows:-

Let $(W, 1/u)$ and (s, t) be the coordinates of the match point.

The coefficients of hydraulic conductivity and specific storage of the main aquifer are given by

$$K = \frac{QW}{4\pi s m} \qquad (2.13a)$$

and

$$S_s = \frac{4Ktu}{r^2} \qquad (2.13b)$$

where $W(u) = 0.40$; $\frac{1}{u} = 0.115 \times 10^6$

$s = 1$ ft; $t = 200$ min.

$r = 7$ ft; $Q = 128$ c.f.m.

Hence

$K = 0.103$ ft/min

$S_s = 0.72 \times 10^{-5}$ ft.$^{-1}$

Let β and $\frac{r}{B}$ be the values of the dimensionless storage and leakage factors for the selected family of type curves. The hydraulic coefficients of the aquitard are obtained from

$$K' = \frac{(\frac{r}{B})^2 \; K \; mm'}{r^2} \qquad (2.10a)$$

and

$$S_s' = \frac{16\beta^2 \; m^2 \; K \; S_s}{K' \; r^2} \qquad (2.10b)$$

where

$\frac{r}{B} = .018$; $\beta = .008$

$m' = 45$ ft; $r = 7$ ft.

$K = 0.103$ ft/min; $S_s = 0.72 \times 10^{-5}$ ft^{-1}

Hence

$K' = .0012$ ft/min

$S_s' = 0.29 \times 10^{-4}$ ft.$^{-1}$

(iii) The values of K, S_s, K' and S_s' calculated in (ii) and the actual data of the field system were fed into the finite element model, and the flow problem was solved for Q = 128 cfm and pumping period t = 4320 min. The calculated drawdown versus time relationships at selected nodes in the aquifer were finally compared with the field data plot for the corresponding points in the field system. Fig. 2.38 shows such a comparison. It is seen that there is good agreement between the predicted and the actual behaviour of the field system.

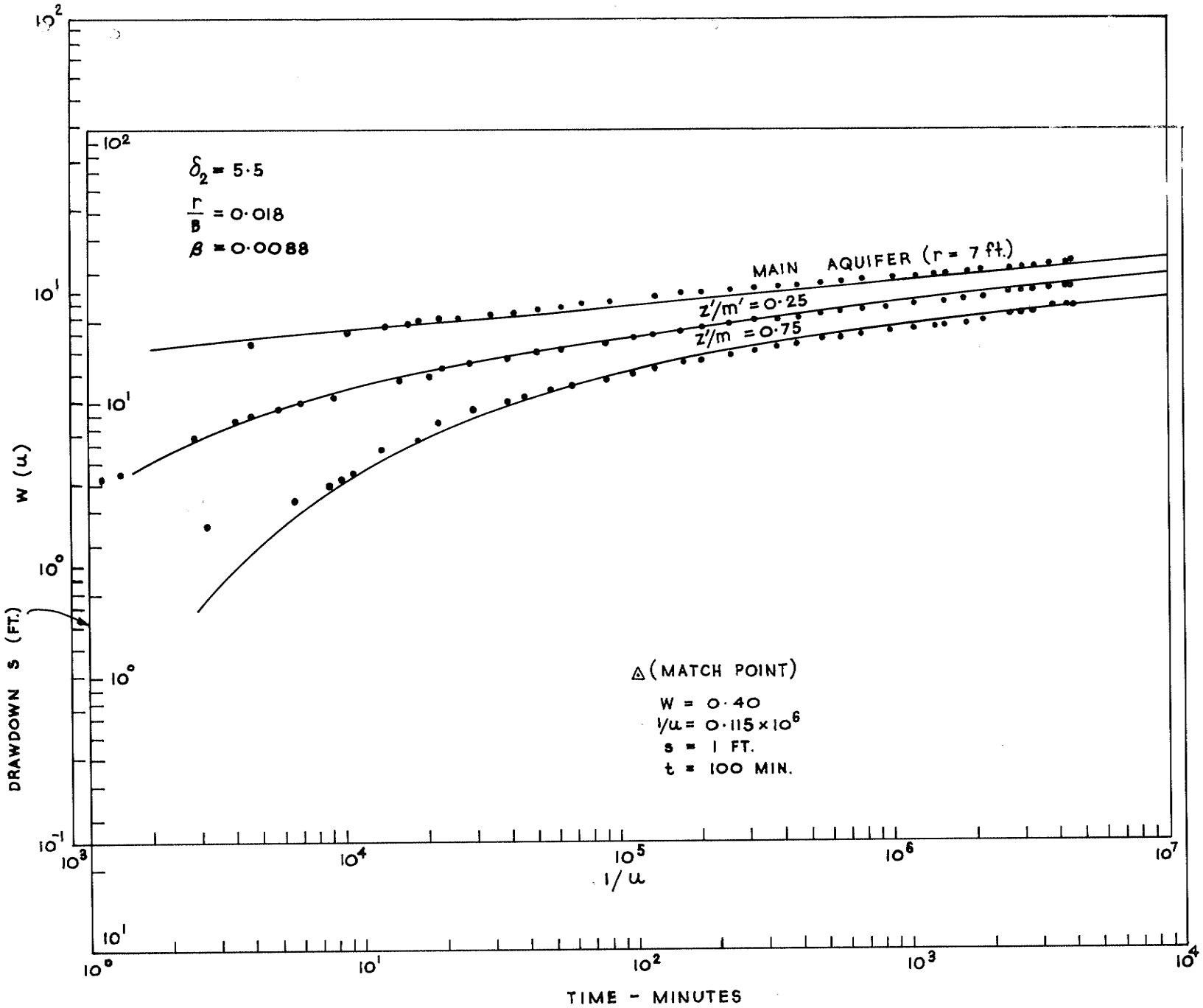

Fig. 2.32: Matching of Field Data on Type Curves for Aquifer-Aquitard System.

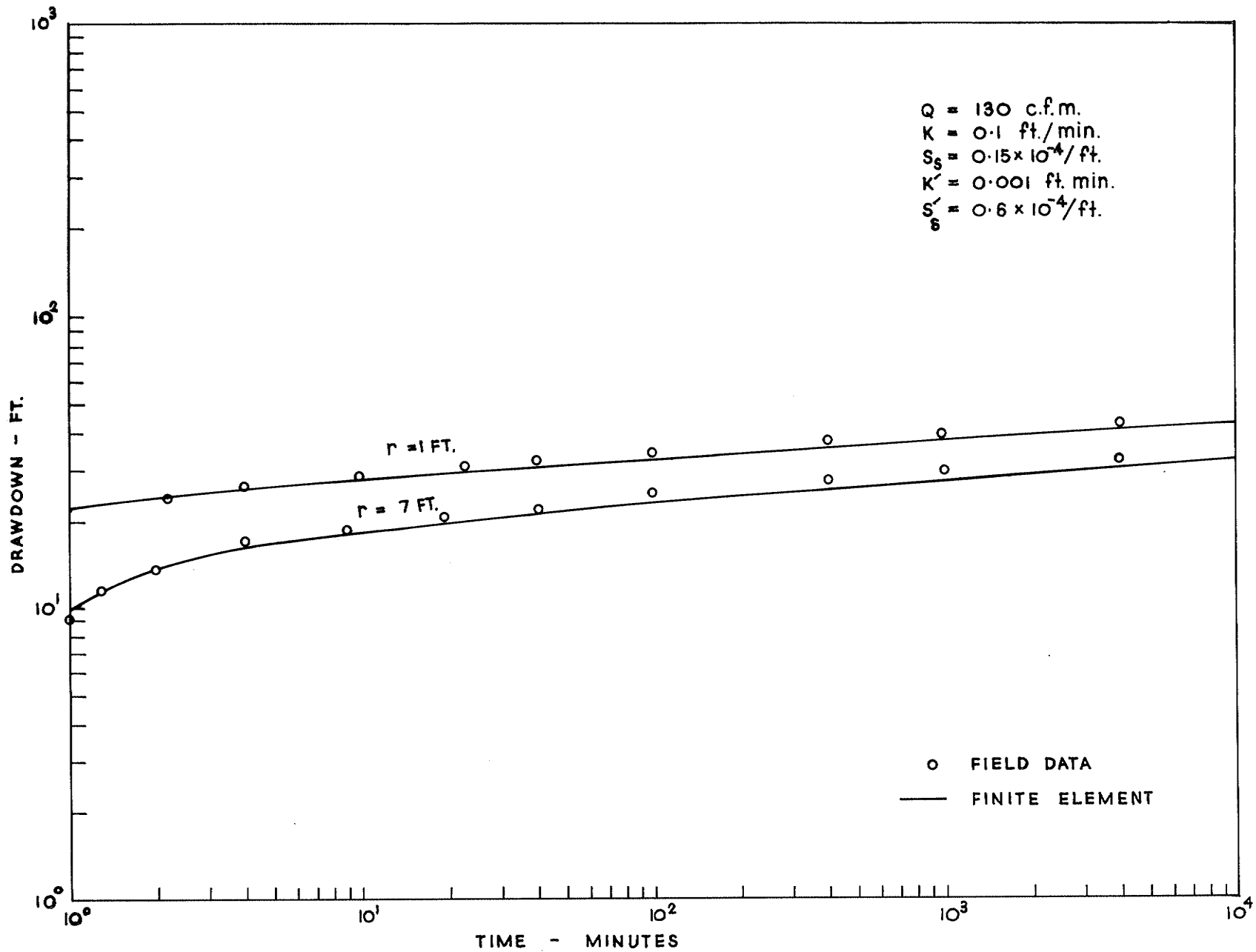

Fig. 2.33: Comparison of Field Data from Main Aquifer with Finite Element Model Results.

3. Site B - Rosevale, South East Queensland

3.1 General

The programme of aquifer tests at this site was performed in co-operation with the Irrigation and Water Supply Commission, Queensland, at a location close to the Bremer River, approximately 1 mile east of Rosevale (Fig. 3.1).

The testing programme conducted was designed in such a manner that the information obtained from preliminary tests on each of two closely spaced trial holes and in-situ two well tests on the pair of holes could be used to predict the performance of a larger production well at the same site. Consequently the testing programme can be considered to be comprised of three stages, namely:-

(i) Preliminary tests
(ii) In-situ two well tests
(iii) Production well verification tests

3.1.1 Preliminary Tests

The group of trial wells and observation wells used for the preliminary tests is as illustrated in Fig. 3.2. The construction features and available drillers logs at the test site are presented in Fig. 3.3. Wells 1, 1A, 2, 3, 4 and 5 were drilled using a percussion drilling rig, with continuous sampling performed on wells 2 and 3. Collected samples were sealed with paraffin wax in metal containers and transported back to the Water Research Laboratory, where a sieve analysis and permeameter test were performed.* A summary of the samples used for the sieve analysis and permeameter tests is presented in Table 3.1.

Table 3.1: Samples used for Sieve Analysis and Permeameter Tests

	Well No.	Interval (R.L. assumed, ft.)
(a) Sieve Analysis	2	56.25-56.95
(b) Permeameter Test	2	52.75-53.85
		53.85-56.25
		56.95-58.75
		58.75-60.35
	3	51.66-52.66
		52.66-54.13
		54.13-56.40
		56.40-57.75
		57.75-60.75

* Samples removed from containers by hand and majority of fines removed by washing. These would then be more representative of the material local to the well.

The results of sieve analysis is presented in Fig. 3.4. Originally it was intended to drill one production well using a rotary drilling rig and thereby make a comparison between samples taken from this rig and those obtained from the percussion drilling rig. However, due to the large size of the material encountered this intention had to be abandoned and all wells completed using the percussion drilling rig.

Wells 2 and 3, spaced 10 ft. apart, were used as trial production wells. Wells 1, 1A, 4, 5 and 14S9A were used as observation wells. The screened intervals of all wells are as presented in Table 3.2.

A schedule of all pumping tests performed is presented in Tables 3.3, 3.4 and 3.5. Pumping tests on production wells 3 and 2 were performed during the periods of June 8 - 15, 1972, and June 19 - 29, 1972 respectively.

Table 3.2: Radial Distances from Wells 2 and 3 and screened intervals of Observation Wells at Site B.

Well	Radial Distance from Well 2 (ft.)	Radial Distance from Well 3 (ft.)	Screened Interval R.L. assumed (ft.)
1	28.0	38.0	52 - 56
1A	29.25	39.25	81 - 83
2	-	10.0	51 - 61
3	10.0	-	51 - 57
4	47.4	57.4	51 - 55
5	2.0	8.0	51 - 55
14S9A	80.0	80.6	53 - 58

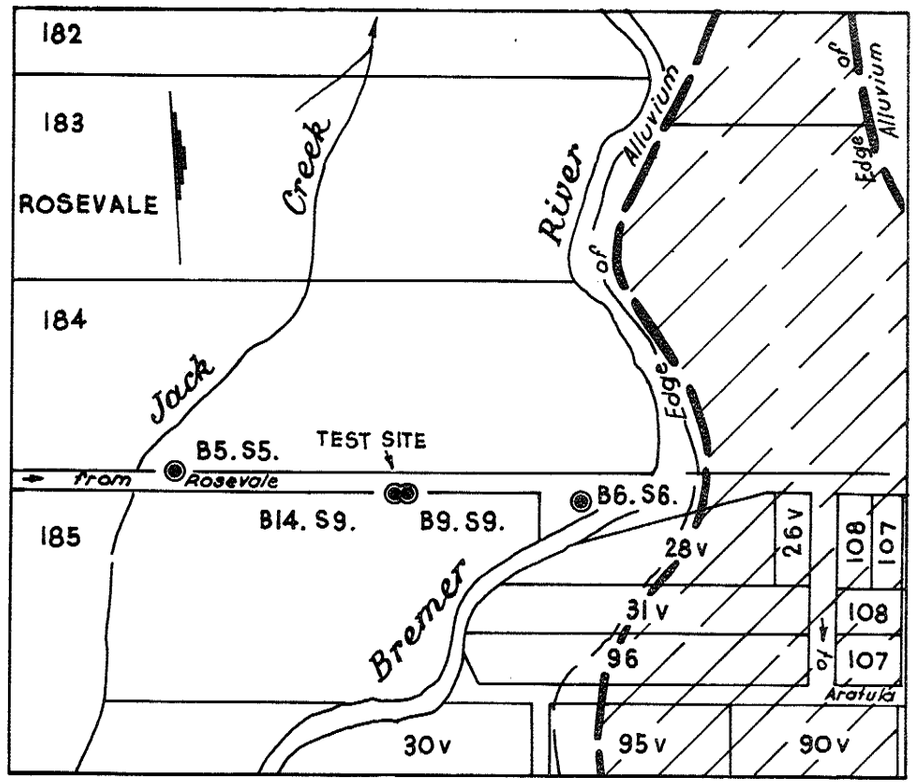

Fig. 3.1: Plan of Site B Testing Site.

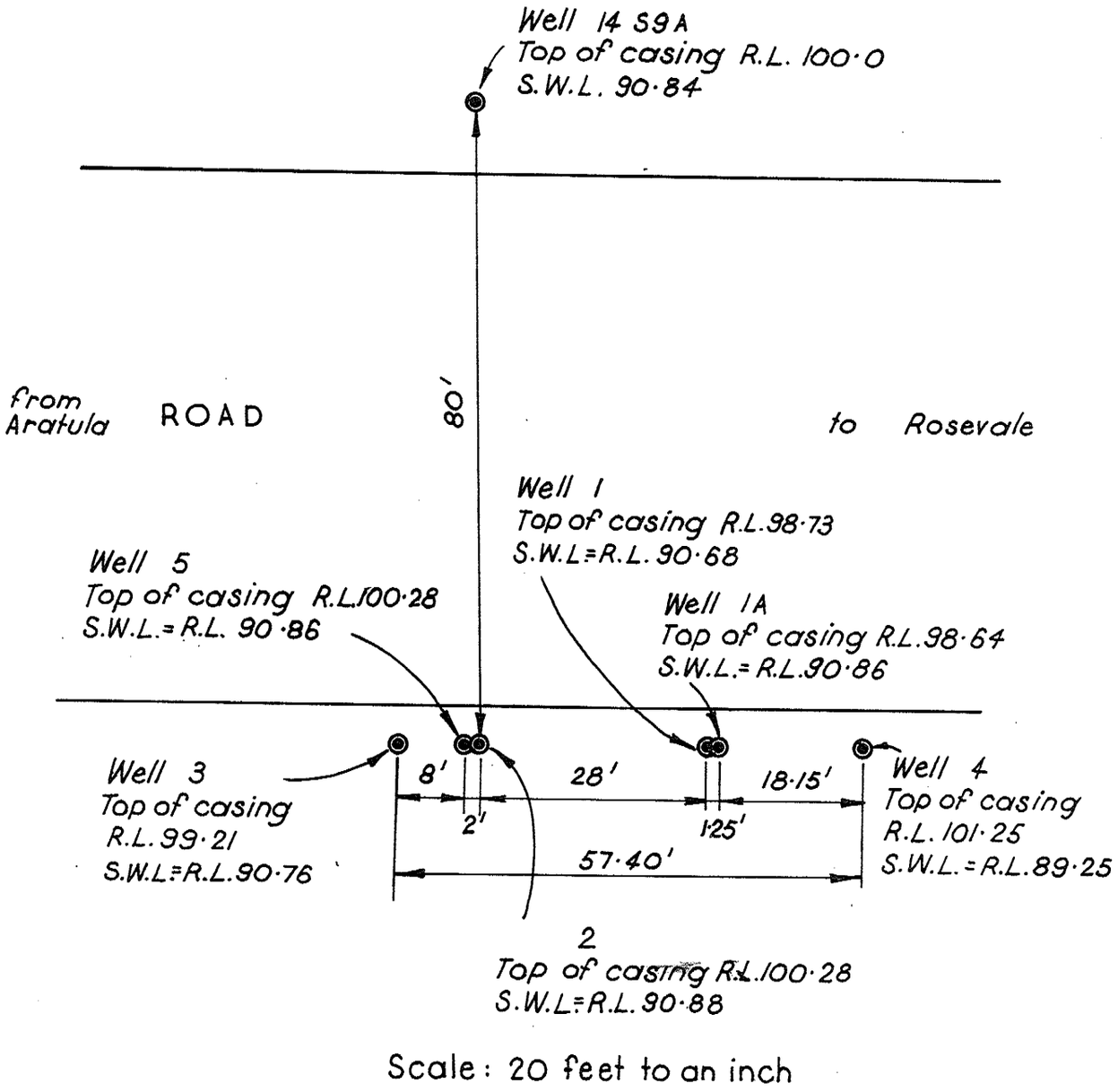

Fig. 3.2: Plan of Field Testing Site at Rosevale.

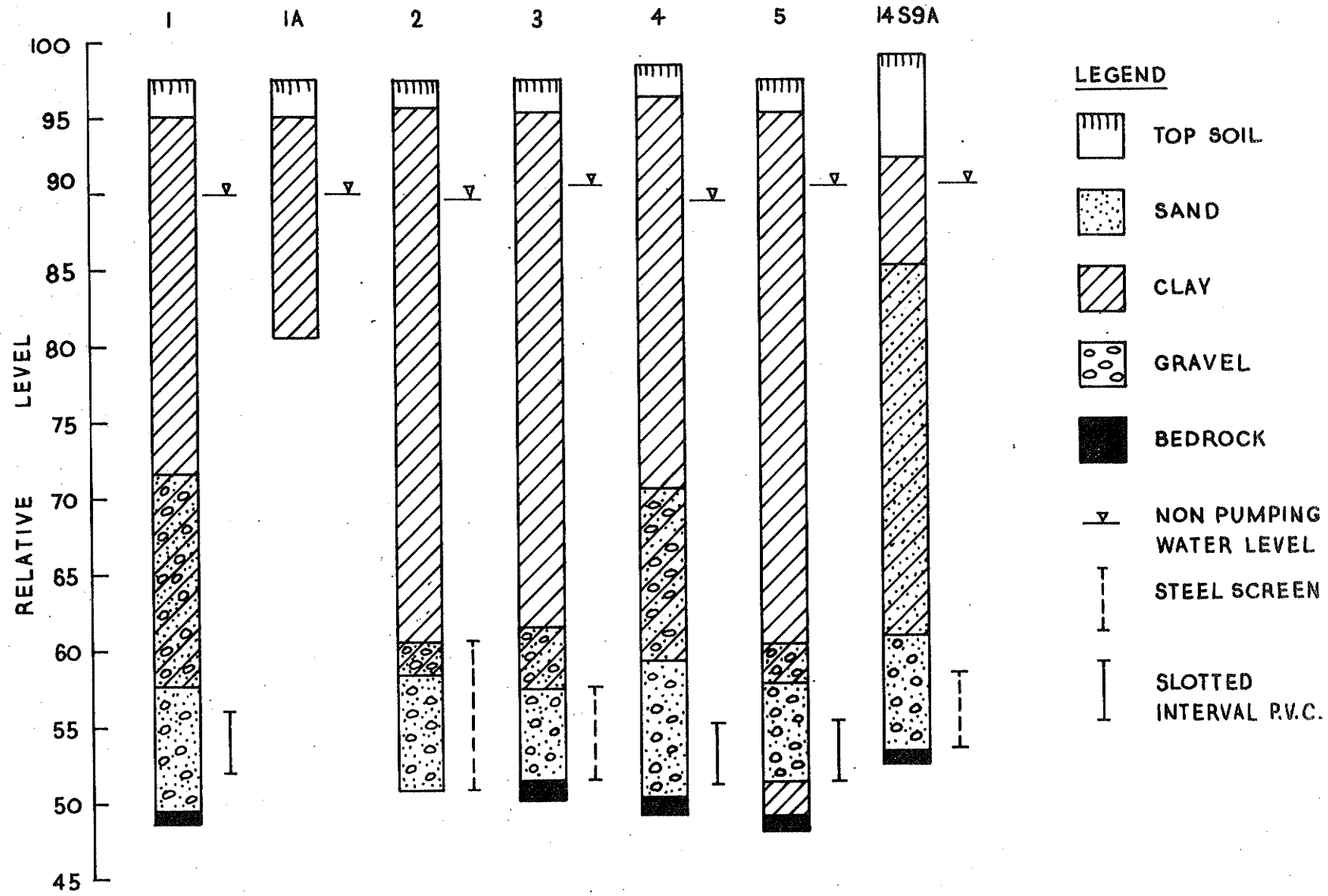

Fig. 3.3: Construction features and available drillers logs of wells at Site B.
(Note: 14S9A logged by different driller to the others)

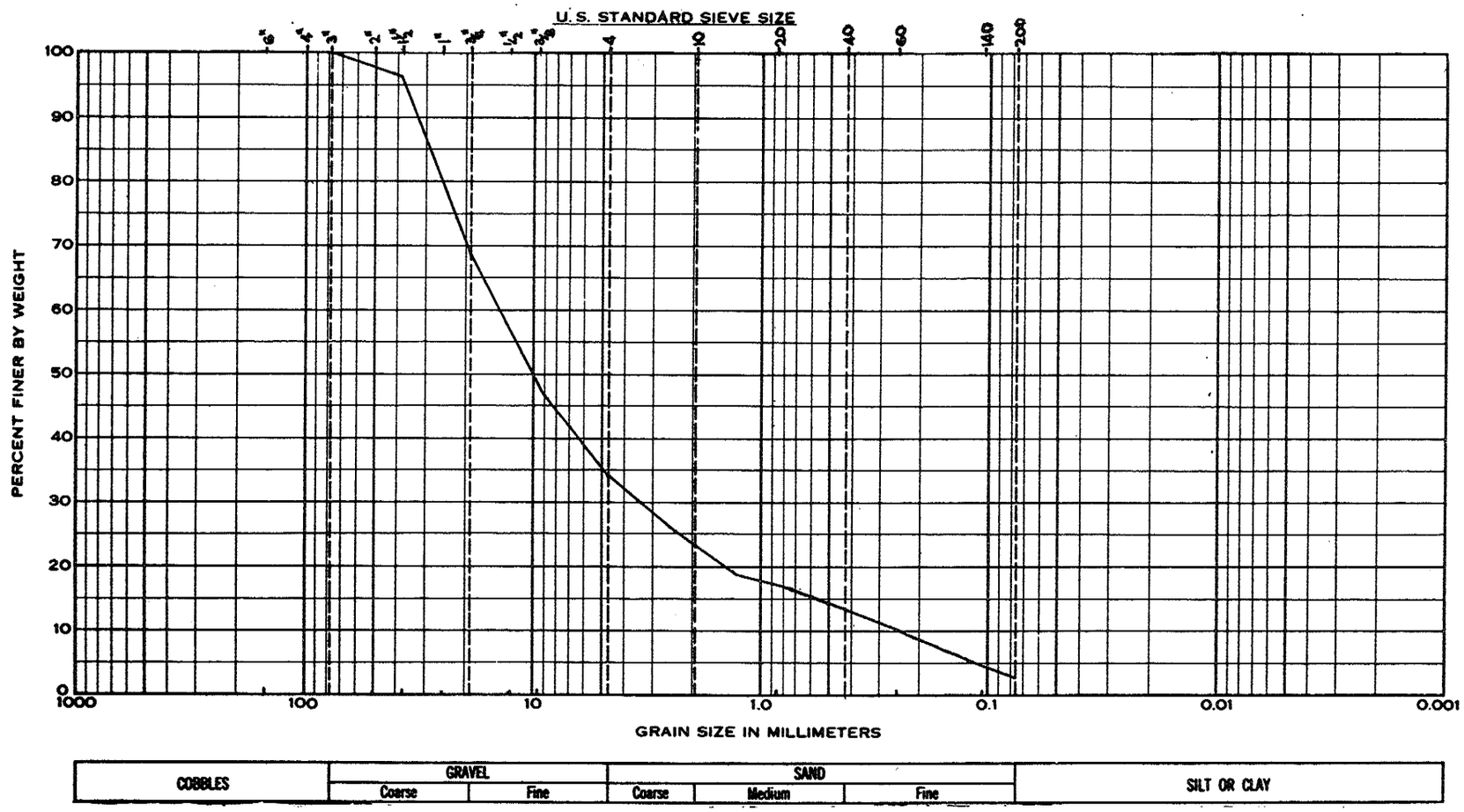

Fig. 3.4: Sieve Analysis of Sample from Prod. Well 2.

Table 3.3: Schedule of Preliminary Tests performed at Site B.

Well No.	Test	Date	Pumping Tests		Description	Pumping Rate igph (c.f.m)	Range	Recovery Tests		Description
			From	To				From	To	
3	1	8.6.72 to 9.6.72	11.00	11.00	24 hr. test	7050 (18.83)	6950-7100	11.00	13.30	3½ hour test
	2	10.6.72	12.00	16.00	4 hr. test	4000 (10.7)	Not available	16.00	17.30	1½ hour test
	3	12.6.72	12.00	16.00	4 hr. test	5700 (15.25)	5650-5750	16.00	18.00	2 hour test
	4	15.6.72	10.00	14.00	4 hr. test	2769 (7.43)	Steady at 2769	14.00	15.30	1½ hour test
2	5	19.6.72	12.00	23.00	11 hr. test	7550 (20.2)	7700-7550	-	-	Not recorded
	6	20.6.72 to 21.6.72	12.00	11.00	23 hr. test	7550 (20.2)	Steady at 7550	-	-	Not recorded
	7	26.6.72	13.00	17.00	4 hr. test	2350 (6.39)	2400-2000	17.00	19.00	2 hour test
	8	27.6.72	8.00	12.00	4 hr. test	5000 (13.38)	Steady at 5000	12.00	14.00	2 hour test
	9	28.6.72	8.00	12.00	4 hr. test	6000 (16.05)	Steady at 6000	12.00	13.20	1-1/3 hr. test
	10	29.6.72	9.00	13.00	4 hr. test	8200 (21.9)	Steady at 8200	13.00	15.00	2 hour test

Table 3.4: Summary of Results of Trial insitu Two Well Tests

Test	Pumping Rate igph	Drawdown (ft.) Well 2	Well 3	Well 5
1	4100	-3.67	+4.97	-1.91
2	4900	-4.00	+5.59	-2.04
3	6100	-6.05	+8.40	-3.08

Table 3.5: Schedule of Production Well Verification Tests

Test	Date	From	To	Description	Pumping Rate igph
11*	13.2.73	9.30	15.30	6 hr. test	7200
12*	14.2.73	6.00	8.00	2 hr. test	4600
13**	14.2.73	13.30	15.30	2 hr. test	16800

* Plus 2 hour recovery test
** No recovery test performed

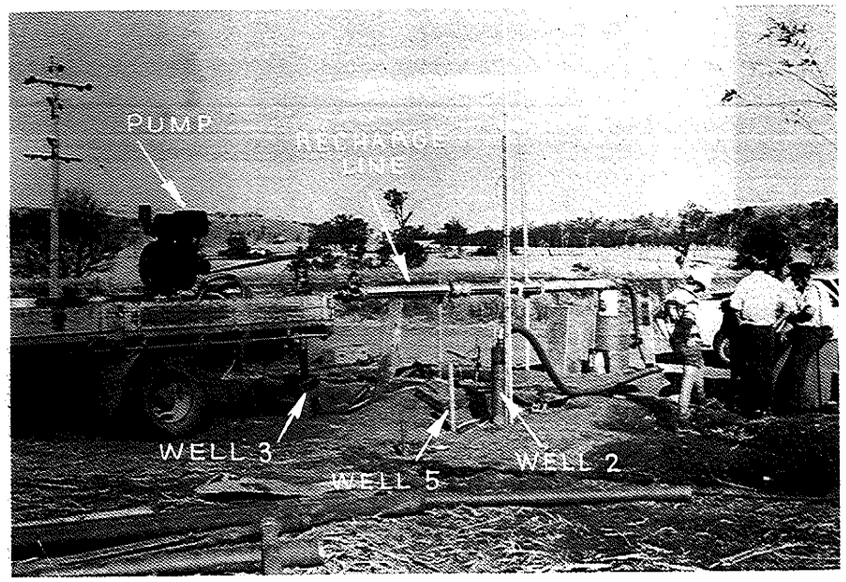

Fig. 3.5: General view of insitu two well testing arrangement.

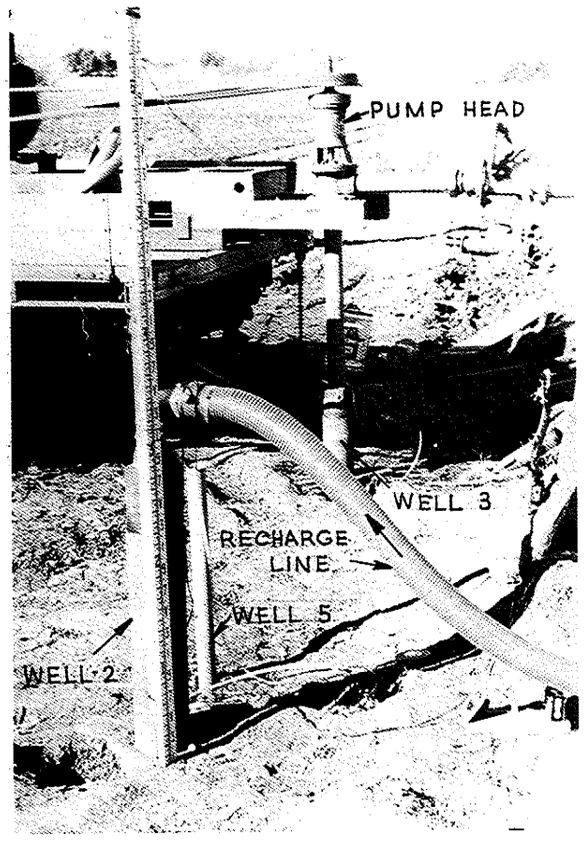

Fig. 3.6: Detailed view of arrangement for insitu two well tests.

The effects of pumping and recovery of wells 3 and 2 were measured in the production wells and all observation wells. No response was recorded in observation well 5 during the 24 hour test (Test 1) on production well 3, as it had become blocked with drilling lubricant. Attempts to clear it failed, and the well was backfilled and redrilled before the start of Test 2. As a consequence, well 2 which is only 2 feet away from it, required prolonged development before the commencement of Test 5.

Test 5, itself, was the first attempt at a 24 hour test on production well 2, but due to a pump column breakage after 11 hours of pumping the test had to be abandoned. No recovery data for this test and test 6 was recorded.

3.1.2 Insitu Two Well Tests

Production wells 2 and 3 were used for the insitu two well tests. The tests were performed on July 6, 1972. A summary of the test results is presented in Table 3.4.

For all the tests, production well 3 was used as the discharge well and production well 2 as the recharge well. The flow rate was measured by means of an orifice plate meter with D and $\frac{D}{2}$ pressure tappings. The arrangement used to connect the two production wells is shown in Figs. 3.5 and 3.6. The pump was allowed to operate at constant discharge, until the water levels had stabilised in both the discharging well and the recharging well.

3.1.3 Verification Tests

Due to on site complications two attempts were made to complete this phase of the field testing at Site B.

The first attempt was made in the period from December 12 to 15, 1972, on an enlarged production well on the site of production well 2. The screen diameter was increased from 4 inches to 8 inches, the screen aperture from 0.05 inches to 0.10 inches, and the casing diameter from 6 inches to 10 inches.

However, during the construction of the larger production well the neighbouring observation well 5 gravel pack collapsed into the redrilled hole creating a cavity under the overlying clay formation. This cavity was not completely refilled, and the overlying clay formation subsequently collapsed during development of the well. At this point the tests on the enlarged production well 2 were abandoned and a new enlarged production well constructed on the site of production well 3.

The second attempt was made in February 1973 on the enlarged production well 3. The details of construction of this well were the same as for the abandoned production well 2.

3.2 Conventional Methods of Pumping Test Analysis

3.2.1 Selection of Applicable Methods

(i) Type Curve Methods

Cooley (1971) presented an analytical solution to the initial-boundary value problem involving a well pumping from an aquifer that is semi-confined between an overlying water table aquitard and underlying aquiclude. The complete solution is divided into short and long time segments. The short time solution ($t = \frac{m's'}{10k'}$ where the prime is used to indicate the parameters belonging to the aquitard) is identical to that given by Hantush (1960) if his underlying aquitard is assumed impermeable. The long time solution is similar to Boulton's solution for drawdown resulting from a pumped well in a water table aquifer.

The results of Cooley's work suggest possible application of the following type curve methods to the time-drawdown field data.

(a) Hantush's type curve method for semi-confined well aquifer system with allowance for water released from storage in the aquitard could be

applied to the early time portion of the field data to obtain the early time values of the coefficients of transmissivity and storage for the main aquifer.

(b) The remaining portion of the field data might be matched on a family of Boulton's type curves to obtain the values of late time aquifer transmissivity and specific yield and delayed yield index for the overlying water table aquitard.

(ii) Straight Line Method

The straight line method introduced by Cooper and Jacob was considered applicable to the late time drawdown data of the observation wells 4 and 14 S9A to determine values of transmissivity T and specific yield S_y.

(iii) Jacob's Method of Well Loss Evaluation

Jacob (1946) expressed the total drawdown in a pumped well in an equation which may be written in the form

$$S_W = AQ + BQ^2 \qquad (3.3)$$

where S_W = well drawdown

A = linear aquifer loss constant (min/ft^2)

B = well loss constant (including nonlinear aquifer loss) (min^2/ft^5)

Q = discharge (c.f.m.)

The series of preliminary tests performed provided the opportunity to study this relationship for the field site. Values of A and B for each production well have been determined from the time-drawdown data of a range of constant discharge tests.

Periods of 12 hours minimum between successive tests were allowed to ensure nearly complete recovery.

3.2.2 Application of the Conventional Methods of Analysis to the Field System

The analysis of the collected field data using the conventional methods of analysis was restricted to the preliminary aquifer tests on production wells 2 and 3.

(i) Type Curve Method

The time drawdown graphs of wells 1, 2, 3 and 5 are very flat and obtaining a reasonable match with the superimposed type curves was difficult. The time-drawdown graph of observation well 1A represents the time drawdown relationship for a point in the aquitard and consequently cannot be analysed by conventional methods. Emphasis was placed on the time-drawdown graphs of wells 4 and 14S9A in determining the early time values of T, S, β and late time values of T, S_y, $\frac{r}{D_t}$.

The results obtained by applying the type curve methods are summarised in Tables3.8 and 3.9.

(a) Pumping Tests

The short time Hantush type curves were superimposed on the early time-drawdown data graphs of observation wells 4 and 14S9A. Figures 3.7 and 3.8 show the fit of the type curve trace for Test 1.

The long time Boulton type curves were then fitted to the late time drawdown data graphs (Figs. 3.7 and 3.8) and values of T, S_y, and $\frac{r}{D_t}$ were obtained.

(b) Recovery Tests

The long time Boulton type curve was superimposed on the time-residual drawdown recovery test data. Values of transmissivity T and specific yield S_y were determined.

Table 3.8: Summary of T & S Values obtained for Production Well 3.

Test	Well	Radial Distance (ft)	Discharge Tests: Type Curve Method: Hantush Method T (ft^2/min)	Hantush Method S	Hantush Method r/D	Boulton Method T (ft^2/min)	Boulton Method S_y	Boulton Method r/D	Straight Line Method T (ft^2/min)	Straight Line Method S_y	Recovery Tests: Type Curve Method T	Type Curve Method S_y	Straight Line Method T	Straight Line Method S
(1)	14	57.4	-	-	-	2.88	3.58×10^{-3}	0.8	2.12	9.3×10^{-3}	*	*	2.76	4.52×10^{-3}
	14	80.0	2.2	3.88×10^{-4}	0.25	2.14	4.1×10^{-3}	0.6	2.06	3.62×10^{-3}	2.88	1.8×10^{-3}	3.13	1.43×10^{-3}
(2)	4	57.4	-	-	-	2.94	3.93×10^{-3}	0.8	2.80	3.82×10^{-3}	*	*	*	*
	14	80.0	3.28	2.05×10^{-4}	0.25	3.27	0.86×10^{-3}	0.6	2.93	1.55×10^{-3}	3.22	1.17×10^{-3}	2.34	2.8×10^{-3}
(3)	4	57.4	-	-	-	2.7	0.89×10^{-3}	0.8	2.54	5.55×10^{-3}	*	*	*	*
	14	80.0	2.95	3.14×10^{-4}	0.25	2.95	1.59×10^{-3}	0.6	3.09	1.28×10^{-3}	3.58	0.9×10^{-3}	3.72	9.15×10^{-3}
(4)	4	57.4	-	-	-	2.2	0.59×10^{-3}	0.8	2.52	4.84×10^{-3}	**	**	3.0	3.07×10^{-3}
	14	80.0	2.2	3.58×10^{-4}	0.25	2.2	0.22×10^{-3}	0.6	2.23	2.35×10^{-3}	2.63	1.81×10^{-3}	2.94	8.25×10^{-3}
			2.46	3.14×10^{-4}	0.25	2.64	2.36×10^{-3}	-	2.54	4.04×10^{-3}	3.08	1.42×10^{-3}	2.98	9.5×10^{-3}

Legend:

* Not recorded

** Record of observations not long enough

Table 3.9: Summary of T & S Values obtained for Production Well 2.

Test	Well	Radial Distance (ft)	Discharge Tests: Type Curve Method: Hantush Method T (ft^2/min)	Hantush Method S	Hantush Method β	Boulton Method T (ft^2/min)	Boulton Method S_y	Boulton Method $\frac{r}{D_t}$	Discharge Tests: Straight Line Method T (ft^2/min)	Straight Line Method S	Recovery Tests: Type Curve Method T	Type Curve Method S	Straight Line Method T	Straight Line Method S
(6)	4	47.4	**	**	**	3.15	1.09×10^{-2}	0.8	2.24	1.12×10^{-2}	*	*	*	*
	14	80.0	2.90	1.82×10^{-4}	0.25	2.91	3.37×10^{-3}	0.6	2.39	3.28×10^{-3}	*	*	*	*
(7)	4	47.4	**	**	**	**	**	-	2.55	6.37×10^{-3}	**	**	3.77	3.96×10^{-3}
	14	80.0	2.55	2.88×10^{-4}	0.25	2.55	2.23×10^{-3}	0.6	2.55	2.24×10^{-3}	2.21	3.55×10^{-3}	3.77	1.01×10^{-3}
(8)	4	47.4	**	**	**	**	***	-	2.85	3.99×10^{-3}	**	**	3.5	4.2×10^{-3}
	14	80.0	3.30	3.64×10^{-4}	0.25	3.32	1.31×10^{-3}	0.6	2.75	1.26×10^{-3}	2.88	2.16×10^{-3}	3.5	1.12×10^{-3}
(9)	4	47.4	**	**	**	**	**	-	2.77	5.7×10^{-3}	**	**	3.93	3.14×10^{-3}
	14	80.0	3.0	2.25×10^{-4}	0.25	3.05	1.2×10^{-3}	0.6	2.85	1.4×10^{-3}	2.91	2.18×10^{-3}	3.93	0.83×10^{-3}
(10)	4	47.4	**	**	**	*	*	-	2.97	5.8×10^{-3}	**	**	4.0	3.2×10^{-3}
	14	80.0	2.9	2.9×10^{-4}	0.25	2.9	1.9×10^{-3}	0.6	2.97	1.57×10^{-3}	3.29	1.65×10^{-3}	4.17	0.88×10^{-3}
			2.95	2.7×10^{-4}	0.25	2.98	3.49×10^{-3}		2.69	4.28×10^{-3}	2.82	2.39×10^{-3}	3.82	2.29×10^{-3}

Legend:

* Not recorded

** Record of observations not long enough

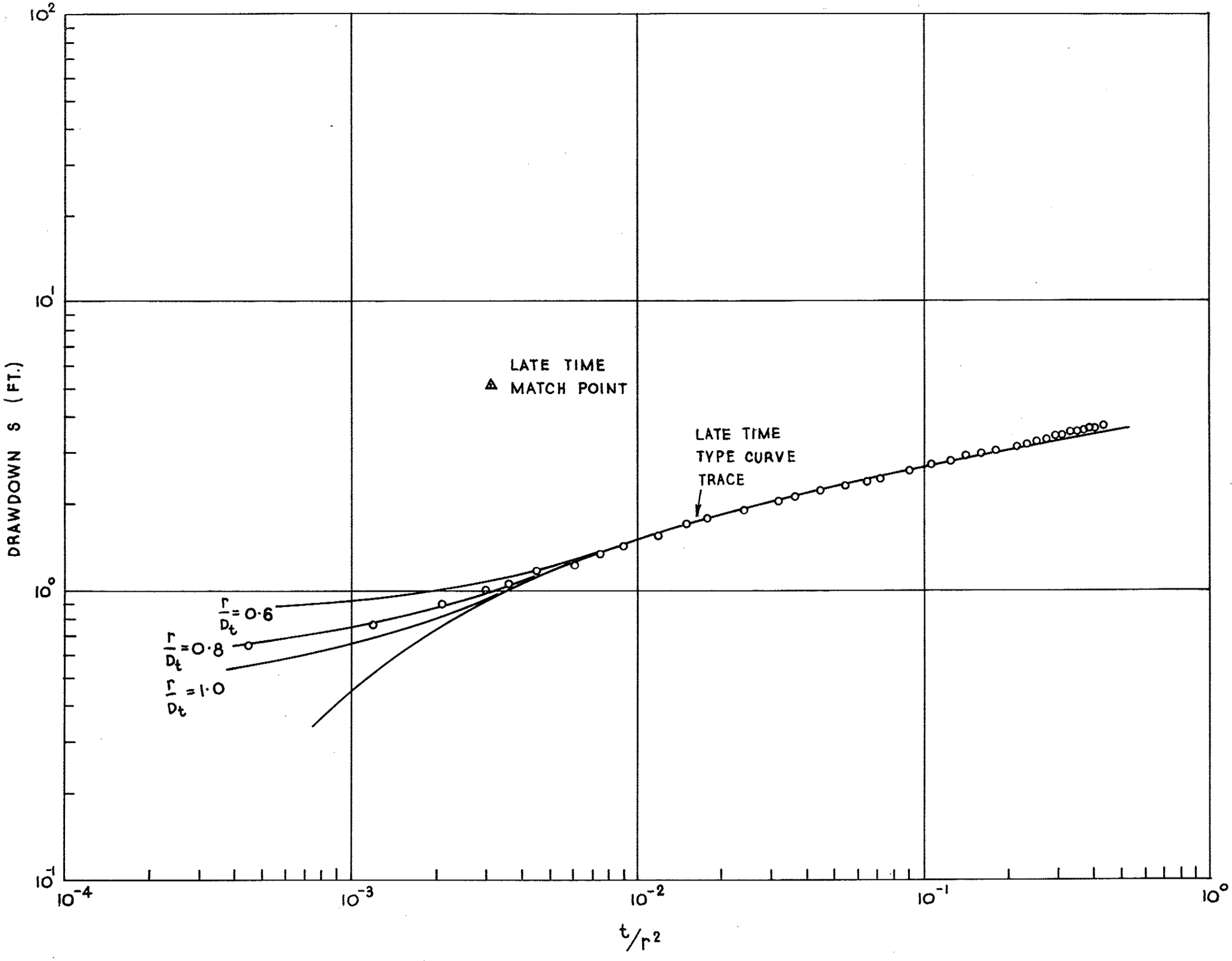

Fig. 3.7: Time-Drawdown graph for observation well 4 - Test 1.

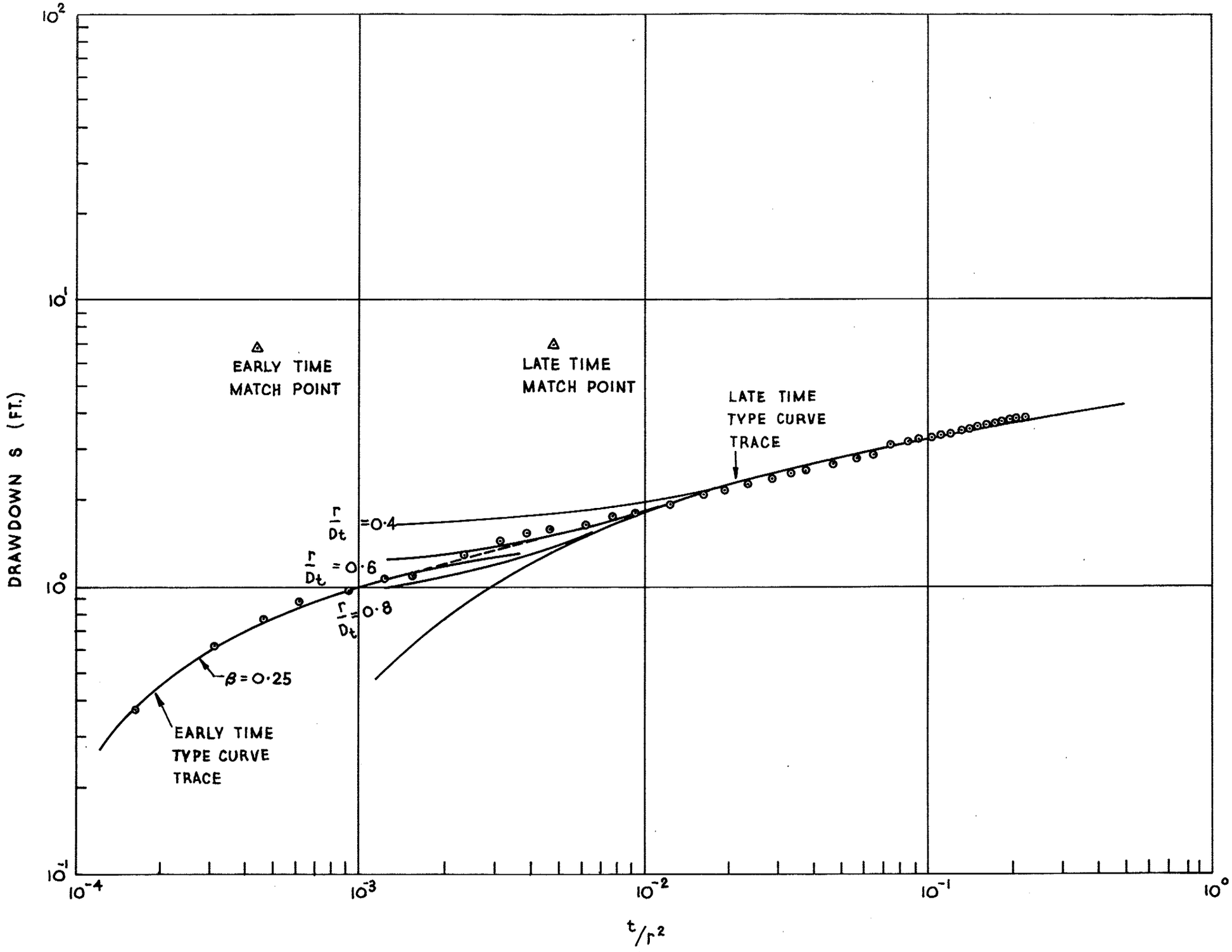

Fig. 3.8: Time-Drawdown Graph for Observation Well 14S9A - Test 1.

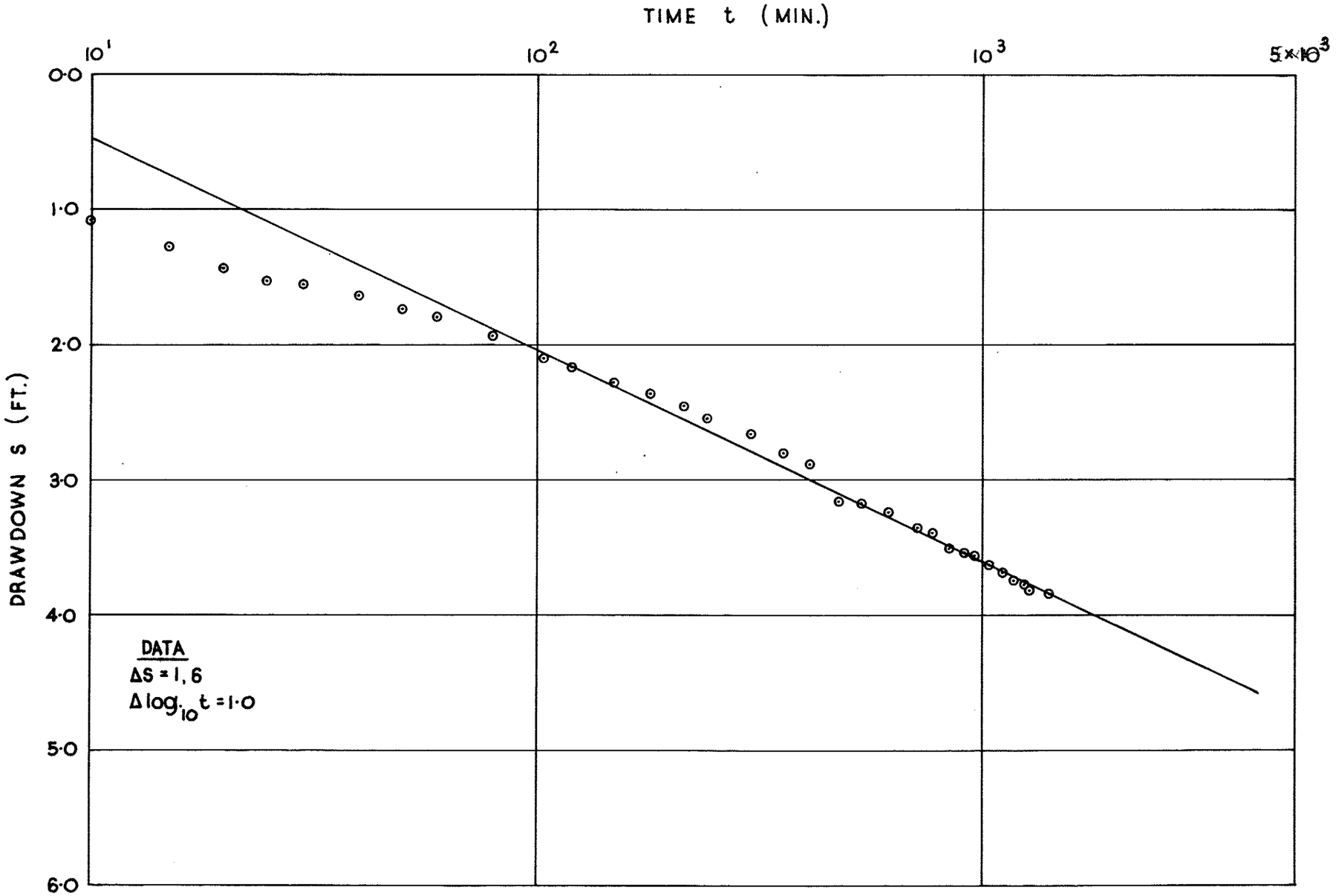

Fig. 3.9: Straight Line Graph of Time-Drawdown Data for Well 4.

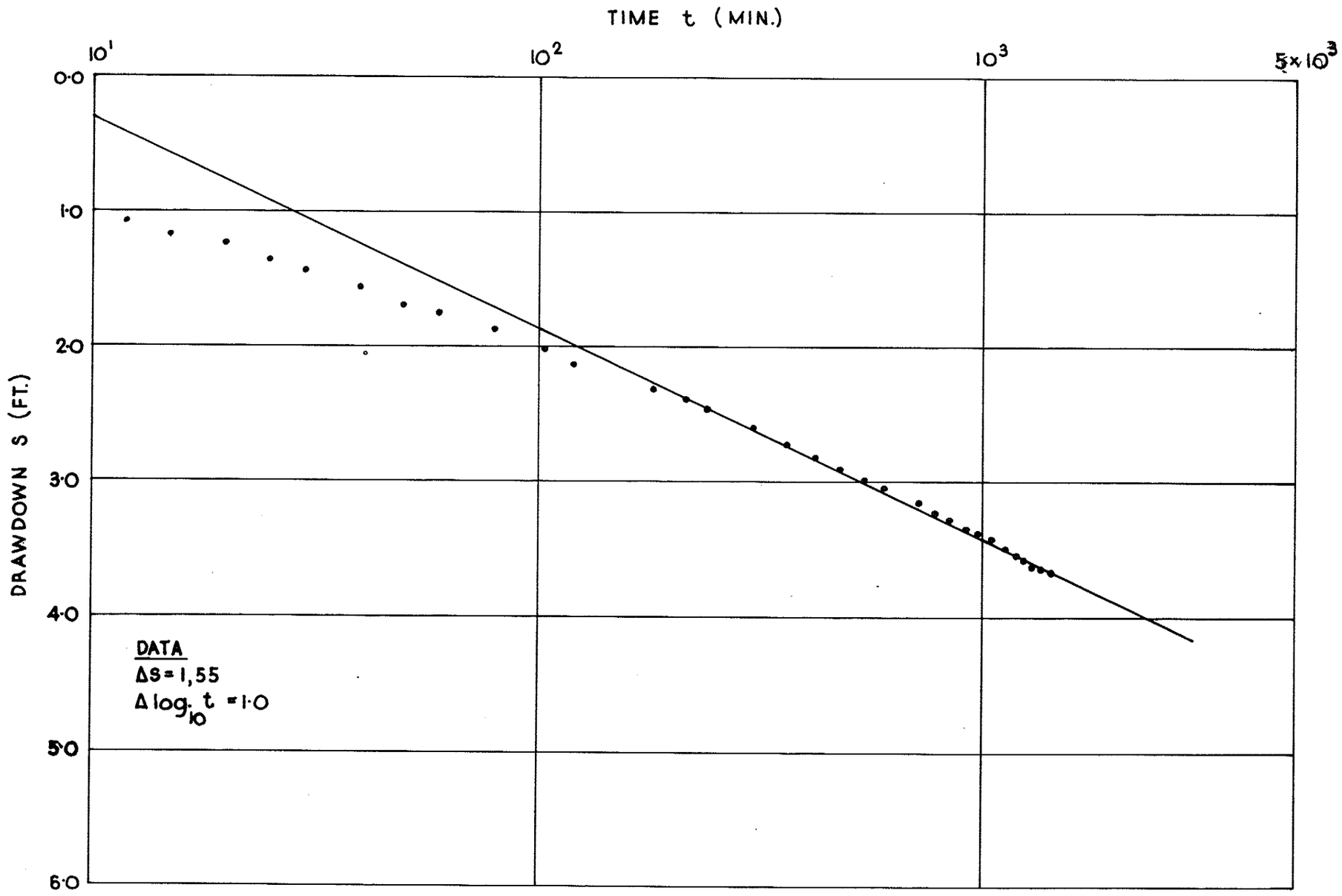

Fig. 3.10: Straight Line Graph of Time-Drawdown Data for Well 14.

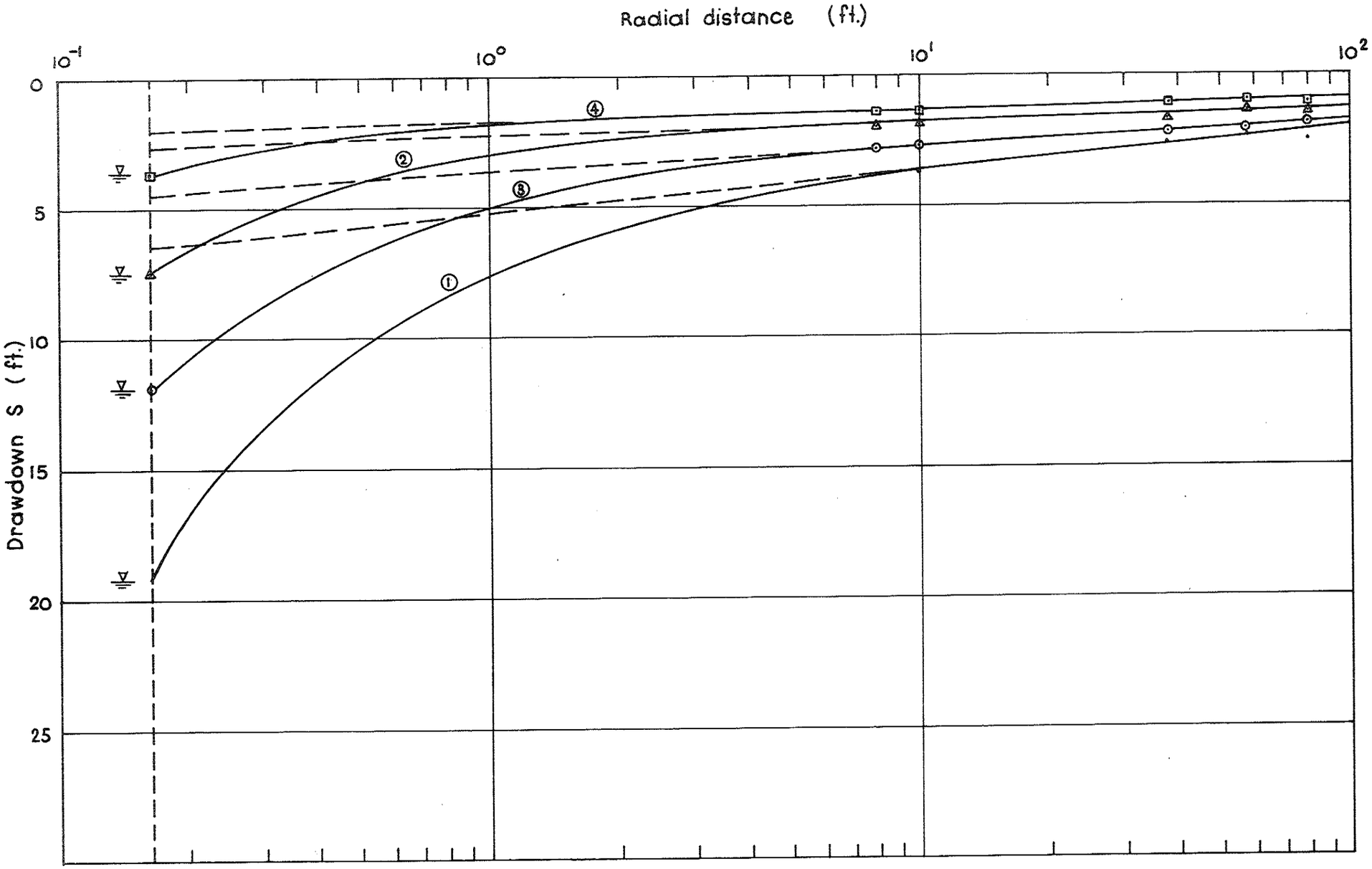

Fig. 3.11: Radial distance-drawdown graphs for well 3 tests.

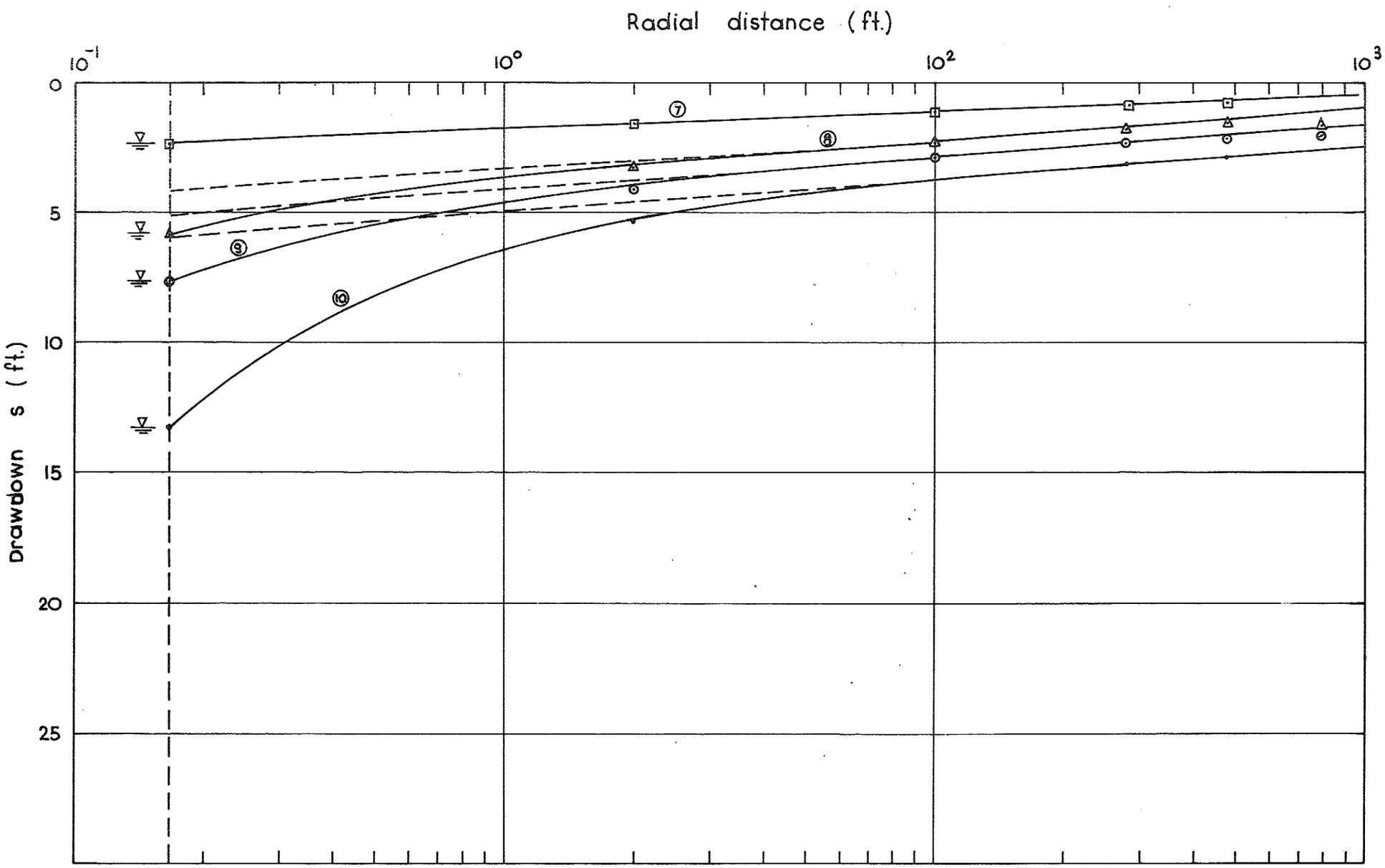

Fig. 3.12: Radial distance-drawdown graphs for well 2 tests

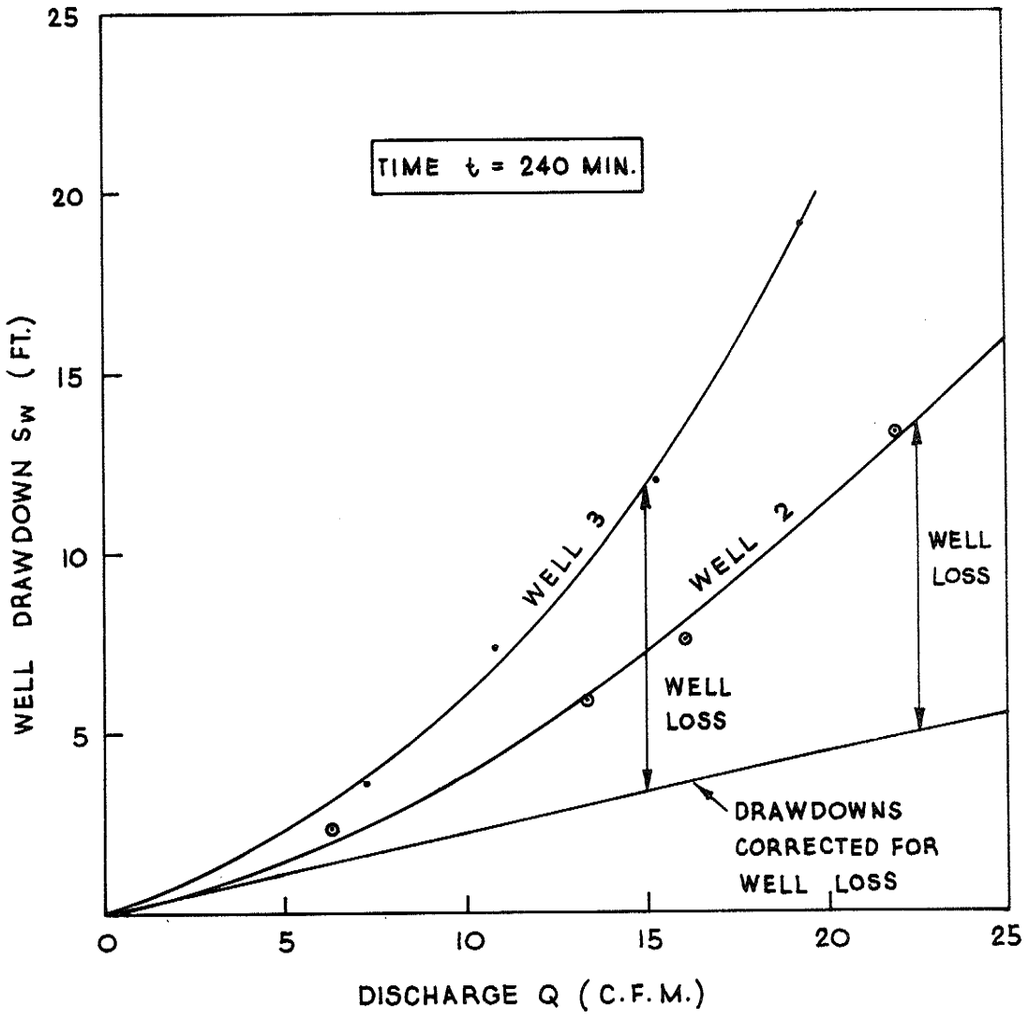

Fig. 3.13: Well Drawdown S_w Discharge Q Graphs for Wells 2 and 3.

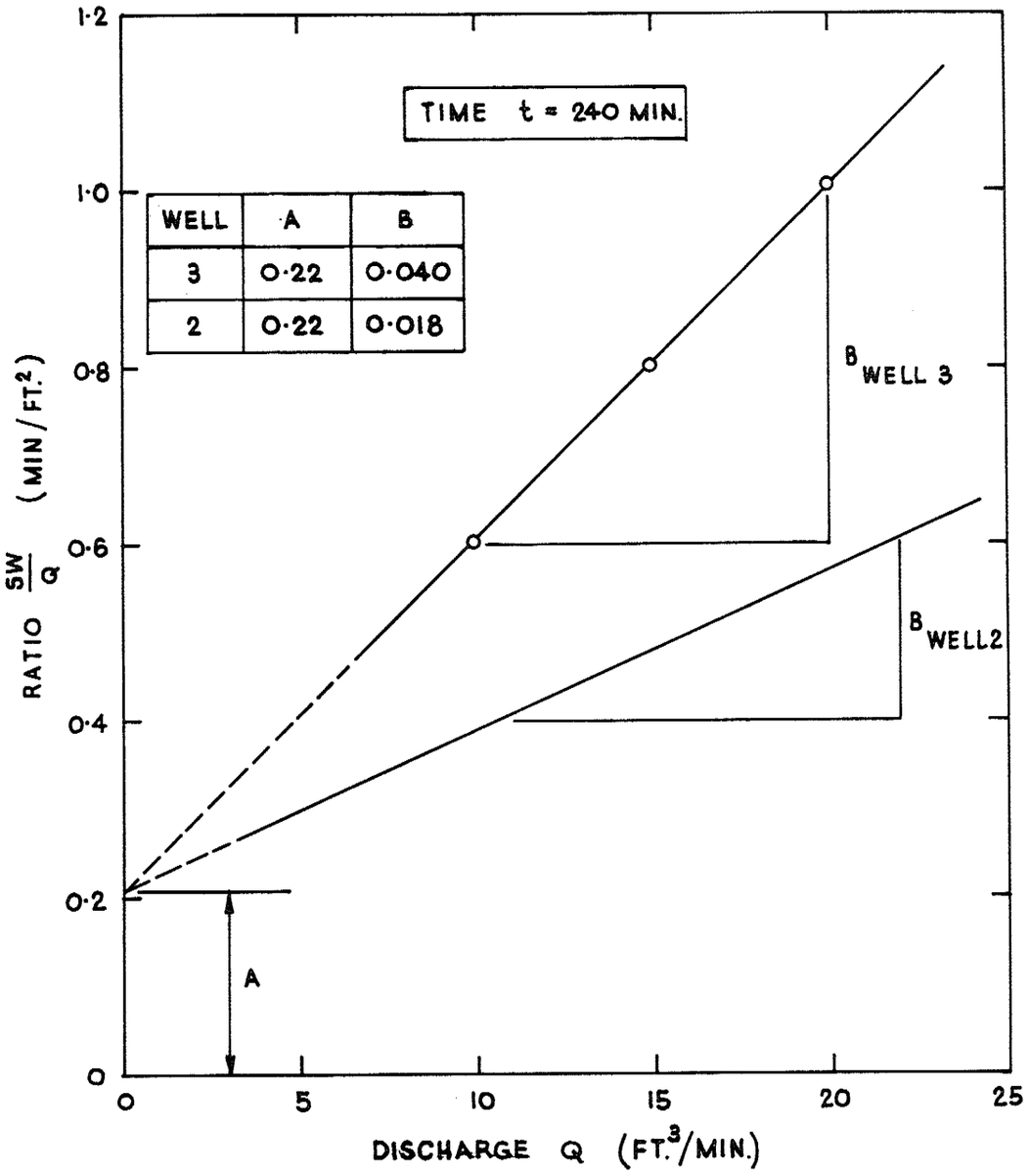

Fig. 3.14: $\frac{S_w}{Q}$ versus Q Graphs for Wells 2 and 3.

(ii) Straight Line Method

The time-drawdown field data for observation wells 4 and 14S9A for both the pumping and recovery tests were plotted on semilogarithmic paper (Figs. 3.9 and 3.10). Straight lines were fitted to the late time drawdown field data of all graphs. The slopes of the straight lines and the intercepts with the zero drawdown axis, t_o were substituted in

$$T = \frac{2.3\ Q}{4\pi \frac{\Delta s}{\Delta \log_{10} t}} \qquad (3.5)$$

and $$S_y = \frac{2.25\ T\ t_o}{r^2} \qquad (3.6)$$

to obtain the coefficients of transmissivity T and specific storage S_y.

The values of T and S_y obtained are summarised in Tables 3.8 and 3.9.

(iii) Radial Distance-Drawdown Graphs

Semilogarithmic graphs of radial distance against drawdown (natural scale) were prepared using the drawdowns in all wells at a time t of 240 minutes (Figs. 3.11 and 3.12).

These graphs would suggest that the flow of water through the system towards production wells 2 and 3 involves both linear and non-linear regimes of aquifer loss.

3.2.3 Application of Jacob's Method

Values of well drawdown S_w and ratio $\frac{S_w}{Q}$ were plotted against values of discharge Q for each production well. The results are shown in Figures 3.13 and 3.14 for a time of 240 minutes.

Values of A and B were determined from Fig. 3.14 for both wells. A check on these values has been made by calculating and plotting the line of drawdowns corrected for well loss.

3.3 Computer Method of Pumping Test Analysis

3.3.1 Introduction

The problem of determining the flow pattern and evaluating the hydraulic coefficients for the aquifer system at this particular site is more complex than that previously handled for the Gumly Gumly Island, Wagga Wagga aquifer system. In the present case, the overlying aquitard is unconfined and the main aquifer is quite variable in thickness and is bounded by barrier boundaries. Examination of core samples from the two 4 inch diameter trial pumped wells and other well log data revealed that the main aquifer is also very variable in physical and hydraulic properties. The field data plot on a log-log scale of time versus drawdown shows significant delayed yield effects during the intermediate and late time periods of pumping. Non-Darcy flow also occurred in close vicinity to the pumped wells, resulting in significant well losses. The occurrence of non-Darcy flow is indicated by non-linear drawdown-discharge relationships. The semi-log plots of drawdown-distance data for late times also show non-linearity in the near-screen-zone.

To overcome these problems, the mathematical formulation and the finite element model previously developed for the Wagga Wagga system were modified to take into account the additional conditions which previously did not exist.

3.3.2 Mathematical Formulation of Flow Problems

A sketch of the mathematical model of the well-aquifer system at this site is shown in Fig. 3.15.

Apart from assumptions (i) to (iii), previously made in Section 2.3.2, the following assumptions were made:-

(iv) Non-Darcy flow occurs in the immediate vicinity of the well screen and Forchheimer's equation may be used to describe the non-linear velocity-hydraulic gradient relationship.

(v) Flow in the unsaturated zone above the water table may be neglected, and Boulton's concept of delayed yield may be applied to approximate the condition of slow vertical drainage due to the falling water table (Boulton 1954, 1963).

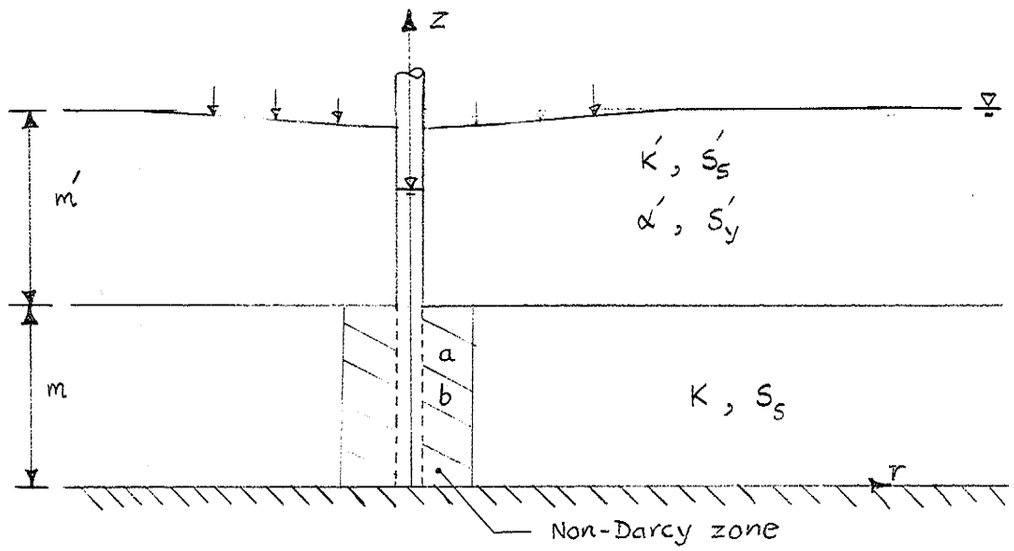

Fig. 3.15: Mathematical model for Rosevale well-aquifer system.

The following partial differential equations and initial and boundary conditions were used to describe the two-regime flow in the main aquifer and Darcy flow in the overlying aquitard respectively.

Let s and s' denote drawdowns in the main aquifer and the overlying aquitard respectively. The differential equations for drawdown in the main aquifer are as follows:-

In the Darcy zone

$$K\left(\frac{\partial^2 s}{\partial r^2} + \frac{1}{r}\frac{\partial s}{\partial r}\right) + \frac{K'}{m}\frac{\partial s'}{\partial z}(r, m, t) = S_s \frac{\partial s}{\partial t} \qquad (3.7)$$

In the non-Darcy zone

$$\frac{\partial}{\partial r}\left(K_e \frac{\partial s}{\partial r}\right) + \frac{1}{r}\frac{\partial}{\partial r}(K_e s) + \frac{K'}{m}\frac{\partial s'}{\partial z}(r, m, t) = S_s \frac{\partial s}{\partial t} \qquad (3.8a)$$

$$Ke = \frac{1}{a + b|V|} \qquad (3.8b)$$

The corresponding initial and boundary conditions are:-

$$s(r, o) = 0 \qquad (3.9a)$$

$$s(\infty, t) = 0 \qquad (3.9b)$$

$$\frac{\partial s}{\partial r}(r_w, t) = -\frac{Q}{2\pi K m r_w} \qquad (3.9c)$$

The differential equation for drawdown in the aquitard is

$$K' \frac{\partial^2 s'}{\partial z^2} = S_s' \frac{\partial s'}{\partial t} \qquad (3.10)$$

With the following initial and boundary conditions

$$s'(r, z, 0) = 0 \qquad (3.11a)$$

$$s'(r, m, t) = s(r, m, t) \qquad (3.11b)$$

$$-K' \frac{\partial s'}{\partial z}(r, m+m', t) = S_y' \alpha' \int_0^t e^{-\alpha'(t-\tau)} \frac{\partial s'}{\partial \tau} d\tau \qquad (3.11c)$$

where

K_e is the effective hydraulic conductivity of the aquifer,

$|v|$ is the absolute value of the radial flow velocity,

α' and S_y' are the reciprocal of the delayed yield index and specific yield of the aquitard respectively and the rest of the symbols have been previously defined. The right hand term of Equation(3.11c)is Boulton's convolutional integral for variable delayed yield.

Analytical solutions of the above system of partial differential equations and the corresponding initial and boundary conditions are extremely difficult to obtain. Asymptotic solutions are available in the literature for short and long time drawdowns in the Darcy zone of the main aquifer and for short time drawdowns in the overlying aquitard. The solutions for short time drawdowns in the aquifer and aquitard are given by equations (2.7) and (2.9) respectively. The short time criterion is identical to that given by Hantush ($t \leqslant \frac{m'^2 S_s'}{10k'}$).

The solution for long times was obtained by Cooley and Case (Cooley, 1971) who solved the initial-boundary value problem identical to the one solved by Hantush with the exception that the boundary condition at the top of the aquitard was replaced by Boulton's integral to approximate the delayed yield from the unsaturated zone. Their solution may be written in the following form:-

$$s = \frac{Q}{4\pi Km} W(\delta_2 u, r/D) \qquad (3.12a)$$

$$\text{for } t \geqslant \frac{10 m'^2 S_s}{K'}$$

where

$$W(\delta_2 u, r/D) = \int_0^\infty 2 J_o(2y) \left\{ 1 - \frac{(r/D)^2}{(r/D)^2 + 4y^2} \cdot \exp\left[\frac{-(r/D)^2 y^2}{\delta_2 u ((r/D)^2 + 4y^2)} \right] \right\} \frac{dy}{y} \qquad (3.12b)$$

$$\delta_2 = 1 + \frac{S_y' + S_s' m'}{S_s m} \qquad (3.12c)$$

$$D = \left[\frac{Km}{\alpha' S_y'} + \frac{Kmm'}{K'} \right]^{1/2} \qquad (3.12d)$$

J_o = Bessel function of the first kind of zero order.

Type curves obtained from Equation 3.12a are identical to those produced by Boulton. A computer subroutine for numerical evaluation of the well function in Equation 3.12b was written in Fortran IV language for the purpose of comparison with the finite element solution.

3.3.3 Modification of Previous Finite Element Model

The two-dimensional model constructed for the Wagga Wagga well-aquifer system was modified to incorporate the boundary condition at the water table, described by Equation (3.11c) and non-Darcy flow in the immediate vicinity of the well screen, described by Equation (3.8). Although the modified model is capable of handling variable saturated thickness of the aquitard when the water table is lowered by pumping, the maximum saturated thickness m' was assigned to the aquitard in this study as the field data showed that the water table was not significantly lowered at the end of the pumping period.

The technique for handling non-Darcy flow in the vicinity of the well screen has already been presented in Section B of this report. The following technique was developed to treat the time-varying boundary condition at the water table.

Referring to Section B, a system of simultaneous algebraic equations for model drawdowns in the two-layered system may be written as

$$\left(\frac{\Delta t}{2} C_{JI}^{t+\Delta t/2} + D_{JI} \right) s_J^{t+\Delta t/2} = D_{JI} s_J^{t} - \frac{\Delta t}{2} F_I^{t+\Delta t/2} \qquad (3.13a)$$

$$s_J^{t+\Delta t} = 2 s_J^{t+\Delta t/2} - s_J^{t} \qquad (3.13b)$$

where s_J are drawdowns at various nodes in the system and the remaining symbols are as previously defined. (For the nodes in the aquitard the symbol s_J is replaced by s_J').

The terms $F_I^{t+\Delta t/2}$ are non-zero at the top of the water table aquitard where vertical drainage occurs due to lowering of the water table.

Let $q_I^{t+\Delta t/2}$ denote vertical flux at node I on the top boundary of the aquitard region. $F_I^{t+\Delta t/2}$ may be expressed as

$$F_I^{t+\Delta t/2} = \sum^{e} \int_{B^e} q_J^{t+\Delta t/2} N_J N_I n_3 \, dB \qquad (3.14)$$

where N_J are the shape functions, n_3 is the vertical component of the unit normal vector

$q_J^{t+\Delta t/2}$ may be approximated as follows:-

$$\begin{aligned} q_J^{t+\Delta t/2} &= \alpha' S_y' \int_0^{t+\Delta t/2} \frac{\partial s_J'}{\partial \tau} e^{-\alpha'(t+\Delta t/2-\tau)} d\tau \\ &\approx \alpha' S_y' \Big[\int_0^{t} e^{-\alpha'(t-\tau)} e^{-\alpha'\Delta t/2} \frac{\partial s_J'}{\partial \tau} d\tau \\ &\quad + \int_t^{t+\Delta t/2} \frac{\partial s_J'}{\partial \tau} e^{-\alpha'(t+\Delta t/2-\tau)} d\tau \Big] \end{aligned} \qquad (3.15a)$$

The second right hand term of equation (3.15a) is further approximated by

$$\alpha' S_y' \int_t^{t+\Delta t/2} \frac{\partial s'}{\partial \tau} e^{-\alpha'(t+\Delta t/2-\tau)} d\tau = \frac{1}{2}\Big(\frac{\partial s_J'}{\partial \tau}\Big|_{\tau=t} + \frac{\partial s_J'}{\partial \tau}\Big|_{\tau=t+\Delta t/2} \Big) S_y' (1 - e^{-\alpha'\Delta t/2}) \qquad (3.15b)$$

Equation (3.15a) may now be written in the following simplified form

$$q_J^{t+\Delta t/2} = e^{-\alpha'\Delta t/2} q_J^{t} + S_e' \frac{\partial s'}{\partial \tau}\Big|_{\tau=t+\Delta t/2} \qquad (3.16a)$$

where

$$S_e' = S_y' (1 - e^{-\alpha'\Delta t/2}) \qquad (3.16b)$$

Following Boulton's concept of delayed yield, the coefficient S_e' may be interpreted as an incremental volume rate of delayed yield drainage from the unsaturated zone per unit area per unit increase in drawdown at the top of the aquitard which takes place over incremental time $\Delta t/2$.

At an earlier time t, the integral represented by the term q_J^t is

conveniently evaluated by applying Simpson's rule of numerical integration. Knowing q_J^t, $q_J^{t+\Delta t/2}$ may be obtained from equation (3.16a)

3.3.4 Calibration of Finite Element Model

A typical flow problem was formulated for the purpose of model calibration. The problem data are given in Fig. 3.16.

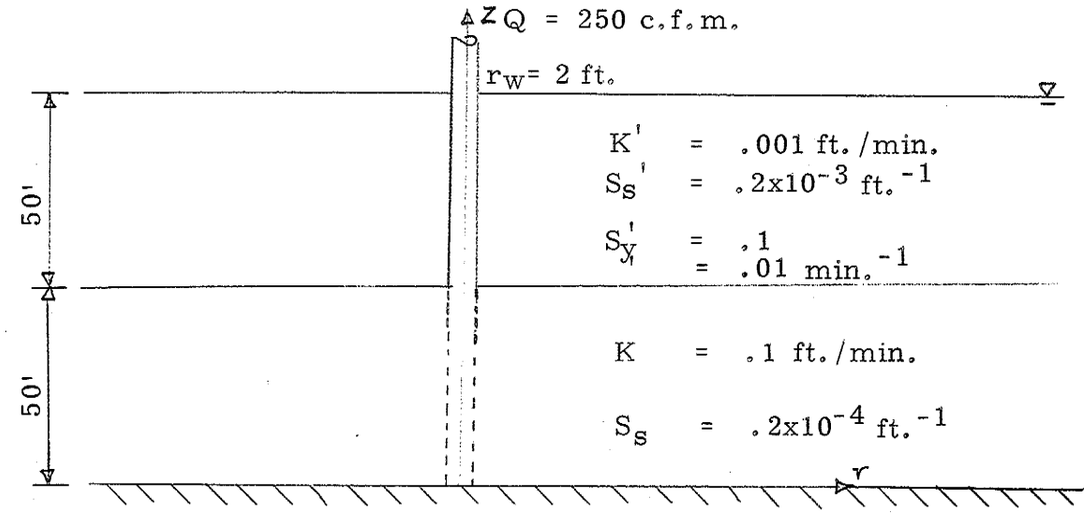

Fig. 3.16: Flow system for test problem.

As described in Section 2.3.4 two combinations of mesh pattern and time discretisation were employed. The two mesh patterns are identical to those shown in Fig. (2.23). Only wholly Darcy flow cases were simulated as exact solutions for transient non-Darcy flow are not available.

Fig. 3.19 shows the comparison of the finite element results and the asymptotic analytical solutions computed separately from the computer subroutines employing Simpson's rule of numerical integration. The plot represents time-drawdown relationships for nodes located at different levels in the aquitard but at the same radial distance from the pumped well. Good agreement between the finite element and exact analytical solutions and improvement of accuracy with mesh refinement may be observed.

3.3.5 Behaviour of Well-Aquifer System

(i) Wholly Darcy Flow

The general dimensionless drawdown-time relationship for a two layered confined aquifer-unconfined aquitard system may be written in the following forms:-

$$\frac{4\pi Ts}{Q} = W(u, \beta, r/B, r/D) \qquad (3.17a)$$

and

$$\frac{4\pi Ts'}{Q} = W(u, \beta, r/B, r/D, z'/m') \qquad (3.17b)$$

where

W = generalised well function

$$u = \frac{r^2 S_s}{4Kt}$$

$$\beta = \frac{r}{4m}\sqrt{\frac{K' S_s'}{K S_s}}$$

$$\frac{r}{B} = r\sqrt{\frac{K'}{Kmm'}}$$

$$D = \left[\frac{T}{\alpha' S_y'} + \frac{Tm'}{K'}\right]^{\frac{1}{2}}$$

$$\frac{z'}{m'} = \frac{z-m}{m'}$$

s and s' = drawdowns in the main aquifer and the unconfined aquitard respectively.

Families of type curves for Equation 3.17a are shown in Figs. 3.17 and 3.21. For the set of curves in each figure, the dimensionless ratios $\beta/\frac{r}{B}$ and $\beta/\frac{r}{D}$ are constant. The early and late time Theis curves are also included. It is seen that for $t \leqslant \frac{m'^2 S_s'}{10K'}$, the type curves for the main aquifer are identical to Hantush type curves and for $t \geqslant \frac{10m'^2 S_s'}{K'}$ these type curves become Boulton type curves. The two Theis curves are separated by a horizontal distance of $1/u\ (\delta_2 - 1)$, where $\delta_2 = 1 + (S_y' + S_s'm')/S_s m$, the distance increasing with increase in δ_2.

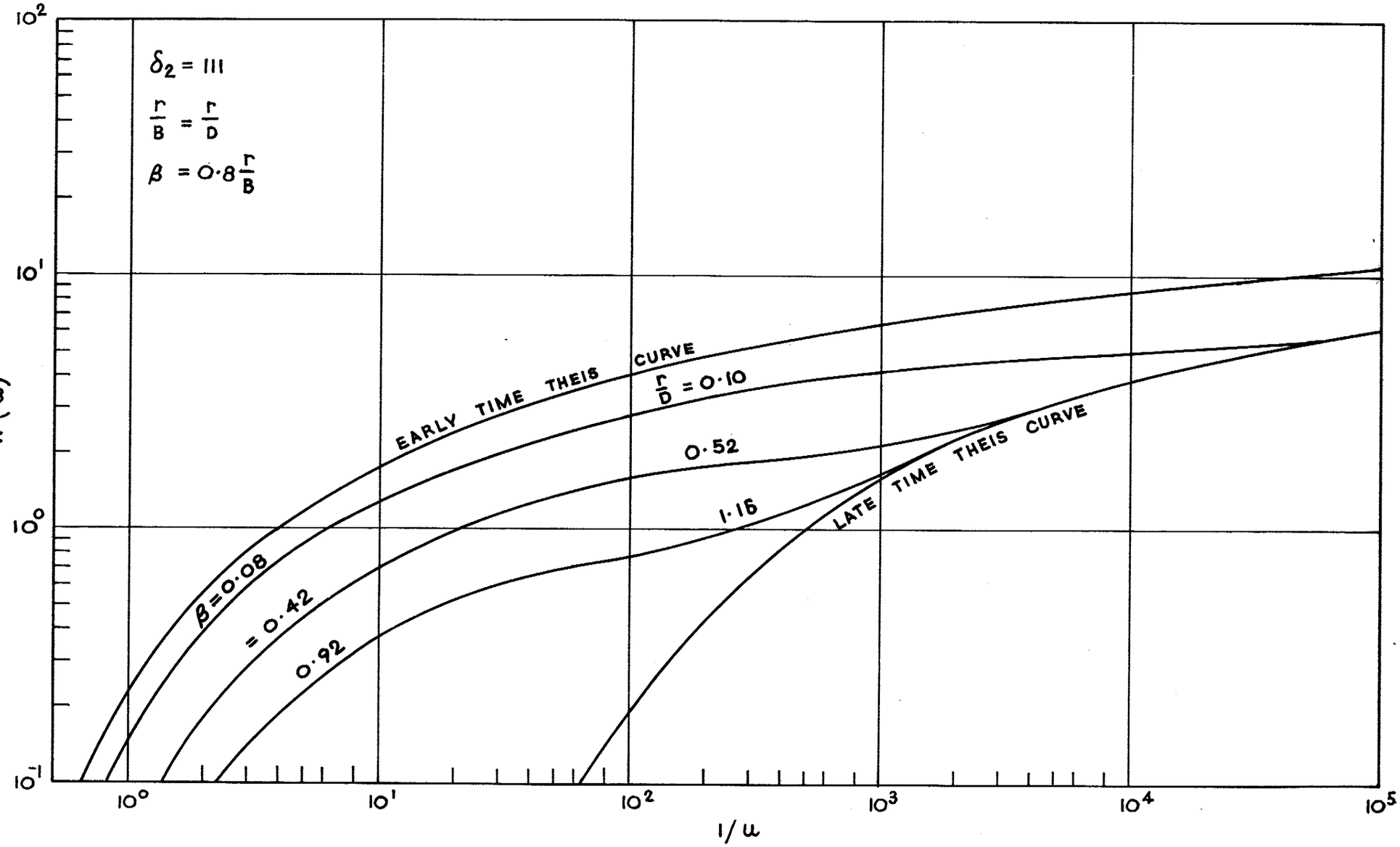

Fig. 3.17: Type curves for the main aquifer of a confined aquifer-unconfined aquitard system.

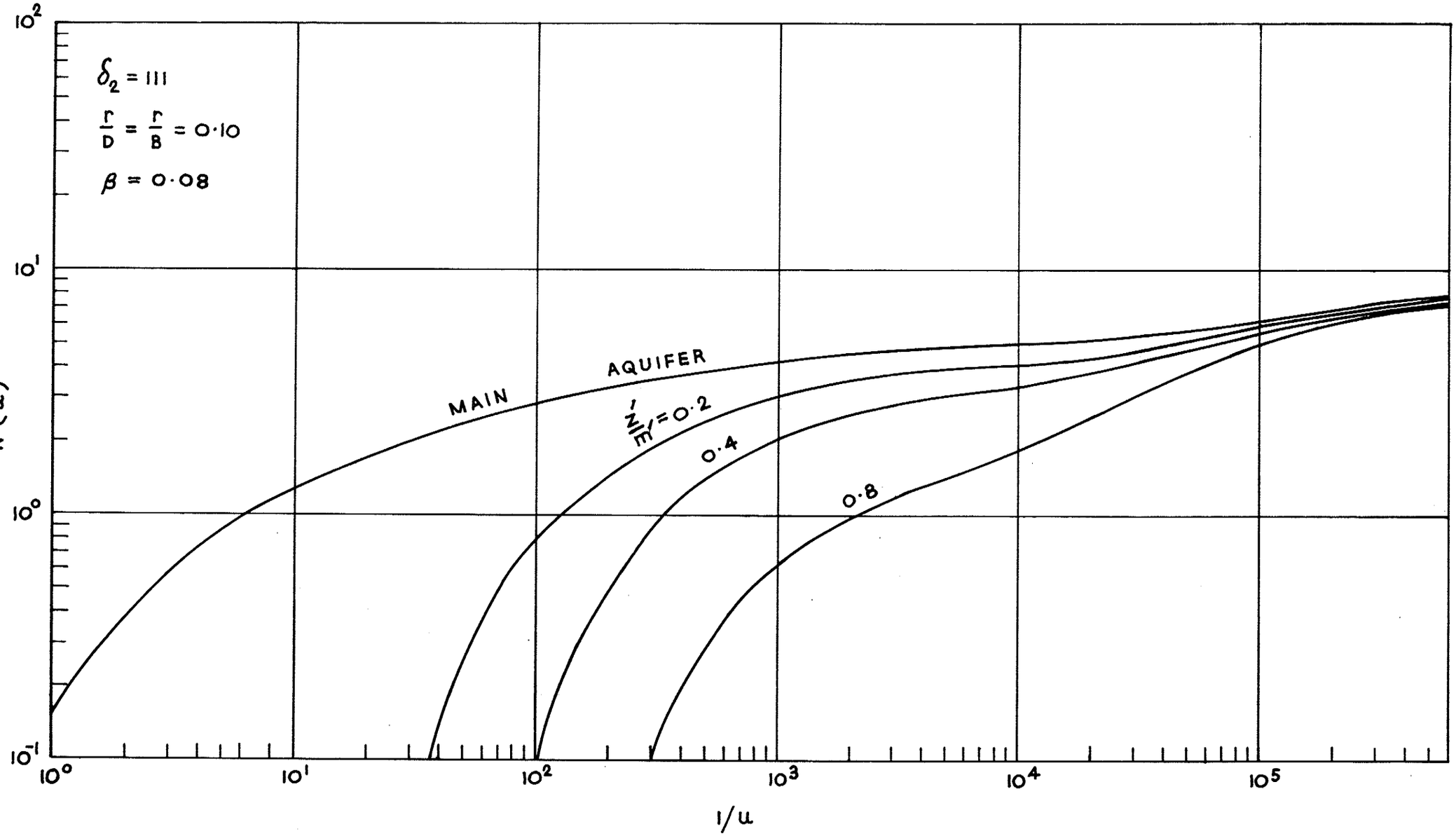

Fig. 3.18: Type curves for the aquitard of a confined aquifer-unconfined aquitard system.

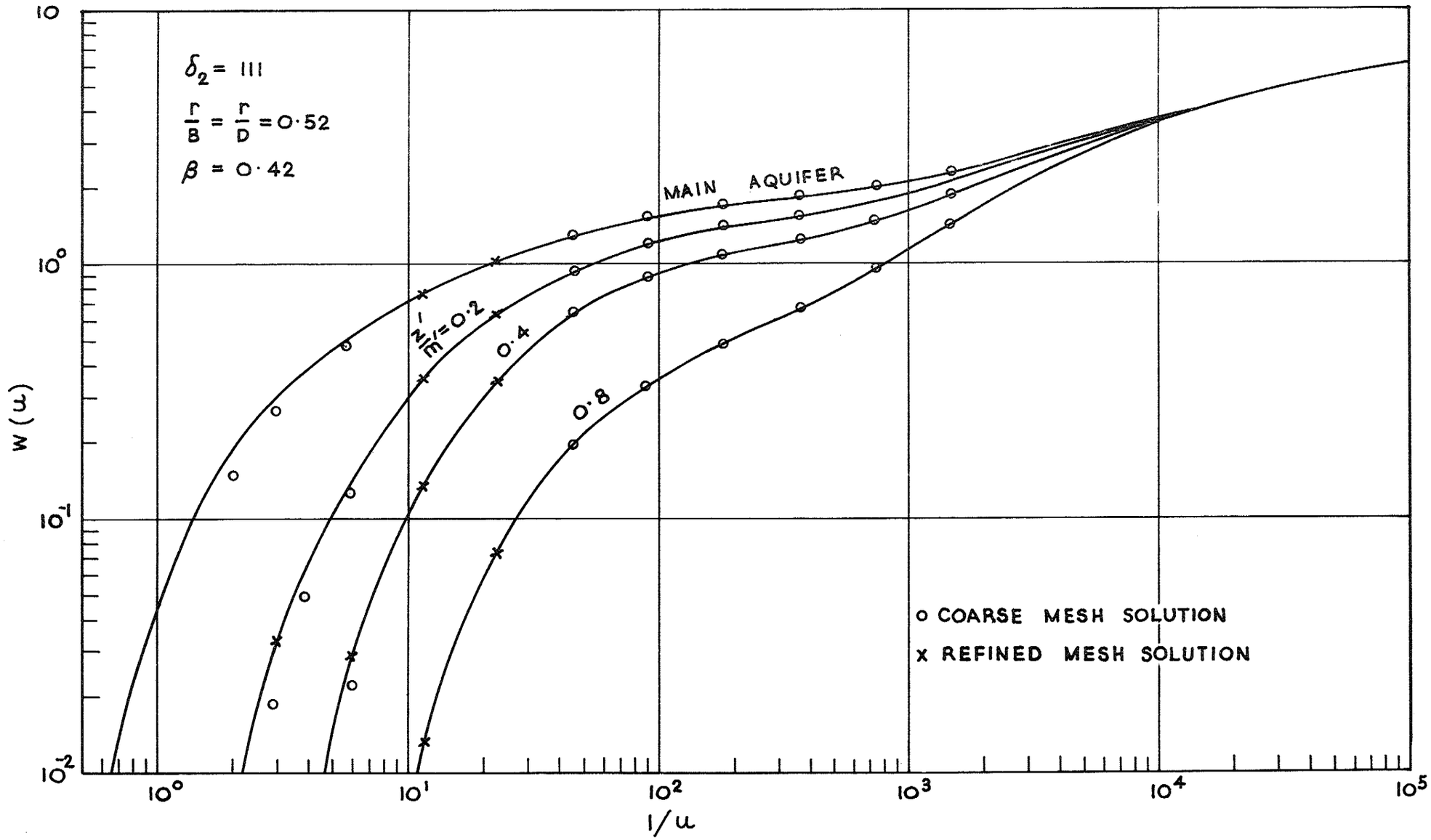

Fig. 3.19: Type curves for the aquitard of a confined aquifer-unconfined aquitard system, showing convergence of finite element solutions.

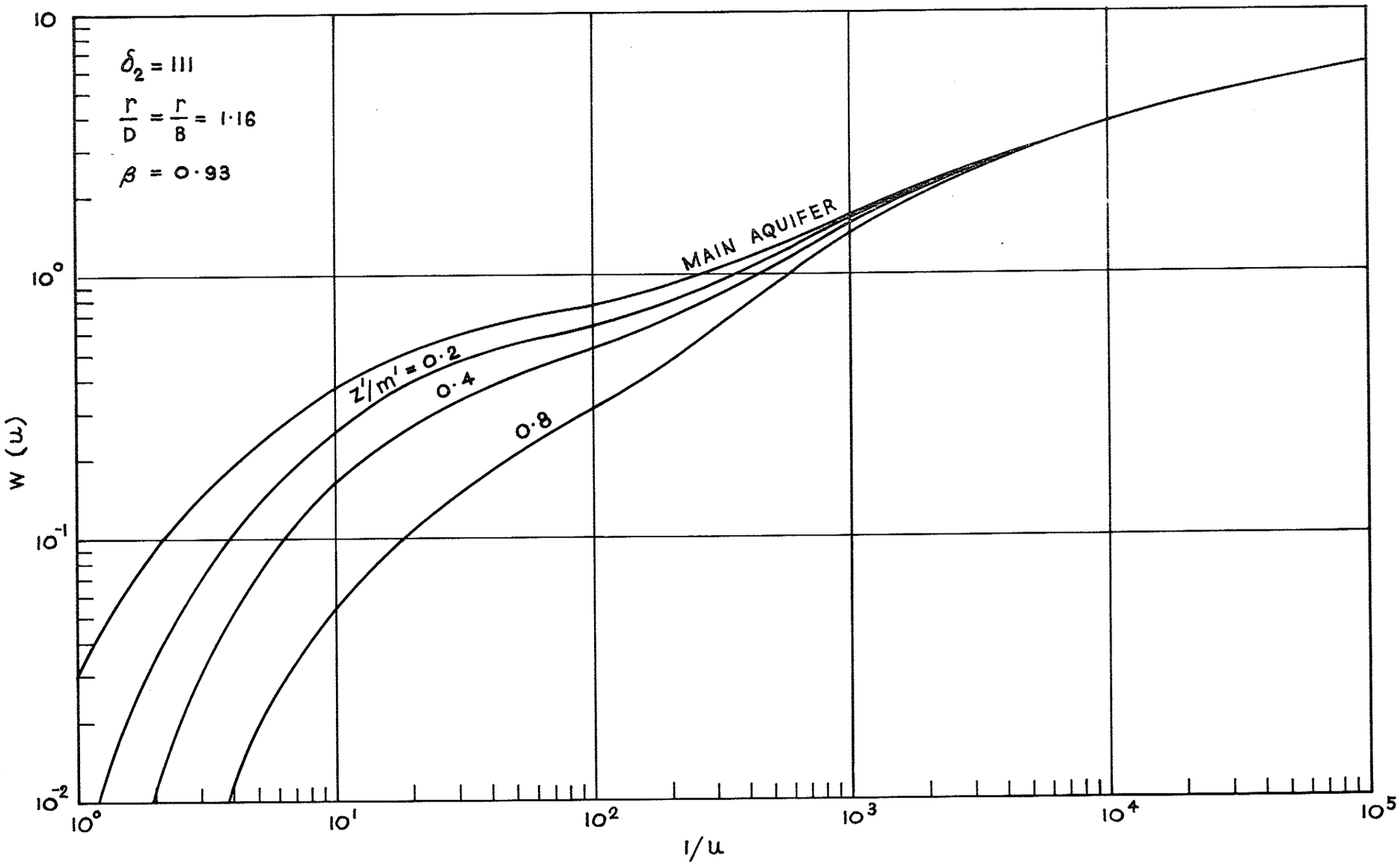

Fig. 3.20: Type curves for the aquitard of a confined aquifer-unconfined aquitard system.

Families of type curves for Equation (3.17b) are shown in Figs. 3.18 to 3.20. Each family was obtained from various nodes along a vertical line in the aquitard region. Each curve in a family shows an increasing gradient at a later time when the delayed yield effect becomes much less significant. For the families of large values of $\frac{r}{B}$ and $\frac{r}{D}$, the spread between the curves decreases and all curves merge into one curve when the vertical flow towards the top of the aquifer becomes negligible.

(ii) Non-Darcy Flow

In the case where non-Darcy flow develops near the well screen, semi-log plots of drawdown in the aquifer versus radial distance for late pumping times become non-linear as the well is approached. The total drawdown at a point in the non-Darcy zone consists of the drawdown computed by assuming wholly Darcy flow and the additional drawdown due to non-Darcy less the general dimensionless drawdown-time relationship may be written as

$$\frac{4\pi T\bar{s}}{Q} = \bar{W}(u, \beta, r/B, r/D, \lambda) = W + \Delta W \qquad (3.18)$$

where $\bar{S}$ = total drawdown = $S + \Delta S_N$

ΔS_N = additional drawdown due to non-Darcy loss

$\bar{W}$ = generalised well function incorporating non-Darcy loss

ΔW = additional well function

λ = a dimensionless parameter which is given by:-

$$\lambda = \frac{bQT}{2\pi m^2 r}$$

Type curves for Equation (3.18) are shown in Fig. 3.23 for $10^4 \leqslant 1/\delta_2\, u \leqslant 10^8$. It is seen that the effect of non-Darcy flow results in a vertical shift of the type curves above the late time Theis curve. The shift is approximately proportional to the value of the dimensionless parameter . It is also noted that for a given aquifer material (b and T constant) is directly proportional to the well discharge and inversely proportional to the radial distance from the pumped well.

3.3.6 Evaluation of Hydraulic Properties of Aquifer and Aquitard

The following procedures were adopted to determine the values of the hydraulic coefficients of the aquifer and aquitard materials local to the pumped well.

(i) The Drawdown-time data collected from observation wells Nos. 2 and 1 (r = 10, 38 ft.) outside the non-Darcy zone were converted to log-log plots of s versus t on two separate sheets of transparent paper. Each plot was then matched on a family of type curves for the main aquifer as shown in Figs. 3.21 and 3.22 respectively. For each observation well a match point was selected and the hydraulic coefficients were computed as follows:-

Well No. 2 (r = 10 ft.)

$$W(u) = 2.30,\ 1/u = 0.5 \times 10^5$$

$$s = 1 \text{ ft.},\ t = 10 \text{ min.}$$

$$r/D = 0.22$$

Hence

$$K = \frac{Q\,W(u)}{4\pi s\,m} = \frac{18.8 \times 2.3}{4 \times 3.14 \times 10} = 0.345$$

$$T = Km = 3.45 \text{ ft.}^2/\text{min.}$$

Assuming

$$S_y' \approx S_y' + S_s'm' + S_sm$$

$$S_y' = \frac{4Tt\sigma_2\, u}{r^2} = \frac{4 \times 3.45 \times 10 \times 251}{100 \times .5 \times 10^5}$$

$$= .0076$$

$$D = \left[\frac{T}{\alpha S_y'} + \frac{T}{K'/m'}\right]^{\frac{1}{2}}$$

$$D = \frac{10}{.22} = 46$$

Well No. 1 (r = 38 ft.)

$W(u) = 1.7,\ 1/u = 2.75 \times 10^4$

$s = 1$ ft., $t = 100$ min.

$r/D = 0.875$

Substituting the above values and m = 10 ft., $m' = 38$ ft., Q = 18.8 cfs, the following coefficients were obtained

$$K = \frac{QW}{4\pi s m}$$

$$= \frac{18.8 \times 1.7}{4 \times 3.14 \times 10} = 0.254$$

$$T = Km = 2.54 \text{ ft}^2/\text{min.}$$

$$S_y' \quad \frac{4\,Tt\,\delta_{2u}}{r^2} = \frac{4 \times 2.54 \times 100 \times 251}{38 \times 38 \times 2.75 \times 10^4}$$

$$= .0064$$

$$D = \left[\frac{T}{\alpha' S_y'} + \frac{T}{K'/m'}\right]^{\frac{1}{2}}$$

$$D = \frac{38}{0.875} = 43.5$$

(ii) Time-drawdown data obtained from wells 1 and 1A

(r = 38 ft., $z'/m' = 0,\ 0.8$) were plotted on the same sheet of transparent paper and matched on a selected family of aquitard type curves. Using the average values of T and r/D obtained from (i), appropriate values β and $\frac{r}{B}$ which gave satisfactory matching were obtained. The remaining hydraulic coefficients S_s, α', K', S_s' were estimated from the following expressions:-

$$K' = \frac{r}{B}^2 \frac{Kmm'}{r^2}$$

$$S_s' = \frac{16\beta^2 m^2 K S_s}{K' r^2}$$

$$D = \left[\frac{T}{\alpha' S_y'} + \frac{T}{K'/m'}\right]^{\frac{1}{2}}$$

(iii) The drawdown-time data collected from pumped well No. 3 (r_w = 0.167 ft) was plotted on another sheet of transparent paper. As the observed drawdowns in this well would also include non-Darcy losses, the corresponding drawdowns for wholly Darcy flow at the same pumping time were obtained by extrapolating the straight line semi-log plot of s versus r to a radius r_w = 0.167 ft. The two plots were shown in Fig. (3.23). To allow the dimensionless non-Darcy flow parameter to be estimated the two plots were matched on the generalised non-Darcy type curves $\bar{W}(u)$ versus $1/\delta_2 u$ as shown in Fig. 3.23. Knowing the non-linear Forchheimer coefficient b was computed. The linear Forchheimer coefficient a was taken to be approximately 1/K.

(iv) The values of the hydraulic coefficients computed from (i) and (ii) were fed back into the finite element model, and the flow problem was solved for Q = 18.8 cfm and pumping period t = 1440 mins. The calculated drawdown versus time relationships at selected nodes in the aquifer and aquitard regions were compared with the field data for the corresponding points in the field system. Figs. 3.24 and 3.25 show such comparisons. It is seen in Fig. 3.24 that reasonable agreement was obtained for the pumped well and observation well No. 2 (r=10 ft.) Less satisfactory agreement was obtained for observation well No. 1 (r = 38 ft.) as shown in Fig. 3.25.

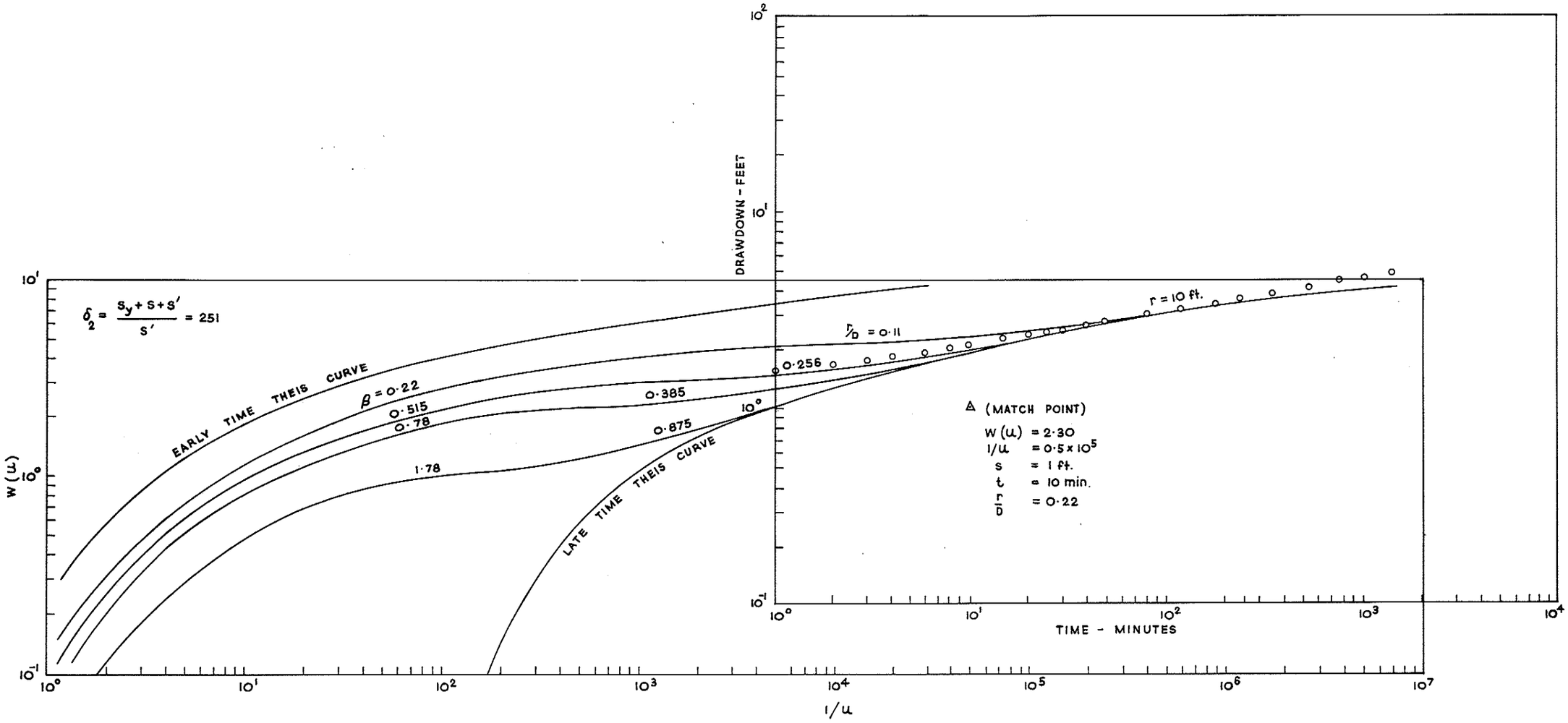

Fig. 3.21: Matching of Field Data on Type Curve for Main Aquifer.

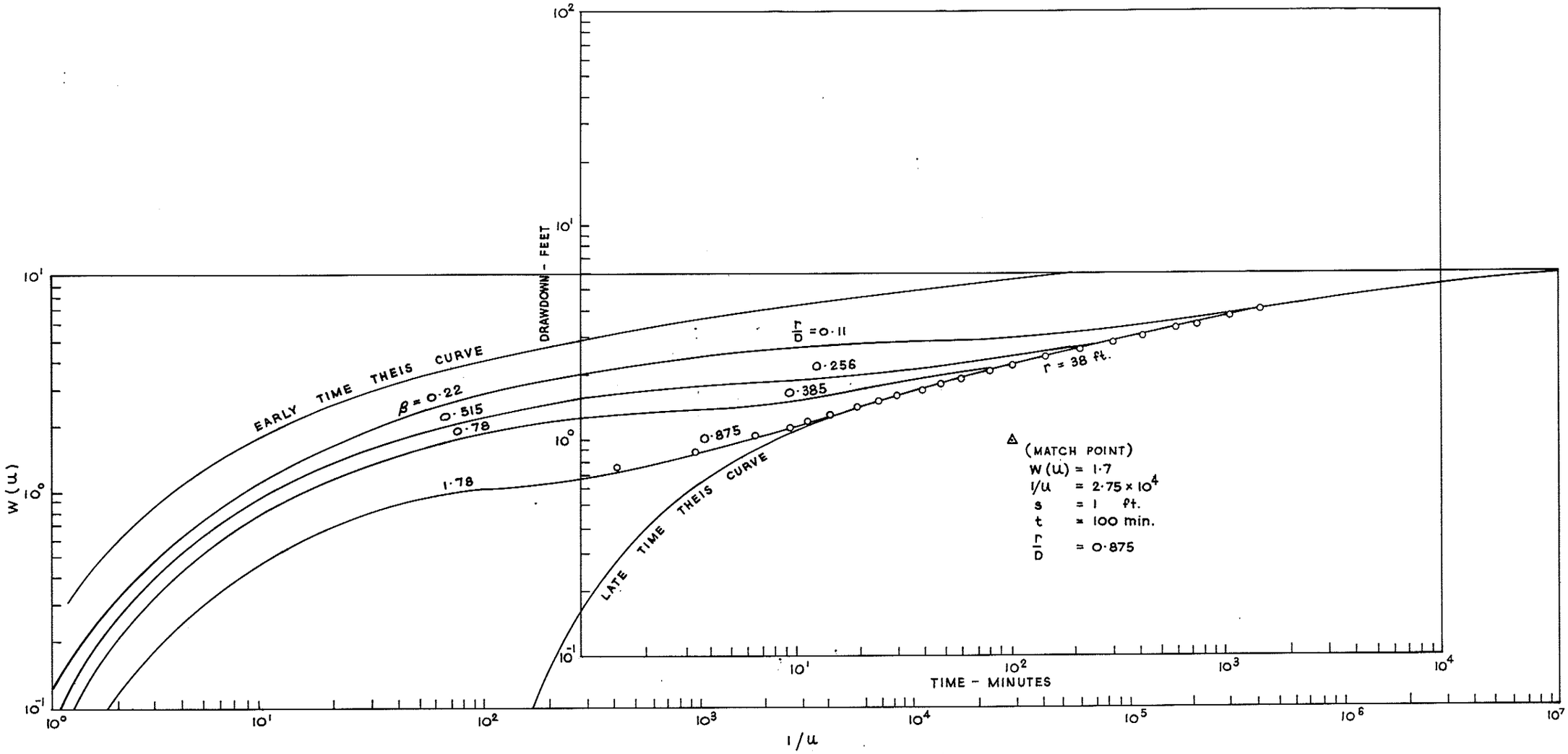

Fig. 3.22: Matching of Field Data on Type Curves for Main Aquifer.

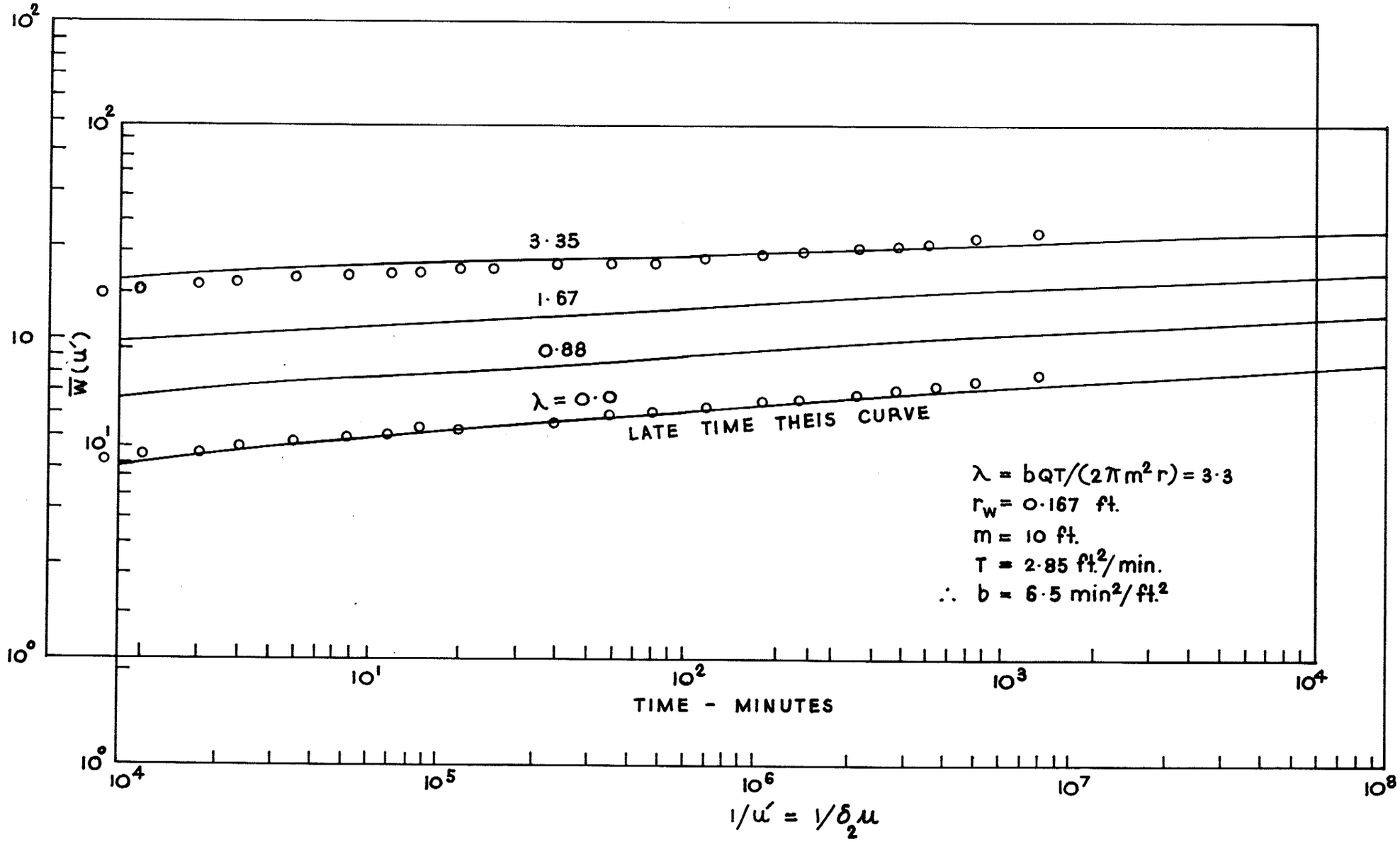

Fig. 3.23: Matching of field data on non-Darcy flow type curves.

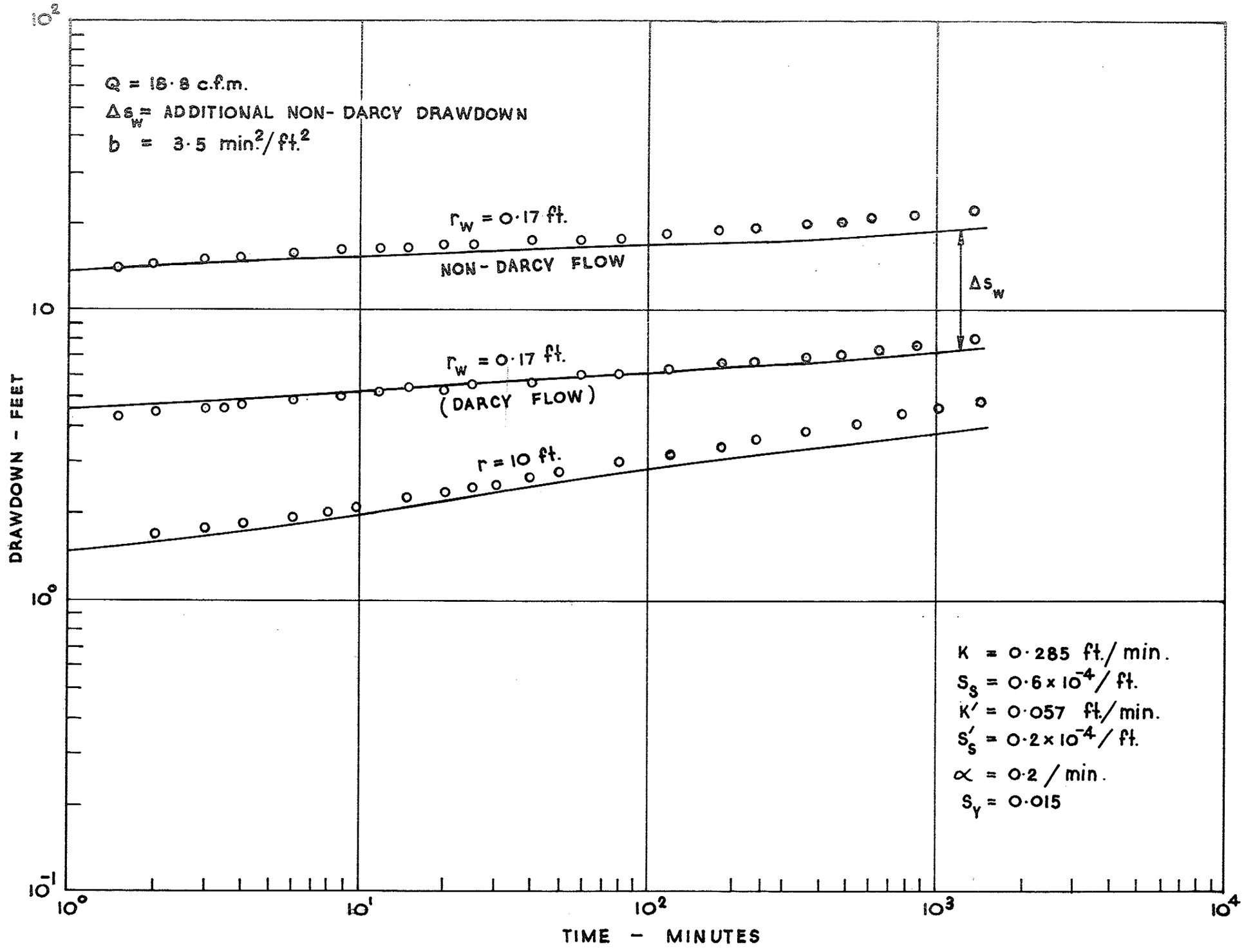

Fig. 3.24: Comparison of finite element model results with field data.

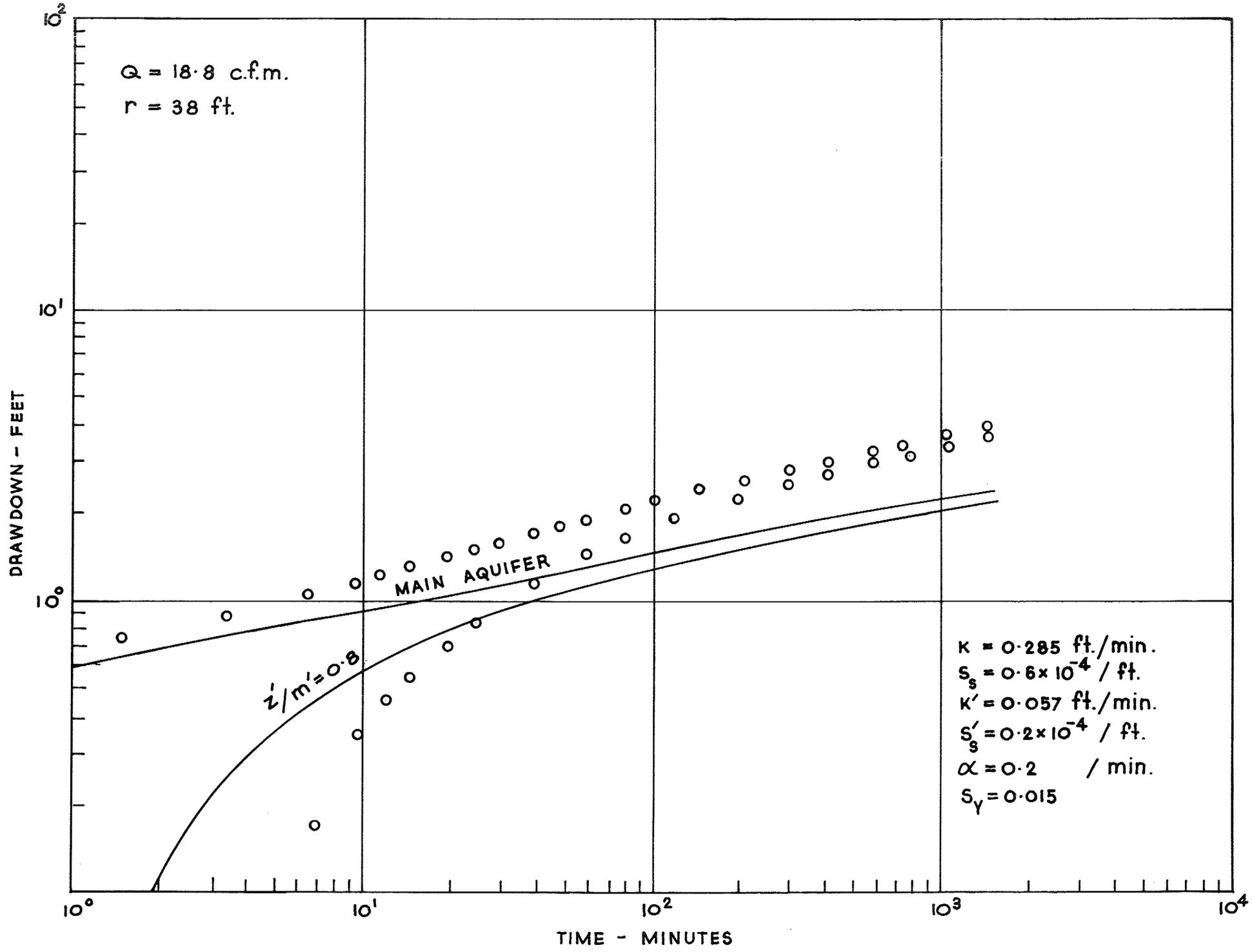

Fig. 3.25: Comparison of finite element model results with field data.

4. Conclusions

Pumping test data collected from the two sites have been analysed by both conventional methods of pumping test analysis and new methods which employ finite element computer programmes. Values of the hydraulic coefficients for the aquifer and aquitard materials local to the pumped wells and the average coefficients pertaining to a wider region of influence have been obtained. These values have been used as initial input data for the computer programmes to simulate the flow conditions existing in the field. Predictions of drawdown-time relationships for the pumped wells and close observation wells have been made and compared with the field data.

For site A, where the aquifer and aquitard are relatively uniform in thickness and hydraulic properties, good agreement between the computer predictions and field data has been achieved. It was found that conventional methods of pumping test analysis gave good estimates of the values of the hydraulic coefficients for the main portion of the aquifer and that these values approximate the values for the material near the pumped well as given by the new computer methods. Although the new methods also allow the Forchheimer non-linear coefficient b to be evaluated, it was not possible to do so from the field data obtained as non-Darcy flow did not occur around the 24 inch diameter gravel pack of the production well at a discharge of 48,000 igph. To induce non-Darcy flow having significant effects on well drawdowns would have required either a reduction in well diameter for the same discharge or a significant increase in discharge if the same diameter were used. For site B, where the main aquifer is quite variable in physical and hydraulic characteristics and the overlying aquitard is unconfined, less satisfactory agreement between the computer results and the field data has been achieved. It was found that the regional hydraulic coefficients evaluated by conventional methods were unreliable as when they were fed into the finite element model, poor agreement between the model predictions and the field data was obtained. This can be explained in terms of the limiting assumptions of the conventional type curve methods which were used and the marked difference between hydraulic coefficients of the aquifer material near the pumped wells and the average value for the aquifer beyond this zone.

Since observations of drawdowns in the two trial wells indicated the existence of non-Darcy losses, the non-linear coefficient b was also evaluated by the computer methods. The evaluation was based on the assumption that screen losses may be separated from the total well drawdown or neglected, thus the value of the coefficient b so obtained would represent an over-estimate of the true value if the screen losses were significant. It would be desirable, if any further testing should be

performed at this particular site, to construct piezometers just outside the pumped wells to enable screen losses to be measured and subtracted from the total well drawdowns.

It has been demonstrated that the new methods of pumping test evaluation may be used as a supplement to conventional methods to obtain more detailed information on the local flow behaviour in the immediate vicinity of pumped wells and the existence of non-Darcy flow and resulting losses. The hydraulic coefficients determined for the material in the near well zone and outside this zone may be used in the selection of a production well design using the computer programmes presented in Section C of this report or design charts produced by the programmes.

DRAWDOWN SHEET

Sheet No. 1

RESULTS of 72 hour pumping test

Job Name AWRC Research Project 68/8 Line Name Gumly Island Wagga Wagga

BORE DESCRIPTION Bore No. 30638 Site No. (P.B.) on Property

TEST NUMBER 1 PUMPING PERIOD 3.00 pm 26.9.72 to 3.00 pm 29.9.72

S.W.L. from Reference Point at Commencement of Test 31.33

Watch Time hr.	min	am or pm	Time reg'd in mins.	Draw-down ft.	ins.	Water Level from Ref. Pt. ft.	ins.	Rate Measurements Measurement	Rate (gph)	Remarks (e.g. was water clear throughout & were D.Ds. measured in any other bores
3	00	pm	0	0.	00	31.	33	223500		Pump started
			1	21.	92	53.	25			
			2	23.	19	55.	52			
			3	25.	36	56.	69			
			4	26.	17	57.	50			
			5	26.	69	58.	02			
			10	28.	52	59.	85			
			15	29.	62	60.	95			
			20	30.	44	61.	77			
			25	30.	92	62.	25			
			30	31.	20	62.	53			
			60	32.	84	64.	17	323300	50100	
			90	33.	61	65.	04			
			120	34.	46	65.	79			
			150	35.	02	66.	35			
			180	35.	42	66.	75	372850	49550	
			210	35.	70	67.	13			
			240	36.	15	67.	48	422000	49250	
			270	36.	46	67.	79			
			300	36.	52	67.	85	471500	49550	
			330	36.	61	67.	94			
			360	36.	75	68.	08	519700	48200	
			420	37.	13	68.	46	568500	48800	
			480	37.	59	68.	92	617300	48800	
			540	37.	92	69.	25	666200	48900	
			600	38.	25	69.	58	715100	48900	
			660	38.	42	69.	75	763300	48900	
			700	38.	59	69.	92	812400	48900	
			840	38.	67	70.	00	909200	48900	
			960	38.	86	70.	19	1006100	48900	
			1080	38.	92	70.	25	11026351	48100	

DRAWDOWN SHEET Sheet No 2

RESULTS of 72 hour pumping test

Job Name AWRC Research Project 68/8 Line Name Gumly Island, Wagga Wagga

BORE DESCRIPTION Bore No. 30638 Site No. (P.B.) on Property

TEST NUMBER 1 PUMPING PERIOD 3.00 pm 26.9.72 to 3.00 pm 29.9.72

S.W.L. from Reference Point at Commencement of Test 31.33

Watch Time			Time reg'd in mins.	Draw-down		Water Level from Ref. Pt.		Rate Measurements		Remarks (e.g. was water clear throughout & were D.Ds. measured in any other bores
hr.	min	am or pm		ft.	ins.	ft.	ins.	Measurement	Rate (gph)	
			1200	39.	32	70.	65	1198700	48100	
			1440	39.	56	70.	89	1390200	48612	
			1680	40.	06	71.	39			
			1920	40.	46	71.	79			
			2220	40.	67	72.	00			
			2400	40.	88	72.	21	2204700	47500	
			2640	41.	04	72.	37	2347400	47700	
			2880	41.	00	72.	33	2535300	47000	
			3120	41.	68	73.	05	2725700	47600	
			3360	42.	04	73.	37	291600	47600	
			3600	42.	17	73.	50			
			3840	42.	25	73.	58			
			4320							Pump stopped